The Scientific World Journal

Cardiac Electrophysiology

Guest Editors: Yanggan Wang, Yimei Du, and Xun Ai

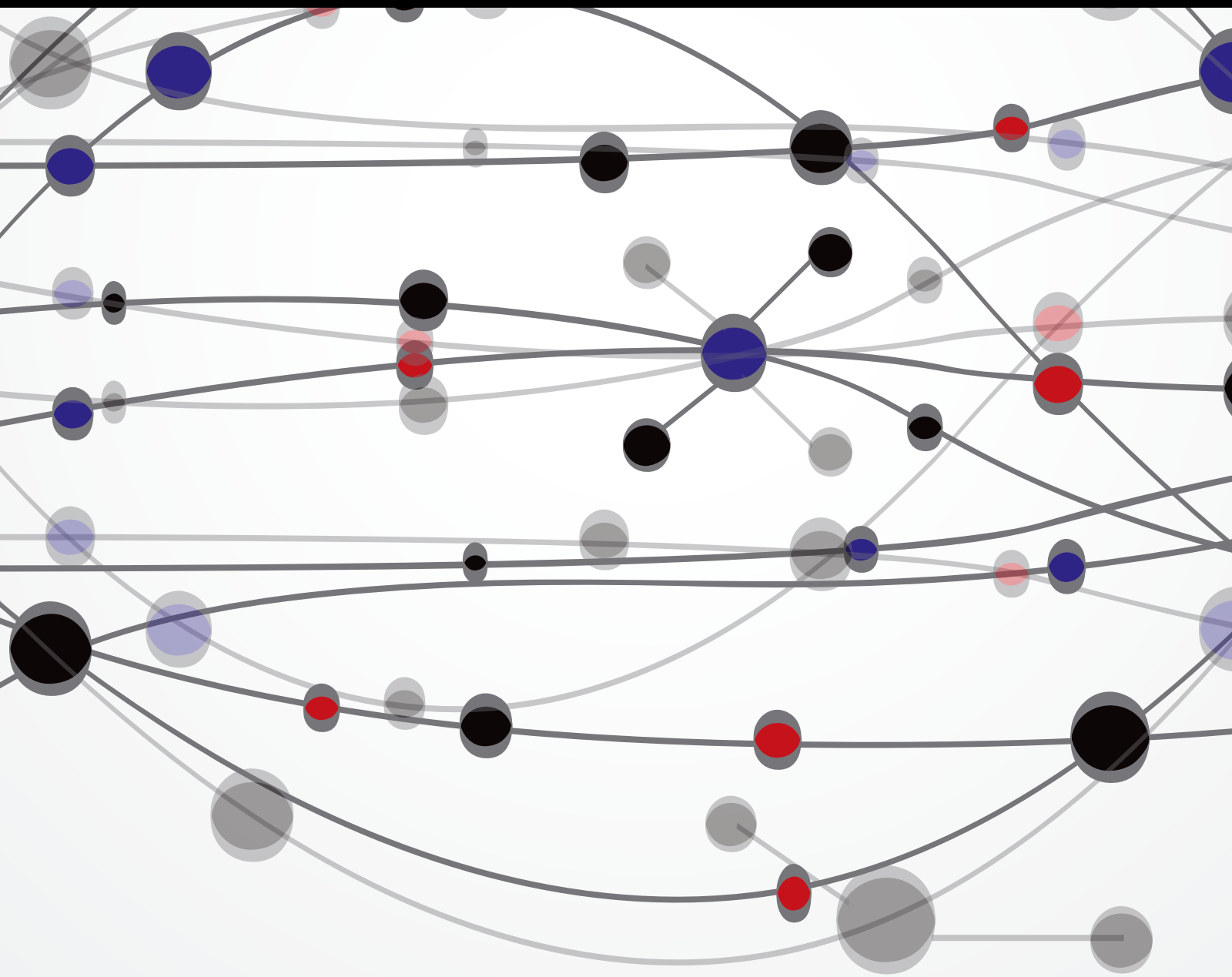

Cardiac Electrophysiology

The Scientific World Journal

Cardiac Electrophysiology

Guest Editors: Yanggan Wang, Yimei Du, and Xun Ai

Contents

Cardiac Electrophysiology, Yanggan Wang, Yimei Du, and Xun Ai
Volume 2013, Article ID 909746, 1 page

Effects of Low-Level Autonomic Stimulation on Prevention of Atrial Fibrillation Induced by Acute Electrical Remodeling, Yubi Lin, Ning Bian, Hairui Li, Jia Chen, Huijie Xing, Hong Li, Dandan Huang, Xianwu Lan, Bojun Gong, Li Zhou, Ruijie Liu, Min Guan, Dongdong Zhang, Gang Du, Zhengyi Huang, Xiaoming Chen, Tao Zhang, Jianyi Feng, Shaorong Wu, Liwei Wang, Aidong Zhang, and Zicheng Li
Volume 2013, Article ID 781084, 9 pages

Polymorphisms but Not Mutations of the KCNQ1 Gene Are Associated with Lone Atrial Fibrillation in the Chinese Han Population, Hui-min Chu, Ming-jun Feng, Yi-gang Li, Yi-xin Zhang, Ji-fang Ma, Bin He, Yi-bo Yu, Jing Liu, and Xiao-min Chen
Volume 2013, Article ID 373454, 6 pages

Calcium Transient and Sodium-Calcium Exchange Current in Human versus Rabbit Sinoatrial Node Pacemaker Cells, Arie O. Verkerk, Marcel M. G. J. van Borren, and Ronald Wilders
Volume 2013, Article ID 507872, 10 pages

Predictors of Cardiac Resynchronization Therapy Response: The Pivotal Role of Electrocardiogram, Yahya S. Al Hebaishi, Halia Z. Al Shehri, and Abdulrahman M. Al Moghairi
Volume 2013, Article ID 837086, 6 pages

Mechanism of and Therapeutic Strategy for Atrial Fibrillation Associated with Diabetes Mellitus, Yubi Lin, Hairui Li, Xianwu Lan, Xianghui Chen, Aidong Zhang, and Zicheng Li
Volume 2013, Article ID 209428, 6 pages

Hindawi Publishing Corporation
The Scientific World Journal
Volume 2013, Article ID 909746, 1 page
http://dx.doi.org/10.1155/2013/909746

Editorial

Cardiac Electrophysiology

Yanggan Wang,[1] Yimei Du,[2] and Xun Ai[3]

[1] *Department of Cardiology, Zhongnan Hospital, Wuhan University, Wuhan 430071, China*
[2] *Department of Cardiology, Xiehe Hospital of Huazhong University of Science and Technology, Wuhan 430022, China*
[3] *Department of Physiology, Loyola University Chicago, Maywood, IL 60153, USA*

Correspondence should be addressed to Yanggan Wang; ygwang2013@163.com

Received 21 July 2013; Accepted 21 July 2013

Recently, significant achievements have been made in cardiac electrophysiology research, including Ca^{2+} regulatory pathways, membrane ion channel-related intracellular signaling, and electrical remodeling in cardiomyopathies. The rapid progress in the basic research has led to applications of numerous new methods and strategies to clinical diagnoses and treatments. The efficacy of antiarrhythmic pharmacotherapy remains a major challenge, but recent insights into complex mechanisms of electrical remodeling and new therapeutic strategies have raised the prospect of targeting arrhythmogenic substrates.

This special issue introduces recent progress in this area with special focus on atrial fibrillation, one of the most common arrhythmias in structural heart diseases. Papers published in this issue include basic research in ion channels, polymorphisms associated with lone atrial fibrillation, low-level autonomic stimulation on prevention of atrial fibrillation, new clinical methods for diagnosis and treatment of atrial fibrillation, and the pivotal role of cardiac imaging and electrocardiogram in assessing the effectiveness of cardiac resynchronization therapy. Due to volume limits, several important areas have not been included in this issue. However, we plan to discuss these topics in future issues.

Yanggan Wang
Yimei Du
Xun Ai

Hindawi Publishing Corporation
The Scientific World Journal
Volume 2013, Article ID 781084, 9 pages
http://dx.doi.org/10.1155/2013/781084

Research Article

Effects of Low-Level Autonomic Stimulation on Prevention of Atrial Fibrillation Induced by Acute Electrical Remodeling

Yubi Lin,[1] Ning Bian,[1] Hairui Li,[1] Jia Chen,[2] Huijie Xing,[3] Hong Li,[1] Dandan Huang,[1] Xianwu Lan,[1] Bojun Gong,[1] Li Zhou,[1] Ruijie Liu,[1] Min Guan,[4] Dongdong Zhang,[5] Gang Du,[1] Zhengyi Huang,[1] Xiaoming Chen,[1] Tao Zhang,[1] Jianyi Feng,[1] Shaorong Wu,[1] Liwei Wang,[6] Aidong Zhang,[1] and Zicheng Li[1]

[1] *Department of Cardiology, The First Affiliated Hospital of Jinan University, Guangzhou 510630, China*
[2] *The Second Department of Cardiology, The Guangdong No. 2 Provincial People's Hospital, Guangzhou 510317, China*
[3] *Laboratory Animal Center of Jinan University, Guangzhou 510632, China*
[4] *Department of Interventional Radiology and Vascular Surgery, The First Affiliated Hospital of Jinan University, Guangzhou 510630, China*
[5] *Department of Cardiothoracic Surgery, The First Affiliated Hospital of Jinan University, Guangzhou 510630, China*
[6] *Department of Physiology of Medical College of Jinan University, Guangzhou 510632, China*

Correspondence should be addressed to Zicheng Li; zichengli@163.net

Received 20 April 2013; Accepted 2 June 2013

Academic Editors: X. Ai, Y. Du, and Y. Wang

Background. Rapid atrial pacing (RAP) can induce electrical and autonomic remodeling and facilitate atrial fibrillation (AF). Recent reports showed that low-level vagosympathetic nerve stimulation (LLVNS) can suppress AF, as an antiarrhythmic effect. We hypothesized that LLVNS can reverse substrate heterogeneity induced by RAP. *Methods and Results*. Mongrel dogs were divided into (LLVNS+RAP) and RAP groups. Electrode catheters were sutured to multiple atrial sites, and LLVNS was applied to cervical vagosympathetic trunks with voltage 50% below the threshold slowing sinus rate by ⩽30 msec. RAP induced a significant decrease in effective refractory period (ERP) and increase in the window of vulnerability at all sites, characterized by descending and elevated gradient differences towards the ganglionic plexi (GP) sites, respectively. The ERP dispersion was obviously enlarged by RAP and more significant when the ERP of GP-related sites was considered. Recovery time from AF was also prolonged significantly as a result of RAP. LLVNS could reverse all these changes induced by RAP and recover the heterogeneous substrate to baseline. *Conclusions*. LLVNS can reverse the electrical and autonomic remodeling and abolish the GP-central gradient differences induced by RAP, and thus it can recover the homogeneous substrate, which may be the underlying mechanism of its antiarrhythmic effect.

1. Introduction

Atrial fibrillation (AF) is the most common cardiac rhythm disorder and contributes to thromboembolism. The presence of AF is an independent risk factor for thromboembolism; especially stroke in association with AF increases mortality and morbidity, leading to greater disability, longer hospital stays, and worse quality of life [1, 2]. AF affects approximately 10 million people in China alone [3]. AF is a complex disease that is initiated by a specific trigger and maintained in the presence of a vulnerable substrate. The autonomic nervous system (ANS), especially the vagosympathetic/vagus nerve, is an important participant in the mechanism of AF initiation.

The cardiac ANS consists of extrinsic and intrinsic components [4, 5]. The extrinsic component comprises cervical and thoracic stellate ganglia, which contribute to complex sympathetic innervation of the heart. Most of the vagosympathetic trunks of the extrinsic system contain vagal nerve fibers; they serve as parasympathetic innervation and converge at the epicardial fat pads around the superior vena cava, pulmonary veins (PVs), and the aorta, postulated to be "integration centers." The extrinsic component modulates

cardiac electrophysiology and the inducibility of AF [6, 7]. The intrinsic cardiac ANS is a complex neural network composed of ganglionated plexi (GP) concentrated within epicardial fat pads, and interconnecting ganglia and axons [8–10]. Stimulation of GP can convert the firing from PVs into AF in dogs and in humans [11–13], then promote maintenance of AF due to markedly reduced atrial effective refractory period (ERP), widen the window of vulnerability (WOV), and increase gradient differences in ERP and WOV towards GP, which serve as heterogeneous substrate caused by GP hyperactivity [14]. This mechanism is largely based on the observation that vagosympathetic nerve stimulation (VNS) can greatly facilitate initiation and maintenance of AF by activating the "integration centers of GP" [7, 15]. Once initiated, AF leads to atrial remodeling, which involves electrical and structural remodeling and even promotes autonomic remodeling; this facilitates maintenance and recurrence of AF.

Ablation of the autonomic substrate suppresses or eliminates focal AF originating from PVs [11]. In particular, GP ablation can result in successful autonomic denervation, thus prevent the induction of AF, attenuate complex fractionated atrial potentials, and suppress vagally induced AF [16–18]. Until recently, the success rate of a single or multiple circumferential PV ablations for paroxysmal AF was 70–90% (followup for about 1 year) [19], and refractory AF was reported in some of the patients. Moreover, although GP ablation significantly reduced the vagal stimulation effect, AF inducibility was strongly augmented by vagal stimulation 4 weeks after GP ablation [20]. It was also reported that, 8 weeks after ARGP and IRGP ablation, AF was induced easily by atrial RAP [21]. Therefore, the long-term effects of GP ablation are debatable. Although the autonomic effect is eliminated after GP ablation, atrial autonomic intervention remodeling and neurohormonal disturbances in the atrium may also be responsible for AF vulnerability: for example, atrial natriuretic peptide, a substrate for arrhythmia, is associated with shortened atrial conduction time and effective refractory period (ERP) [21]. Therefore, there is a need for new therapeutic strategies.

Low-level VNS (LLVNS) is being explored as another strategy. Strong-level VNS that produces >60% prolongation of the sinus cycle length facilitates AF; it produces long pauses and even sinus arrest, which are generally required to induce and maintain AF [16, 22–24]. However, moderate-level VNS (MLVNS) that produces <40% prolongation of the sinus cycle length appears not to induce AF. It has been reported that MLVNS that slowed the sinus rate by 10% for 4 weeks did not induce AF, and was not associated with arrhythmogenic risk [23]. Some recent evidence suggests that LLVNS, with voltage levels 10–50% below threshold, which does not slow the sinus rate, has an antiarrhythmic effect [25–28].

Based on all these reported results, we hypothesized that the antiarrhythmic effect of LLVNS is brought about by elimination of the heterogeneous substrate surrounding the GP areas, which is induced by rapid atrial pacing (RAP). This study was specifically designed to test the previous hypothesis in dogs with acute electrical remodeling.

2. Methods

2.1. Animal Preparation. The Institutional Animal Care and Use Committee of JINAN University of Experimental Animal Management Centre reviewed and approved the design of all animal experiments. All animal studies were reviewed and approved by the animal experimental administration of JINAN University of China. A total of 20 adult mongrel dogs weighing 13–17 kg were anesthetized with sodium pentobarbital (initial bolus, 30 mg/kg body weight, i.v.), with an additional dose of 2 mg/kg given at the end of each hour. All dogs were ventilated with room air using a positive pressure respirator, and oxygen saturation was maintained at 95–100%. The animals were fixed on an operating table, the temperature of which thermostatically controlled at 37°C. The chest was entered via bilateral thoracotomy at the bilateral fourth intercostal space. Several 10-bipolar electrodes were sutured using a noninjurious method to allow recording and stimulation at the left superior pulmonary vein (LSPV), left inferior pulmonary vein (LIPV), left appendage (LAA, catheter: LA1,2), left atrium (LA, catheter: LA5,6), area around the Marshall ligament (MSL, catheters: LA9,10) [15, 29], right superior pulmonary vein (RSPV), right inferior pulmonary vein (RIPV), right appendage (RAA, catheter: RA1,2), right atrium (RA, catheter: RA5,6), and margin of the anterior right ganglionated plexi (ARGPM, catheter: RA9,10) (Figure 1). The capture threshold of the electrodes was tested and stabilized at 1-2 V. The incisions were sutured, and then the thoracic cavity was pumped till negative pressure was achieved and closed completely.

Standard ECG and electrophysiological channels (IECG) were continuously recorded and filtered at 0.05–100 Hz and 200–1200 Hz, respectively. All tracings from the electrode catheters were amplified and digitally recorded using a computer-based electrophysiological system (Lead2000B; Jingjiang Inc., China).

2.2. Programmed Stimulation. In both groups, RAP was delivered (1200 bpm, 4 V, 1 msec in duration) at the LA. After each pacing hour, RAP was temporarily stopped to measure the electrophysiological data.

Programmed stimulation was performed with Lead-2000B stimulator. Regular atrial pacing as S_1-S_1 interval was set at 330 msec, ERP was determined using S_1-S_2 programmed stimulation (S_1-S_1 : S_1-S_2 = 8 : 1), which decreased from 150 msec by 10 msec decrements; as the S_1-S_2 intervals approached the ERP, the last S_1-S_2 interval increased by 8 msec, and the decrement was reduced by 1 msec again, until precise ERP was reached. ERP dispersion (ERPD) was defined as the coefficient of variation (standard deviation/mean) of the ERP at all 8 or 10 sites [30], and was calculated using MATLAB-R2008. ERPD1 was calculated for RSPV, RIPV, RA, RAA, LSPV, LIPV, LA, and LAA. When adding the ERP of ARGPM and MSL into calculation together with the previous 8 sites, we would get the values of ERPD2.

The WOV was used as a quantitative measure of AF inducibility. During ERP measurements, if AF or >2 echo was induced by decremental S_1-S_2 stimulation, the difference

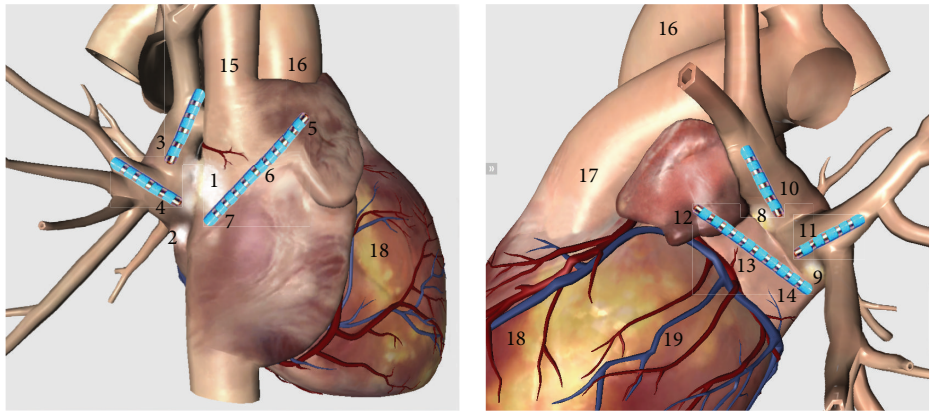

(a) (b)

Figure 1: Position of catheters in the atrium. 1, anterior right ganglionated plexi (ARGP); 2, inferior right ganglionated plexi (IRGP); 3, right superior pulmonary vein (RSPV); 4, right inferior pulmonary vein (RIPV); 5, right appendages (RAA); 6, right atrium (RA); 7, margin of anterior right ganglionated plexi (ARGPM); 8, superior left ganglionated plexi (SLGP); 9, inferior left ganglionated plexi (ILGP); 10, left superior pulmonary vein (LSPV); 11, left inferior pulmonary vein (LIPV); 12, left appendages (LAA); 13, left atrium (LA); 14, Marshall ligament area (MSL); 15, superior vena cava (SVC); 16, aorta; 17, pulmonary artery (PA); 18, right ventricle (RV); and 19, left ventricle (LV).

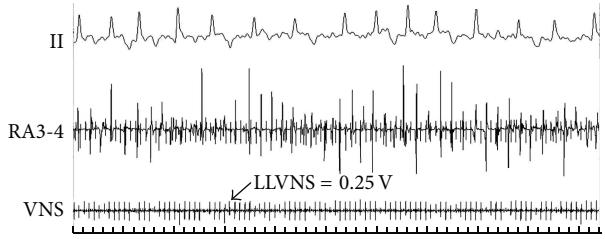

Figure 2: Low-level vagosympathetic nerve stimulation (LLVNS) during rapid atrial pacing (RAP). The voltage of LLVNS was 0.25 V (VNS channel). RAP was delivered at the LA site. RA3,4 channel recorded the signal of RAP and LLVNS.

between the longest and the shortest S_1-S_2 interval was designated as the WOV. The ∑WOV was counted as the sum of WOV at each site [14].

The stimulation of the atrium was delivered at the LA site with S_1-S_1 intervals set at 100 msec and sustained for 10 seconds, which induced atria tachycardia or AF easily when it was continued or stopped. The recovery time (RT) was represented as the duration from AF triggered by persistent S_1-S_1 stimulation to sinus rhythm.

2.3. Low-Level Vagosympathetic Nerve Stimulation. Bilateral cervical vagosympathetic trunks were decentralized by surgical procedures. Two pairs of electrodes insulated with surrounding tissue were embedded in the vagosympathetic trunks located adjacent to the cervical artery for LLVNS [31]. LLVNS was induced by applying high-frequency electrical stimulation (HFS, 20 Hz, 0.1 msec in duration, square waves, voltage 0.1–0.5 V) to vagosympathetic nerves via an electronic stimulator (BL-420E Experimental System; Tai Meng, Chengdu, China) (Figure 2). The lowest voltage of VNS that prolonged the cycle length of sinus rhythm (A-A intervals) by no more than 30 msec was considered the threshold. The LLVNS voltage was approximately 50% below the threshold. Prior to each hour of LLVNS, the threshold of VNS was determined again to adjust the LLVNS voltages for the next hour [25, 26, 28].

2.4. Experimental Protocol. Twenty dogs were randomly divided into the experimental group (n = 10), which underwent RAP remodeling concomitant with LLVNS for 3 hours (Figure 2), and the control group (n = 10), which only underwent RAP remodeling for 3 hours. In the experimental group, LLVNS was delivered to bilateral cervical vagosympathetic nerves by applying HFS as described previously. The ERP and WOV were measured at LSPV, LIPV, LA, LAA, MSL, RSPV, RIPV, ARGPM, RA, and RAA at baseline levels and the end of every hour during the 3 hours pacing period.

2.5. Statistical Analysis. All values were expressed as the mean ± standard deviation of the mean. Paired t-test was used for comparisons of ERP and WOV of baseline levels and each pacing period. Analysis of variance (ANOVA) by SPSS20 was used to compare ERP, WOV, ERP dispersion, and RT in both groups, and graphs were drawn with Microsoft Excel2010. P values ≤0.05 were considered to indicate statistical significance.

3. Results

The systolic and diastolic blood pressures were stable during the entire experimental period, with no sign of heart failure throughout. Oxygen saturation was maintained at 95–100% during the experiments.

3.1. Effective Refractory Period. In the control group, the ERP at RSPV, RIPV, RA, RAA, ARGPM, LSPV, LIPV, LA, LAA, and MSL was markedly shortened in the second and third hour (Figure 3). The decrease in ERP at ARGPM,

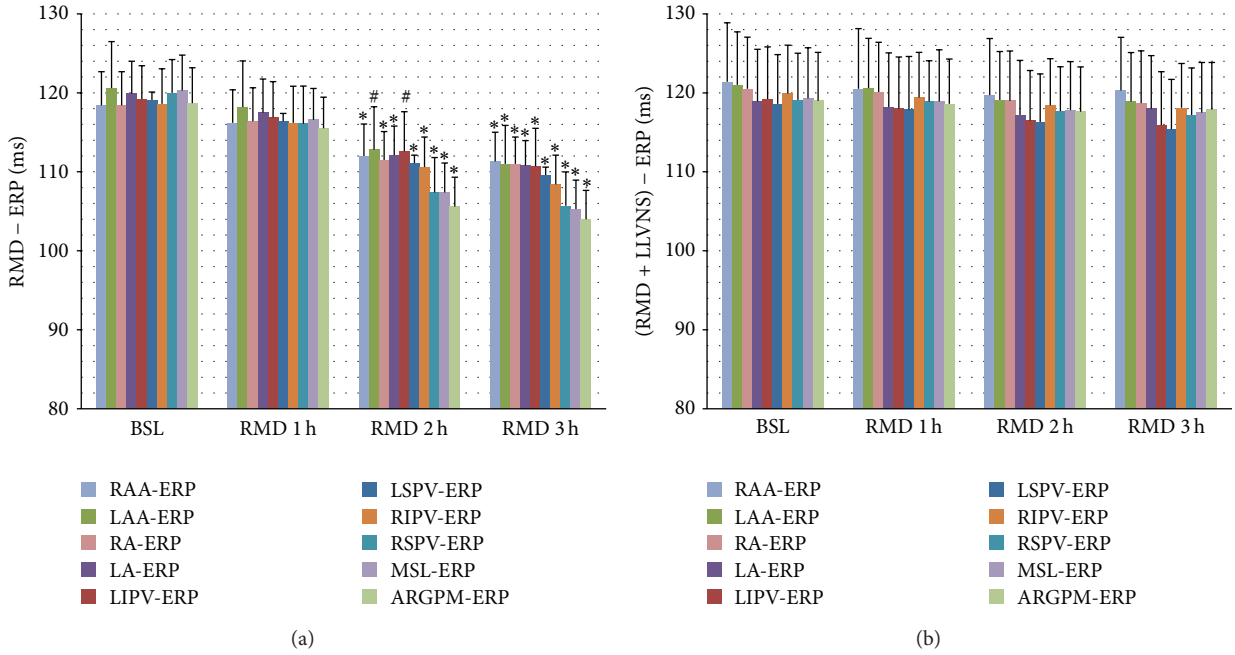

Figure 3: Effects of LLVNS on ERP and its gradient. LLVNS reversed the decrease in ERP and increase in ERP gradient that was induced by RAP. $^{\#}P < 0.05$ and $^{*}P < 0.01$ compared with baseline levels using the paired t-test. ERP: effective refractory period; BSL: baseline level; RMD: remodeling; LLVNS: Low-level vagosympathetic nerve stimulation.

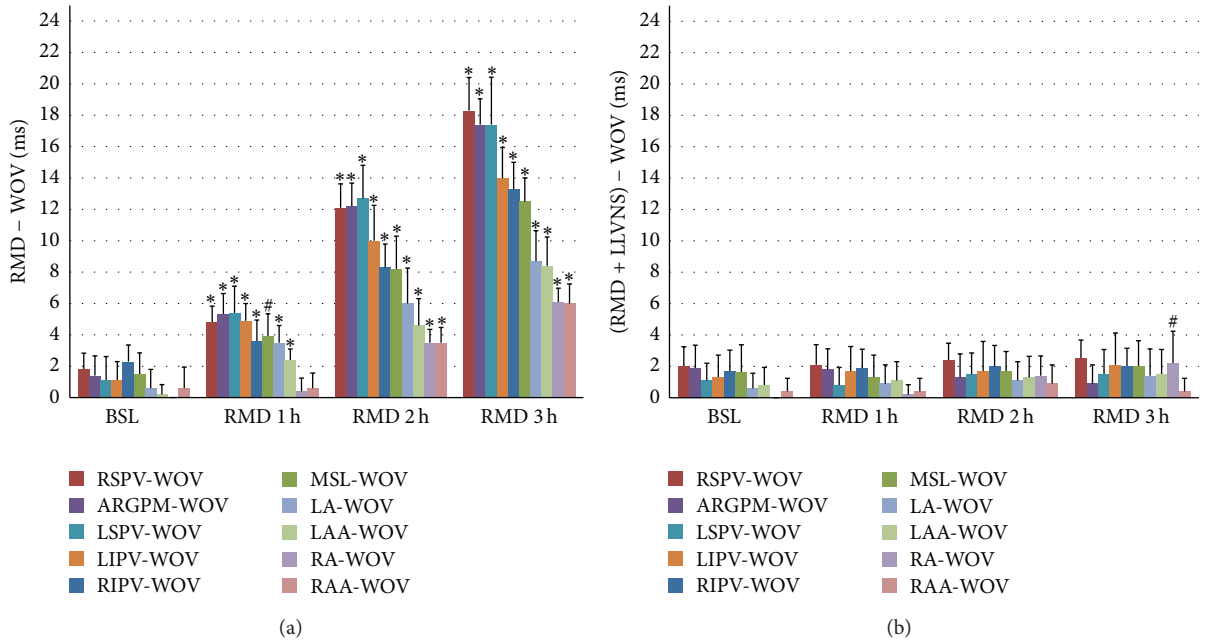

Figure 4: Effects of LLVNS on WOV and its gradient. LLVNS reversed the increase in WOV and its gradient caused by RAP. WOV: window of vulnerability; the remaining symbols and abbreviations are the same as those used in Figure 3.

MSL, RSPV, RIPV, and LSPV was more significant compared to other sites of the atrium. Moreover, there were apparent ERP gradients in the atrium at the second and third hour.

In contrast, in the experimental group, the ERP of each site of the atrium showed no significant variance at the end of each hour, compared to baseline levels. Moreover, ERP gradients were not observed at the end of each hour, as observed at the baseline.

3.2. Window of Vulnerability. In the control group, the WOV at each site of the atrium showed a significantly progressive increase during each hour of RAP (Figure 4). Moreover, a significant WOV gradient was observed in the atrium, and

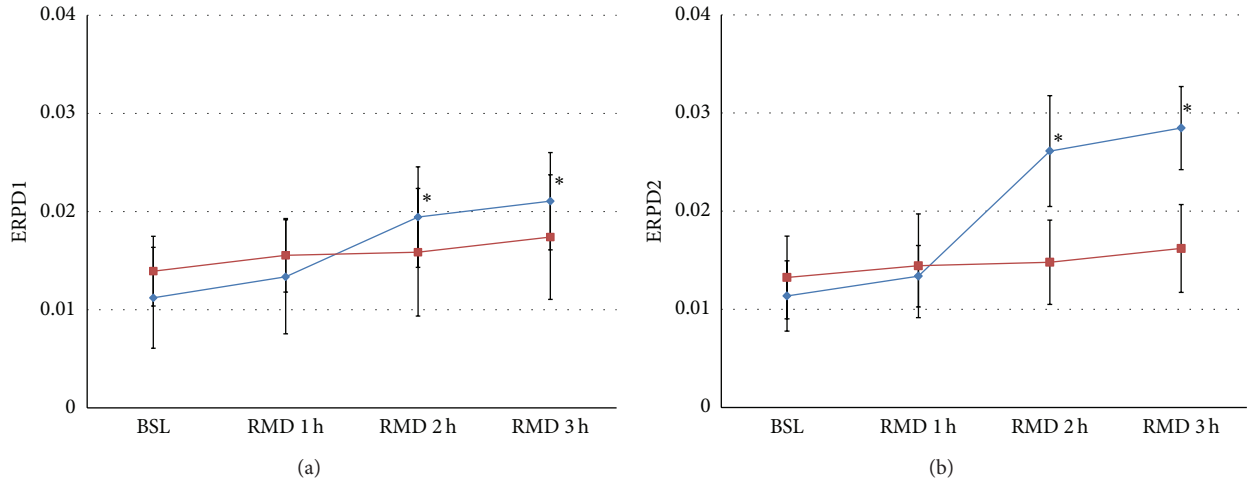

Figure 5: Effects of LLVNS on ERP dispersion. LLVNS reversed the effects of RAP on ERP dispersion. The blue (◇) and red (□) curves represent the control group and experimental group, respectively. The symbols and abbreviations are the same as those in Figure 3.

the WOV progressively increased across sites in the given order: RAA and RA, LAA, LA, MSL, RIPV, LIPV, LSPV, ARGPM, and RSPV.

In the experimental group, the WOV at each site of the atrium was not different between each period of RAP, except for RA at the third period ($P < 0.05$), compared to the baseline value; also, there was no significant WOV gradient at each site of the atrium.

3.3. Dispersion of the Effective Refractory Period. In the control group, ERPD1 and ERPD2 showed progressive increase and reached statistical significance in the second and third hour of RAP (Figure 5). In contrast, the experimental group showed no significant difference in ERPD1 and ERPD2 for each RAP period. Moreover, ERPD2 was more obviously enlarged than ERPD1 in the control group, but there was no significant difference between ERPD1 and ERPD2 in the experimental group during each period.

3.4. Recovery Time and Low-Level Voltage. The recovery time (RT) was represented as the duration from atrial arrhythmia that is facilitated by fast pacing triggers in atrium to sinus rhythm. In control group, RAP remodeling progressively increased RT (Figure 6). While RAP was persistent for 3 hours, the RT was obviously longer than that of baseline (5.078 ± 2.266 seconds versus 1.886 ± 1.059 seconds, $P < 0.01$). In experimental group, combining RAP with LLVNS for 3 hours, the RT at each period has no difference from that of baseline levels. During the judgments of threshold, the voltage at 0.5 V that slowed the sinus rate apparently can lead to atrial premature and then facilitate AF at baseline (Figure 7). The AF was persistent during the VNS. While the VNS was removed, AF still maintained (Figure 8). When RAP that is persistent for 3 hours concomitant with LLVNS (0.25 V) was stopped, the AF progressively terminated even though the LLVNS still continued (Figure 9). The low-level voltages for LLVNS that is 50% below the threshold that prolonged the A-A intervals of sinus rhythm by no more than

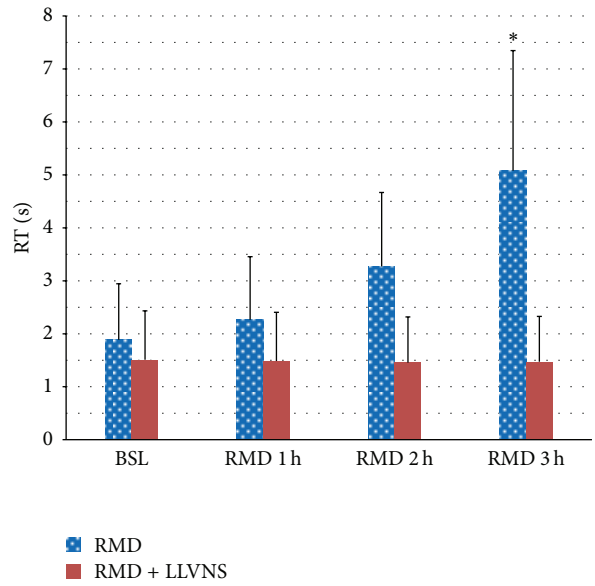

Figure 6: The effect of LLVNS on recovery time. The recovery time (RT) was represented as the duration from AF triggered by persistent S_1-S_1 stimulation to sinus rhythm. Abbreviations are the same as those in Figure 3.

30 msec had not changed, prior to the first, second, and third remodeling (Pre-RMD 1 h, 0.154 ± 0.058 V; Pre-RMD 2 h, 0.22 ± 0.071 V; Pre-RMD 3 h, 0.225 ± 0.115 V, $P > 0.05$).

4. Discussion

We have successfully proved our hypothesis about the benefits of LLVNS for treating AF. This is clear from the results, which show that application of LLVNS to canine models of RAP remodeling markedly reversed the decrease in ERP and increase in WOV at each site. Moreover, it abolished gradient differences in the electrophysiological substrate surrounding

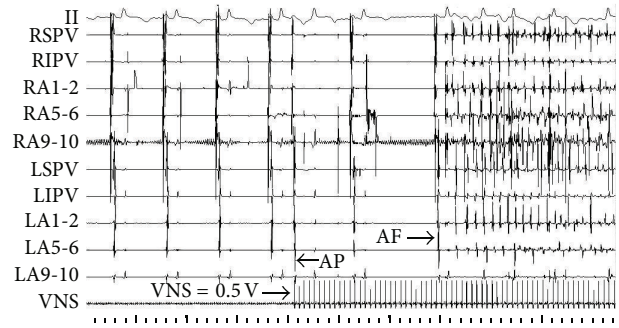

Figure 7: Vagosympathetic nerve stimulation (VNS) promoted atrial arrhythmia. VNS with the voltage at 0.5 V triggered atrial premature and then facilitated AF. AP: atrial premature. AF: atrial fibrillation.

GP and thus maintained ERP dispersion at baseline levels. It also reduced the RT from AF.

In our research, as we measured the threshold, the VNS with the voltage at 0.5 V triggered atrial premature and then facilitated AF at baseline. The AF was persistent during the VNS. While the VNS was removed, AF still maintained. These results suggest that vagosympathetic trunks as extrinsic components play an important role in the initiation and maintenance of AF. The arrhythmic effect of VNS may be mediated by activating the "integration centers of GP" [7, 15].

The hyperactivity of the autonomic element in MSL may contribute to the initiation of AF and even ventricular tachyarrhythmia [32]. It is reported that MSL participates in the interaction between integration centers and GP [15]. High-level stimulation of GP can progressively reduce atrial ERP, widen the WOV, and lead to gradient differences in ERP and WOV towards GP [14], and it is even associated with complex fractionated atrial potentials [33]. Similar to these reports, in our study too, RAP remodeling for 2-3 hours led to a significant decrease in ERP and caused an obvious decrease in the ERP gradient from the appendages towards PV, MSL, and ARGP, which serve as GP areas. Moreover, ERP dispersion progressively increased and reached a significant difference at the end of RAP, and when the ERP dispersion values for ARGP and MSL were added, ERP dispersion was further augmented. The WOV progressively increased during RAP, and it was noted that the increase in WOV at PV, MSL, and ARGP was more apparent, which caused an increase in the gradient difference from the non-GP area towards the GP sites. Based on all these results, we concluded that the ERP and WOV gradients were reflective of the electrophysiological substrate surrounding GP, since autonomic remodeling is characterized by hyperactive GP caused by RAP.

In the RAP remodeling, when electrical remodeling occurs concomitantly with autonomic remodeling, it is believed to indicate progressive enhancement of neural activity [34]; in this study, heterogeneous differences in both ERP and WOV were observed at atrial sites, especially around the GP, so it is possible that RAP resulted in obvious hyperactivity of GP and thus increased vulnerability to AF because of the increased heterogeneity of the substrate.

It has been reported that LLVNS that is 10–50% below the threshold voltage, required to slow the sinus rate or atrioventricular conduction, may prevent episodic AF caused by rapid PV and non-PV firing, due to a progressive increase in AF threshold at all PVs and atrial appendages sites, particularly RSPV, RIPV, LSPV, and RAA. Moreover, this type of antiarrhythmic effect is not dependent on the activation of the afferent vagal nerve fibers that project to the brain [28]. The activation of neural elements within the ARGP, SLGP, and stellate ganglion was attenuated by LLVNS application to both [28, 35] or one vagosympathetic trunk [26, 27], auricular branch of the vagus nerve of the right ear (low-level tragus stimulation) [36], or superior vena cava [34]. Therefore, the antiarrhythmic effect of LLVNS may be brought about via its action on GP sites. When the voltage of LLVNS was further reduced to 80% below the threshold, it still induced a similarly antiarrhythmic effect [36]. LLVNS at these values eliminated the spatial gradient of ERP and WOV induced by ARGP stimulation from the PV-atrial junction toward the atrial appendage [25]. Moreover, it could prevent and reverse atrial remodeling induced by RAP as well as suppress AF induced by strong cholinergic stimulation, for example, by injection of acetylcholine (10 mM) into the ARGP or RAA. The duration and cycle length of AF decreased obviously during LLVNS [35]. In contrast, stimulation of ARGP and SLGP for 6 hours with a voltage that causes a 10% decrease in sinus rate does not appear to have an antiarrhythmic effect [37]. In our study, we used LLVNS values at 50% below the threshold (which slowed the sinus rate by no more than 30 msec). We found that this reversed the electrical and autonomic remodeling, restoring ERP and WOV to baseline levels. LLVNS maintained the two kinds of ERP dispersion at baseline levels. Also, the ERP and WOV around ARGP, PV, and MSL were not significantly different from those in other areas. Thus, LLVNS resulted in substrate homogeneity. Thus, they are in agreement with previously published results. Based on our current study and previous studies, we think that hyperactivation of intrinsic nerves or "integration centers" was suppressed by LLVNS. It brought about this effect by abolishing gradient differences in the substrate surrounding GP, which contributed to the homogeneity of ERP and WOV in the atrium. More importantly, the duration of AF promoted by fast-pacing triggers at the end of each period was significantly decreased. During the process of RAP and LLVNS at the third period, when the RAP was removed, the AF induced by RAP recovered to sinus rhythm immediately, even though LLVNS was still continued.

Based on our results, the mechanism of action of LLVNS may be explained as follows: (1) suppression of the neural activity of GP, which abolishes gradient differences in the substrate surrounding GP and (2) enhanced recovery of the homogeneous substrate with baseline susceptibility to AF. In addition, there are other mechanisms that have been proposed by researchers: (3) decrease in transient intracellular Ca^{2+} levels, owing to reduced release of sympathetic neurotransmitters via inhibition of activity of the stellate ganglion [27, 38], (4) desensitization of autonomic receptors, such as β-adrenergic receptors [25, 39, 40], (5) increase

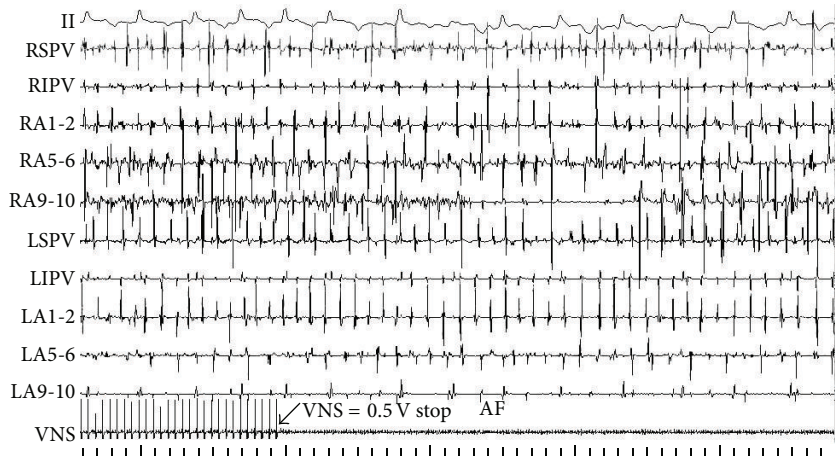

Figure 8: VNS maintained AF. The AF was persistent during VNS with the voltage at 0.5 V. While the VNS was removed, AF still maintained. AF: atrial fibrillation.

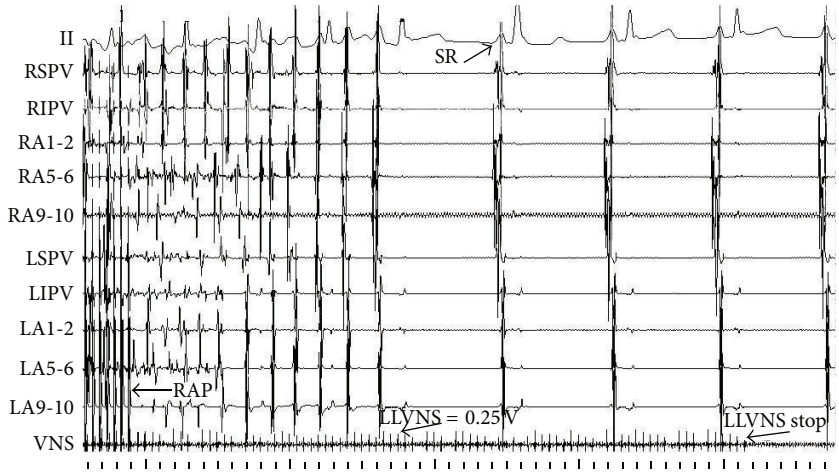

Figure 9: LLVNS cannot maintain the AF. When RAP that is persistent for 3 hours concomitant with LLVNS (0.25 V), was stopped, the AF progressively terminated even though the LLVNS still continued. RAP: rapid atrial pacing. SR: sinus rhythm.

in nitric oxide availability mediated by upregulation of the PI3K/NO signaling pathway [41], which subsequently leads to inhibition of GP function, (6) increase in the levels of neuropeptides or neurotransmitters inhibiting GP function, for instance the neuropeptide Y2 and vasostatin-1, which exert strong antiadrenergic and anticholinergic effects [41–43]. Future studies should be conducted to integrate and explain these mechanisms in relation to one another.

A limitation of this study is that we have no direct evidence indicating inhibition of neuronal firing within GP and MSL, and the results are therefore limited to short-term RAP and LLVNS. This hypothesis will have to be verified in the future by using RAP and LLVNS of longer duration. This will help evaluate the antiarrhythmic effects of LLVNS in chronic AF models. Moreover, research will be required to determine the optimal parameters and sites for LLVNS that will have the greatest degree of AF inhibition with minimal side effects. We hope to devise future treatment methods to treat chronic AF, in which autonomic nerve stimulators can be inserted using noninvasive methods.

5. Conclusions

LLVNS can reverse the electrical and autonomic remodeling induced by RAP. The mechanism involves abolishing gradient differences in the substrate surrounding GP and recovery of the homogeneous substrate.

Disclosure

The authors takes responsibility for all aspects of the reliability and freedom from bias of the data presented and their discussed interpretation.

Conflict of Interests

The authors declare that they have no conflict of interests.

Acknowledgments

The authors thank Professors Lianjun Gao, Yanzong Yang, Yunlong Xia, Shulong Zhang, and Dong Chang of the First

Hospital Affiliated to the Dalian Medical University for their assistance. They thank Jingjiang Electronic Science and Technology Company, Inc. (Chengdu, China) and APT Medical Company, Inc. (Shenzhen, China) for providing the electrophysiological catheters and technical assistance. This work was supported by Grants from the Fundamental Research Funds for Central Universities (no. 21611333), the Science and Technological Program of Guangdong Province (no. 2010-1096-136; 2011B031800336), the Science and Technological Projects of Guangzhou (no. 2010Y1-C941), and the Key Disciplines' Funds and Special Research Funds (no. 2012207) of the First Clinical Medical College of Jinan University, Basic Research Expenses of Jinan University.

References

[1] T. Watson, E. Shantsila, and G. Y. Lip, "Mechanisms of thrombogenesis in atrial fibrillation: virchow's triad revisited," *The Lancet*, vol. 373, no. 9658, pp. 155–166, 2009.

[2] C. Steger, A. Pratter, M. Martinek-Bregel et al., "Stroke patients with atrial fibrillation have a worse prognosis than patients without: data from the Austrian Stroke registry," *European Heart Journal*, vol. 25, no. 19, pp. 1734–1740, 2004.

[3] C. Ma and W. Qi, "Management of atrial fibrillation in Chinese patients," *CVD Prevention and Control*, vol. 4, no. 1, pp. 79–83, 2009.

[4] J. A. Armour, "Cardiac neuronal hierarchy in health and disease," *American Journal of Physiology*, vol. 287, no. 2, pp. R262–R271, 2004.

[5] J. A. Armour, "Functional anatomy of intrathoracic neurons innervating the atria and ventricles," *Heart Rhythm*, vol. 7, no. 7, pp. 994–996, 2010.

[6] C.-W. Chiou, J. N. Eble, and D. P. Zipes, "Efferent vagal innervation of the canine atria and sinus and atrioventricular nodes: the third fat pad," *Circulation*, vol. 95, no. 11, pp. 2573–2584, 1997.

[7] Y. Hou, B. J. Scherlag, J. Lin et al., "Ganglionated plexi modulate extrinsic cardiac autonomic nerve input. effects on sinus rate, atrioventricular conduction, refractoriness, and inducibility of atrial fibrillation," *Journal of the American College of Cardiology*, vol. 50, no. 1, pp. 61–68, 2007.

[8] J. A. Armour, D. A. Murphy, B. X. Yuan, S. Macdonald, and D. A. Hopkins, "Gross and microscopic anatomy of the human intrinsic cardiac nervous system," *The Anatomical Record*, vol. 247, no. 2, pp. 289–298, 1997.

[9] B.-X. Yuan, J. L. Ardell, D. A. Hopkins, A. M. Losier, and J. A. Armour, "Gross and microscopic anatomy of the canine intrinsic cardiac nervous system," *The Anatomical Record*, vol. 239, no. 1, pp. 75–87, 1994.

[10] D. H. Pauza, V. Skripka, and N. Pauziene, "Morphology of the intrinsic cardiac nervous system in the dog: a whole-mount study employing histochemical staining with acetylcholinesterase," *Cells Tissues Organs*, vol. 172, no. 4, pp. 297–320, 2002.

[11] Z. Lu, B. J. Scherlag, J. Lin et al., "Autonomic mechanism for initiation of rapid firing from atria and pulmonary veins: evidence by ablation of ganglionated plexi," *Cardiovascular Research*, vol. 84, no. 2, pp. 245–252, 2009.

[12] B. J. Scherlag, W. Yamanashi, U. Patel, R. Lazzara, and W. M. Jackman, "Autonomically induced conversion of pulmonary vein focal firing into atrial fibrillation," *Journal of the American College of Cardiology*, vol. 45, no. 11, pp. 1878–1886, 2005.

[13] P. B. Lim, L. C. Malcolme-Lawes, T. Stuber et al., "Intrinsic cardiac autonomic stimulation induces pulmonary vein ectopy and triggers atrial fibrillation in humans," *Journal of Cardiovascular Electrophysiology*, vol. 22, no. 6, pp. 638–646, 2011.

[14] J. Zhou, B. J. Scherlag, J. Edwards, W. M. Jackman, R. Lazzara, and S. S. Po, "Gradients of atrial refractoriness and inducibility of atrial fibrillation due to stimulation of ganglionated plexi," *Journal of Cardiovascular Electrophysiology*, vol. 18, no. 1, pp. 83–90, 2007.

[15] J. Lin, B. J. Scherlag, G. Niu et al., "Autonomic elements within the ligament of marshall and inferior left ganglionated plexus mediate functions of the atrial neural network," *Journal of Cardiovascular Electrophysiology*, vol. 20, no. 3, pp. 318–324, 2009.

[16] K. Lemola, D. Chartier, Y.-H. Yeh et al., "Pulmonary vein region ablation in experimental vagal atrial fibrillation : role of pulmonary veins versus autonomic ganglia," *Circulation*, vol. 117, no. 4, pp. 470–477, 2008.

[17] C. Pappone, V. Santinelli, F. Manguso et al., "Pulmonary vein denervation enhances long-term benefit after circumferential ablation for paroxysmal atrial fibrillation," *Circulation*, vol. 109, no. 3, pp. 327–334, 2004.

[18] Z. Lu, B. J. Scherlag, J. Lin et al., "Autonomic mechanism for complex fractionated atrial electrograms: evidence by fast Fourier transform analysis," *Journal of Cardiovascular Electrophysiology*, vol. 19, no. 8, pp. 835–842, 2008.

[19] J. P. Piccini, R. D. Lopes, M. H. Kong, V. Hasselblad, K. Jackson, and S. M. Al-Khatib, "Pulmonary vein isolation for the maintenance of sinus rhythm in patients with atrial fibrillation a meta-analysis of randomized, controlled trials," *Circulation: Arrhythmia and Electrophysiology*, vol. 2, no. 6, pp. 626–633, 2009.

[20] S. Oh, Y. Zhang, S. Bibevski, N. F. Marrouche, A. Natale, and T. N. Mazgalev, "Vagal denervation and atrial fibrillation inducibility: epicardial fat pad ablation does not have long-term effects," *Heart Rhythm*, vol. 3, no. 6, pp. 701–708, 2006.

[21] Q. Y. Zhao, H. Huang, S. D. Zhang et al., "Atrial autonomic innervation remodelling and atrial fibrillation inducibility after epicardial ganglionic plexi ablation," *Europace*, vol. 12, no. 6, pp. 805–810, 2010.

[22] P. Schauerte, B. J. Scherlag, J. Pitha et al., "Catheter ablation of cardiac autonomic nerves for prevention of vagal atrial fibrillation," *Circulation*, vol. 102, no. 22, pp. 2774–2780, 2000.

[23] Y. Zhang, I. Ilsar, H. N. Sabbah, T. Ben David, and T. N. Mazgalev, "Relationship between right cervical vagus nerve stimulation and atrial fibrillation inducibility: therapeutic intensities do not increase arrhythmogenesis," *Heart Rhythm*, vol. 6, no. 2, pp. 244–250, 2009.

[24] R. Nadeau, R. Cardinal, J. A. Armour et al., "Cervical vagosympathetic and mediastinal nerves activation effects on atrial arrhythmia formation," *Anadolu Kardiyoloji Dergisi*, vol. 7, no. 1, pp. 34–36, 2007.

[25] L. Yu, B. J. Scherlag, S. Li et al., "Low-level vagosympathetic nerve stimulation inhibits atrial fibrillation inducibility: direct evidence by neural recordings from intrinsic cardiac ganglia," *Journal of Cardiovascular Electrophysiology*, vol. 22, no. 4, pp. 455–463, 2011.

[26] Y. Sha, B. J. Scherlag, L. Yu et al., "Low-level right vagal stimulation: anticholinergic and antiadrenergic effects," *Journal of Cardiovascular Electrophysiology*, vol. 22, no. 10, pp. 1147–1153, 2011.

[27] M. J. Shen, T. Shinohara, H.-W. Park et al., "Continuous low-level vagus nerve stimulation reduces stellate ganglion nerve activity and paroxysmal atrial tachyarrhythmias in ambulatory canines," *Circulation*, vol. 123, no. 20, pp. 2204–2212, 2011.

[28] S. Li, B. J. Scherlag, L. Yu et al., "Low-level vagosympathetic stimulation a paradox and potential new modality for the treatment of focal atrial fibrillation," *Circulation: Arrhythmia and Electrophysiology*, vol. 2, no. 6, pp. 645–651, 2009.

[29] D. T. Kim, A. C. Lai, C. Hwang et al., "The ligament of Marshall: a structural analysis in human hearts with implications for atrial arrhythmias," *Journal of the American College of Cardiology*, vol. 36, no. 4, pp. 1324–1327, 2000.

[30] Z. Lu, B. J. Scherlag, J. Lin et al., "Atrial fibrillation begets atrial fibrillation: autonomic mechanism for atrial electrical remodeling induced by short-term rapid atrial pacing," *Circulation: Arrhythmia and Electrophysiology*, vol. 1, no. 3, pp. 184–192, 2008.

[31] D. Chang, S. Zhang, D. Yang et al., "Effect of epicardial fat pad ablation on acute atrial electrical remodeling and inducibility of atrial fibrillation," *Circulation Journal*, vol. 74, no. 5, pp. 885–894, 2010.

[32] J. Lin, B. J. Scherlag, Z. Lu et al., "Inducibility of atrial and ventricular arrhythmias along the ligament of marshall: role of autonomic factors," *Journal of Cardiovascular Electrophysiology*, vol. 19, no. 9, pp. 955–962, 2008.

[33] J. Lin, B. J. Scherlag, J. Zhou et al., "Autonomic mechanism to explain complex fractionated atrial electrograms (CFAE)," *Journal of Cardiovascular Electrophysiology*, vol. 18, no. 11, pp. 1197–1205, 2007.

[34] L. Yu, B. J. Scherlag, Y. Sha et al., "Interactions between atrial electrical remodeling and autonomic remodeling: how to break the vicious cycle," *Heart Rhythm*, vol. 9, no. 5, pp. 804–809, 2012.

[35] X. Sheng, B. J. Scherlag, L. Yu et al., "Prevention and reversal of atrial fibrillation inducibility and autonomic remodeling by low-level vagosympathetic nerve stimulation," *Journal of the American College of Cardiology*, vol. 57, no. 5, pp. 563–571, 2011.

[36] L. Yu, B. J. Scherlag, S. Li et al., "Low-level transcutaneous electrical stimulation of the auricular branch of the vagus nerve: a noninvasive approach to treat the initial phase of atrial fibrillation," *Heart Rhythm*, vol. 10, no. 3, pp. 428–435.

[37] L. Wu, Z. Lu, H. Jiang et al., "Low-level ganglionated plexus stimulation facilitates atrial fibrillation: in vivo and in vitro studies," *Autonomic Neuroscience: Basic and Clinical*, vol. 168, no. 1-2, pp. 58–65, 2012.

[38] E. Patterson, S. S. Po, B. J. Scherlag, and R. Lazzara, "Triggered firing in pulmonary veins initiated by in vitro autonomic nerve stimulation," *Heart Rhythm*, vol. 2, no. 6, pp. 624–631, 2005.

[39] T. Iwao, M. Ito, N. Takahashi, T. Saikawa, and T. Sakata, "Sustained left ansae subclaviae stimulation for a 5-hour period inhibits cesium-induced ventricular arrhythmogenesis in rabbits," *Journal of Molecular and Cellular Cardiology*, vol. 30, no. 11, pp. 2237–2245, 1998.

[40] E. Patterson, X. Yu, S. Huang, M. Garrett, and D. C. Kem, "Suppression of autonomic-mediated triggered firing in pulmonary vein preparations, 24 hours postcoronary artery ligation in dogs," *Journal of Cardiovascular Electrophysiology*, vol. 17, no. 7, pp. 763–770, 2006.

[41] S. Stavrakis, B. J. Scherlag, Y. Fan et al., "Inhibition of atrial fibrillation by low-level vagus nerve stimulation: the role of the nitric oxide signaling pathway," *Journal of Interventional Cardiac Electrophysiology*, vol. 36, no. 3, pp. 199–208, 2012.

[42] A. Ilebekk, J.-A. Björkman, and M. Nordlander, "Influence of endogenous neuropeptide Y (NPY) on the sympathetic-parasympathetic interaction in the canine heart," *Journal of Cardiovascular Pharmacology*, vol. 46, no. 4, pp. 474–480, 2005.

[43] B. Tota, A. M. Quintieri, V. Di Felice, and M. C. Cerra, "New biological aspects of chromogranin A-derived peptides: focus on vasostatins," *Comparative Biochemistry and Physiology Part A*, vol. 147, no. 1, pp. 11–18, 2007.

Hindawi Publishing Corporation
The Scientific World Journal
Volume 2013, Article ID 373454, 6 pages
http://dx.doi.org/10.1155/2013/373454

Clinical Study

Polymorphisms but Not Mutations of the *KCNQ1* Gene Are Associated with Lone Atrial Fibrillation in the Chinese Han Population

Hui-min Chu,[1] Ming-jun Feng,[1] Yi-gang Li,[2] Yi-xin Zhang,[3] Ji-fang Ma,[2] Bin He,[1] Yi-bo Yu,[1] Jing Liu,[1] and Xiao-min Chen[1]

[1] *Department of Cardiology, Ningbo No. 1 Hospital Affiliated to Medical College of Ningbo University, 59 Liuting Street, Haishu District, Ningbo 315211, China*
[2] *Department of Cardiology, Xinhua Hospital Affiliated to Shanghai Jiaotong University School of Medicine, 227 Chongqing Southern Road, Shanghai 200092, China*
[3] *Department of Human Population Genetics, Institute of Molecular Medicine, Peking University, 5 Yiheyuan Road, Beijing 100871, China*

Correspondence should be addressed to Xiao-min Chen; markchu@126.com

Received 10 January 2013; Accepted 18 March 2013

Academic Editors: Y. Du and Y. Wang

Background. Recent studies suggest that mutation of the slow delayed rectifier potassium channel (IKs) contributes to familial atrial fibrillation (FAF). In the current study, we identified common genetic variants of *KCNQ1* and explored the potential association between *KCNQ1* polymorphism with lone AF (LAF). *Methods*. Clinical data and blood samples were collected from 190 Han Chinese patients with sporadic AF and matched healthy controls. Variants of the *KCNQ1* gene were identified using single-strand conformational polymorphism (SSCP) analysis. A case-control association study in *KCNQ1* identified six known single-nucleotide polymorphisms (SNPs) during SSCP screening of the 190 LAF patients and 190 healthy controls. *Results*. One of the SNPs in *KCNQ1* was strongly associated with LAF; significant allelic association was detected rs59233444 ($P = 0.013$, OR = 1.469, 95% confidence interval (CI): 1.083–1.993). A multiple regression analysis indicated that rs59233444 is an independent risk factor for LAF. Twelve new variants were identified in *KCNQ1*, including one in the 5′-UTR, two in the 3′-UTR, six in introns, two synonymous substitutions, and one missense substitution. Variants c.1009C>T, c.1860C>T, and c.+2285C>T were not present in the 190 controls, and the others were identified in controls at various frequencies. *Conclusions*. rs59233444, a common SNP but not mutation in the coding regions of the *KCNQ1* gene, is a risk factor for LAF in Chinese Han population.

1. Background

Atrial fibrillation (AF), a common type of cardiac arrhythmia, is a major risk factor for stroke, heart failure, and other cardiovascular morbidities [1, 2]. In 15%–30% of the AF patients, no underlying heart disease could be identified; these cases are referred to as lone AF (LAF). In about 5% of the cases, family history could be clearly established; these are known as familial AF (FAF). Genetic defect was first reported in Chinese kindred in 2003 [3]. A mutation (S140G) was found in the first transmembrane spanning domain of the cardiac slow delayed rectifier potassium channel (IKs), encoded by the *KCNQ1* gene [4]. Functional analysis of the mutation revealed a "gain-of-function" effect on both KCNQ1-KCNE1 and KCNQ1-KCNE2 ion channels. Since then, "gain-of-function" mutations in other genes encoding potassium ion channels have been found to be associated with FAF, including *KCNE2* [5], *KCNE3* [6], *KCNA5* [7], and *KCNJ2* [8]. Q147R [9], R231C [10], and S209P [11] mutations of the *KCNQ1* gene were also reported.

Interestingly, the gain-of-function mutation of KCNE5 is also linked to LAF [12]. The *KCNE5* gene product MiRP4 suppresses the IKs current and downregulates the β-subunit of the KCNQ1. The mutant KCNE5 L65F fails to suppress

IKs, yielding a current indistinguishable from that recorded in the absence of KCNE5. There is evidence of a heritable contribution to LAF, where a polymorphism (S38G) in Mink (KCNE1) was associated with nonfamilial AF [13] (the sporadic LAF). These results indicate that a polymorphism (S38G) and a mutation (S140G) in different genes (*KCNE1* and *KCNQ1*, resp.) encoding different subunits of the same ionic channel (IKs) may be responsible for the development of nonfamilial and familial AF. These results also suggest that familial and nonfamilial AF (sporadic LAF) may share a common pathological mechanism and provide justification to test *KCNQ1* as a candidate gene for LAF.

In the current study, we compared *KCNQ1* variants in 190 Chinese Han patients with LAF and 190 healthy controls. We also performed a case-control association study for several common SNPs in *KCNQ1*.

2. Methods

2.1. Study Subjects. Consecutive patients with LAF referred to the cardiology department of Ningbo No. 1 Hospital and Shanghai Xinhua Hospital from June 1, 2007 to September 27, 2009 were enrolled. AF was defined as replacement of the sinus P waves by rapid oscillations of fibrillation waves that varied in size, shape, and timing and were associated with an irregular ventricular response when atrioventricular conduction was intact. LAF was defined as AF occurring in patients <60 years of age without identifiable causes, including hypertension, overt structural heart disease, or thyroid dysfunction. FAF was defined as the presence of LAF in one or more first-degree relative of the indexed case. Each patient underwent a physical examination and a standardized interview to identify past medical conditions, medications, symptoms, family history, and possible triggers for the initiation of AF. All patients were evaluated by 12-lead electrocardiogram (ECG), echocardiogram, and laboratory studies.

Normal control individuals were selected from a cross-sectional, population-based cohort of 190 individuals from Chinese Han people in Southern China. Each subject underwent a comprehensive medical evaluation consisting of a medical history, a physical examination, echocardiography, and electrocardiography. We selected age-, gender-, and ethnicity-matched controls for our study from this population cohort. Control subjects did not have a history of or clinical evidence for AF or any structural disease. Genomic DNA was isolated from peripheral blood leukocytes using standard protocols with the Wizard Genomic DNA Purification Kit (Agilent). This study was approved by the Institution of Ningbo Medical Societies, and all patients gave written informed consent.

2.2. Mutation Analysis by SSCP and DNA Sequencing. Exons and exon-intron boundaries of the *KCNQ1* gene were amplified by PCR using standard conditions with primers designed from the published *KCNQ1* sequences in the NCBI database (Accession number: NG_008935.1). PCR was performed in a 25 μL volume containing 200 pmol of each primer, 10 ng of genomic DNA, 2.5 μL of 10 × PCR buffer with 1.5 mmol $MgCl_2$, 100 μmol deoxynucleotide triphosphates, and 1 unit of Taq DNA polymerase (Solarbio).

Amplified samples were diluted twofold with 6 μL of formamide buffer (90% formamide, 1 mmol EDTA, 0.2% bromophenol blue, and 0.1% xylene cyanol). The mixture was denatured at 96°C for 3 minutes, then cooled rapidly on ice, and held for 5 minutes. For each sample, 7 μL was loaded onto 10% nondenaturing polyacrylamide gels (acrylamide to bisacrylamide ratio = 40 : 10) and electrophoresed at 80 V for one half hour to two hours at room temperature. The gel was stained with 0.1% silver nitrate and visualized with a 2% NaOH solution (containing 0.1% formaldehyde). Aberrant conformers were directly sequenced with ABI 3130XL instruments (Applied Biosystem), and the sequence was analyzed with Sequence Scanner Software (Version 1.0).

2.3. SNP Genotyping. Subsequently, a case-control association study was performed with known SNPs, which were identified from mutation screening. Six SNPs (rs59233444, rs1057128, rs163150, rs760419, rs163160, and rs2075870) were genotyped using direct DNA sequencing (ABI 3130XL, Applied Biosystems). The PCR products were sequenced using forward and/or reverse PCR primers.

2.4. Statistical Analysis. Hardy-Weinberg equilibrium calculations were applied to analyze the distribution of genotypes. A χ^2 test was used to compare allele and genotype frequencies between the cases and controls and to obtain odds ratios (ORs) with 95% confidence intervals (CIs). The SPSS statistical software (Version 18.0) was used for analyzing LD, and haplotypes were calculated using the Haploview software package. Statistical differences were judged significant at $P < 0.05$. The multivariate logistic analysis included age, gender, diabetes, drinking, and smoking habits as covariates.

3. Results

3.1. Characteristics of the Study Population. A total of 190 patients with LAF and 190 controls were enrolled for the study. Among the 190 patients with LAF, 3 had at least one first-degree relative with AF. The clinical characteristics of these 190 patients are summarized in Table 1. No significant differences were seen between the case patients and control subjects with regard to age, sex, diabetes, smoking and drinking habits, left ventricle ejection fraction, left ventricular end-diastolic diameter, and left ventricular end-systolic diameter. However, the left atrial dimension in the case patient cohort is larger than that in the control cohort (38.8 ± 6.6 mm versus 35.4 ± 4.8, $P < 0.01$). All subjects in our study were of Han ethnic origin.

3.2. Identification of Variants in LAF. To identify mutations or rare polymorphisms associated with AF, all exons and exon-intron boundaries of *KCNQ1* were screened by SSCP analysis. PCR products of aberrant conformers were directly sequenced to identify polymorphisms. A representative portion of the aberrant conformers found in LAF by SSCP

Table 1: Clinical characteristics of the study population.

	Case (n = 190)	Control (n = 190)	P
Age[a] (years, mean ± SD)	55.4 ± 6.3	55.2 ± 7.6	0.211
Gender (female, n (%))	68 (35.8%)	71 (37.4)	0.831
Diabetes[b] (n (%))	8 (4.2%)	10 (5.3%)	0.810
Smoking habit (n (%))	60 (31.6%)	54 (28.4%)	0.576
Drinking habit (n (%))	55 (33.7%)	43 (22.6%)	0.197
Family history	3 (1.6%)	NA	NA
Left atrial dimension (mm)	38.8 ± 6.6	35.4 ± 4.8	<0.01
Left ventricle ejection fraction (%)	64.8 ± 8.9	66.1 ± 9.1	0.215
LVEDD (mm)	48.9 ± 4.9	48.9 ± 7.2	0.542
LVESD (mm)	31.3 ± 4.2	31.1 ± 5.6	0.253

NA: data not available.
[a]Age was defined as the age at the sample collection.
[b]Diabetes was defined as ongoing therapy of diabetes or a fasting plasma glucose level of ≥7.0 mmol.

and DNA sequencing is shown in Figure 1. A total of 12 variants were identified by our analysis (Table 2). One variant at the 5′-UTR, c.−22T>C, was detected in 2 patients and 1 control, indicating that this variant is a rare polymorphism. Six variants were found in the exon-intron boundaries, including c.511-19_511 18delTG, c.1128+3G>A, c.1590+31A>T, c.1684+23G>A, c.1685−43G>A, and c.1795−18C>T. We analyzed these six intronic variants with Human Splicing Finder (version 2.4.1) and found that they were unlikely to affect a splicing site. Three variants were identified in the coding region of *KCNQ1*, including two synonymous mutations, c.1009C>T and c.1860C>T, that were only detected in three total patients and were not found in the controls, suggesting that they are potentially mutations. The other missense change was identified in exon16, c.1945G>A, and results in a D to N substitution at amino acid 649. This appears to be a polymorphism that is not associated with LAF, because it was present in four of the cases and five of the controls. Two variants were identified in the 3′-UTR, one of which, c.+2285C>T, was found in one patient out of 190 cases and in none of the 190 controls. The other variant, c.+2976G>A, was found in five of 190 LAF patients and in three of the 190 controls. We analyzed these two variants with Patrocles Finder (http://www.patrocles.org/) and did not find evidence of microRNA binding; therefore, they are likely rare nonfunctional polymorphisms. In addition to the 12 novel variants that we reported above, we found 12 known polymorphisms with different frequencies in the cohort of 190 LAF patients (Table 3).

3.3. Association of SNPs in KCNQ1 with LAF. Mutation analysis of all translated *KCNQ1* exons in 190 LAF patients did not reveal a single mutation that clearly altered the splice junction or changed amino acid polarity. Therefore, we focused on six previously characterized SNPs that we identified in our cohort from gene mutation sequencing. Genotyping for six SNPs was done through direct DNA sequencing of rs59233444, rs1057128, rs163150, rs760419, rs163160, and rs2075870. The genotypic frequencies of the six SNPs in the controls were not significantly different from Hardy-Weinberg equilibrium. One of the six SNPs was associated with LAF in the additive and dominant genetic patterns (Table 4). For rs59233444, the genotype distribution is significantly different between (—/—, GG—, GG/GG) LAF patients and controls (49.5, 44.2, and 6.3% versus 34.7, 56.8, and 8.5%, $P = 0.014$). An allelic association with LAF was found by both [2] analysis and a regression test (Table 5). The GG minor allele frequency was 36.8% in the LAF group, compared with 28.4% in the normal controls (OR 1.469, 95% CI: 1.083–1.993, $P = 0.013$), and the A minor allele frequency was 23.4% in the LAF patients, compared with 16.3% in the normal controls (OR 1.885, 95% CI: 1.328–2.676, $P < 0.01$) (Table 6).

In this study, we found rs59233444 were the risk factors for LAF. Moreover, we analyzed all confounding factors for LAF including sex, age, smoking, drinking and hypertension using multiple regression analysis. We found that rs59233444 was the independent risk factor for LAF excluding other risk factors (Table 7). We performed a linkage disequilibrium test and demonstrated a low LD for rs59233444 ($D' = 0.342$) (data not shown).

4. Discussion

KCNQ1 (KVLOT1) channel subunits coassemble with KCNE1 (Mink) subunits to form channels that conduct the slow delayed rectifier K^+ current, IK_s in the heart which is important for normal termination of the plateau phase, and repolarization of atrial and ventricular action potentials. Mutations in *KCNQ1* were first identified as being the molecular basis of autosomal dominant atrial fibrillation in a single family from China in 2003 [3]. Subsequent studies have implicated potassium ion channel mutations in the pathogenesis of AF [3, 5–8, 10–12]. Although the study of rare familial forms of atrial fibrillation provides insight into the molecular pathways involved in selective cases of the disease, these genetic defects may not be representative of the pathogenesis in the more common, nonfamilial forms found in sporadic AF patients. Therefore, we focused on whether the *KCNQ1* gene was associated with LAF and screened for *KCNQ1* mutations in a cohort of 190 unrelated individuals with LAF.

Despite a plausible rationale for *KCNQ1* as a candidate gene for LAF, we did not identify any *KCNQ1* mutations in our cohort of 190 patients with sporadic LAF. There are several possible explanations for this. First, although AF has an inheritance tendency recognized by many studies, most of the gene mutations found in AF are those that are associated with a family history [3, 6–8, 10–12, 14–18]. Patients with sporadic AF are more likely to be associated with functional polymorphisms rather than mutations [19–23]. Second, AF is a genetically heterogeneous disorder, so a large sample is generally required to sufficiently screen for *KCNQ1* mutations that cause LAF. Finally, certain types of *KCNQ1* mutations would be missed by our SSCP methodology owing to this

Table 2: List of all *KCNQ1* variants identified in the present study.

Variation	Amino acid change	Frequency in patients	Conserved	Frequency in controls
c.−22T>C	—	2/190	No	1/190
c.51119_51118delTG	—	2/190	No	3/190
c.1009C>T	A336A	1/190	Yes	0/190
c.1128+3G>A	—	2/190	No	1/190
c.1590+31A>T	—	5/190	No	3/190
c.1684+23G>A	—	2/190	No	3/190
c.1685−43G>A	—	1/190	No	2/190
c.1795−18C>T	—	3/190	No	2/190
c.1860C>T	H620H	2/190	Yes	0/190
c.1945G>A	D649N	4/190	No	5/190
c.+2285C>T	—	1/190	Yes	0/190
c.+2976G>A	—	5/190	No	3/190

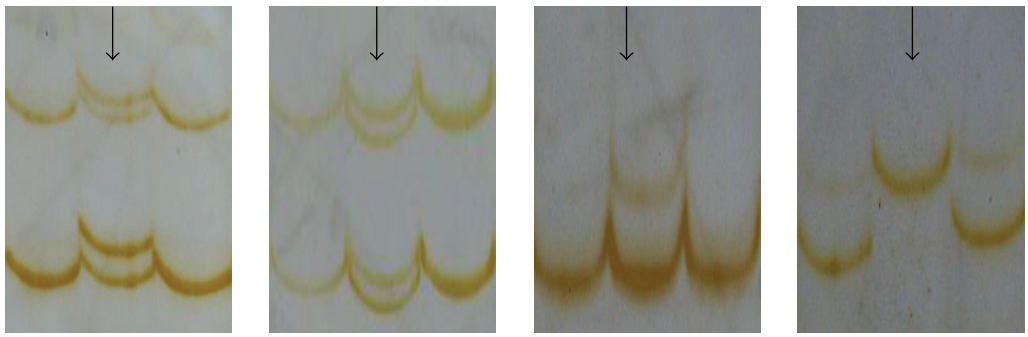

(a)

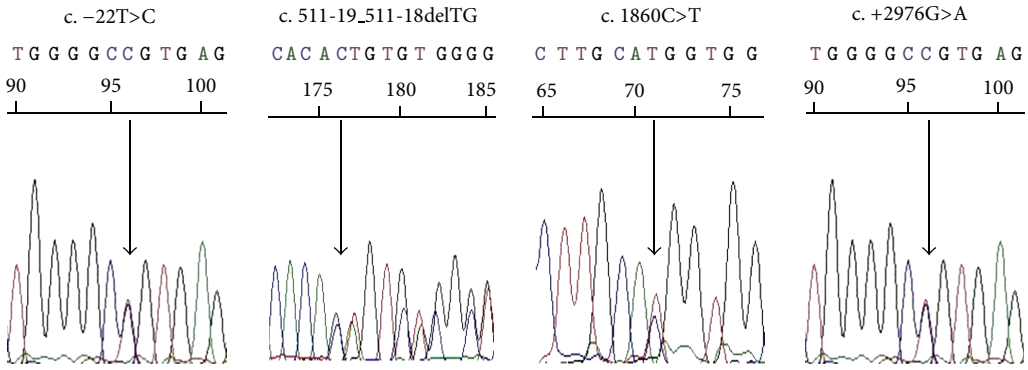

(b)

Figure 1: A representative image of an aberrant single-strand conformation found in the LAF using the single-strand conformation polymorphism (SSCP) procedure (a) and confirmed with direct DNA sequencing (b).

method's <100% sensitivity. Despite these limitations, our results are consistent with other published results [24].

In addition to the 12 variants in *KCNQ1* that we identified in LAF cases, we uncovered 12 known SNPs from LAF groups at different frequencies. After initial comparison of each of the 12 SNP frequencies that we obtained from the case group with the Han Chinese population in HapMap, six of twelve SNPs were targeted for the case-control association study. Finally, one of the six SNPs was determined to be associated with LAF which located in the *KCNQ1* intron2. The GG minor allele conferred an odds ratio (OR) for developing LAF of 1.469 (95% CI: 1.083–1.993, $P = 0.013$), and the A minor allele conferred a higher OR of 1.885 (95% CI: 1.328–2.676, $P < 0.01$). After correcting for the confounding factors, rs59233444 was found to be a risk factor for LAF. Given the incidence of AF, it would be of importance to determine the functional relevance of the one SNP. It is formally possible that the association described here is attributable to LD

Table 3: Twelve known polymorphisms found in LAF patients.

SNPs	Regions	Minor allele	Amino acid change	Han Chinese MAF
rs1800170	Exon2	T	I145I	0.091
rs59233444	Intron2	GG	—	N.A
rs12786951	Intron6	G	—	0.489
rs12577654	Intron12	T	—	0.057
rs760419	Intron12	G	—	0.318
rs163160	Intron12	G	—	0.244
rs2075870	Intron12	A	—	0.170
rs1057128	Exon13	A	S546S	0.289
rs163150	Intron14	A	—	0.289
rs2519184	3′-UTR	A	—	0.034
rs45510192	3′-UTR	A	—	N.A
rs394656	3′-UTR	C	—	N.A

MAF (minor allele frequency) of Han Chinese is based on HapMap Data; N.A: not available from HapMap Data for Han Chinese population.

Table 4: Genotypic association of one SNP in *KCNQ1* with LAF in the Han Chinese population.

SNP	Model	*P*	OR (95% CI)
rs59233444	Add	0.014	1.579 (1.128–2.210)
	Rec	0.432	1.364 (0.627–2.967)
	Dom	0.004	1.840 (1.218–2.779)

Add: additive model; Rec: recessive model; Dom: dominant model; *P*: *P* value from logistic regression; OR (95%): odds ratio with 95% confidence interval.

Table 5: Distribution of rs59233444 genotypes in patients and controls.

rs59233444	*N*	Genotype		
		—/—	GG/—	GG/GG
Case	190	66 (34.7%)	108 (56.8%)	16 (8.5%)
Control	190	94 (49.5%)	84 (44.2%)	12 (6.3%)
		$\chi^2 = 8.471$, $P = 0.014$		

Table 6: Allelic association for rs59233444 in LAF.

SNP	Allele (major/minor)	MAF (case/control)	*P*	OR (95% CI)
Rs59233444	—/GG	0.368/0.284	0.013	1.469 (1.083–1.993)

between *KCNQ1* gene polymorphisms or to another nearby susceptibility gene.

5. Conclusions

Mutations in the coding regions of *KCNQ1* are not a common cause for LAF. Several SNPs were identified in coding and noncoding regions of *KCNQ1*. One SNP in *KCNQ1* (rs59233444) is associated with LAF. Rs59233444 can be deemed as a risk factor for being susceptible to AF in Han Chinese people.

Table 7: Multiple regression analysis for LAF in rs59233444.

Risk factors	*P* value
Sex	0.789
Age	0.530
Smoking	0.689
Drinking	0.744
Hypertension	<0.001
rs59233444	0.005

Disclosure

The authors declare that the submitted paper does not contain previously published material and is not under consideration for publication elsewhere. All authors listed have read the complete paper and have approved submission of the paper. The paper is truthful original work without fabrication, fraud, or plagiarism.

Conflict of Interests

The authors declare that they have no conflict of interests.

Authors' Contribution

Each author has made an important scientific contribution to the study and is thoroughly familiar with the primary data. Hui-min Chu and Ming-jun Feng are co-first authors, they contributed equally to this work; they carried out the molecular genetic studies, participated in the sequence alignment, and drafted the paper. Yi-xin Zhang participated in the sequence alignment. Yi-gang Li participated in the design of the study and performed the statistical analysis. Xiao-min Chen conceived of the study and participated in its design and coordination and helped to draft the paper. Bin He helped to revise the paper. Yi-bo Yu helped to collect the clinical data and the statistical analysis. Jing Liu participated in the design of the study. Ji-fang Ma provided the partial of case and control samples. All authors read and approved the final paper.

Acknowledgments

This work was funded by the City Natural Science Foundation of Ningbo, China (no. 2009A610176). The authors would like to thank Lin Zhao, Chong Wu (Department of Human Population Genetics, Institute of Molecular Medicine, Peking University), and Feng Jiang (Department of Cardiology, The Fourth Affiliated Hospital of Harbin Medical University).

References

[1] L. Frost, G. Engholm, S. Johnsen, H. Møller, and S. Husted, "Incident stroke after discharge from the hospital with a

diagnosis of atrial fibrillation," *American Journal of Medicine*, vol. 108, no. 1, pp. 36–40, 2000.

[2] M. Grogan, H. C. Smith, B. J. Gersh, and D. L. Wood, "Left ventricular dysfunction due to atrial fibrillation in patients initially believed to have idiopathic dilated cardiomyopathy," *American Journal of Cardiology*, vol. 69, no. 19, pp. 1570–1573, 1992.

[3] Y. H. Chen, S. J. Xu, S. Bendahhou et al., "*KCNQ1* gain-of-function mutation in familial atrial fibrillation," *Science*, vol. 299, no. 5604, pp. 251–254, 2003.

[4] Q. Wang, M. E. Curran, I. Splawski et al., "Positional cloning of a novel potassium channel gene: KVLQT1 mutations cause cardiac arrhythmias," *Nature Genetics*, vol. 12, no. 1, pp. 17–23, 1996.

[5] Y. Yang, M. Xia, Q. Jin et al., "Identification of a KCNE2 gain-of-function mutation in patients with familial atrial fibrillation," *American Journal of Human Genetics*, vol. 75, no. 5, pp. 899–905, 2004.

[6] A. Lundby, L. S. Ravn, J. H. Svendsen, S. Haunsø, S. P. Olesen, and N. Schmitt, "KCNE3 mutation V17M identified in a patient with lone atrial fibrillation," *Cellular Physiology and Biochemistry*, vol. 21, no. 1–3, pp. 47–54, 2008.

[7] T. M. Olson, A. E. Alekseev, X. K. Liu et al., "Kv1.5 channelopathy due to KCNA5 loss-of-function mutation causes human atrial fibrillation," *Human Molecular Genetics*, vol. 15, no. 14, pp. 2185–2191, 2006.

[8] K. Calloe, L. S. Ravn, N. Schmitt et al., "Characterizations of a loss-of-function mutation in the Kir3.4 channel subunit," *Biochemical and Biophysical Research Communications*, vol. 364, no. 4, pp. 889–895, 2007.

[9] A. Lundby, L. S. Ravn, J. H. Svendsen, S. P. Olesen, and N. Schmitt, "*KCNQ1* mutation Q147R is associated with atrial fibrillation and prolonged QT interval," *Heart Rhythm*, vol. 4, no. 12, pp. 1532–1541, 2007.

[10] D. C. Bartos, S. Duchatelet, D. E. Burgess et al., "R231C mutation in *KCNQ1* causes long QT syndrome type 1 and familial atrial fibrillation," *Heart Rhythm*, vol. 8, no. 1, pp. 48–55, 2011.

[11] S. Das, S. Makino, Y. F. Melman et al., "Mutation in the S3 segment of *KCNQ1* results in familial lone atrial fibrillation," *Heart Rhythm*, vol. 6, no. 8, pp. 1146–1153, 2009.

[12] L. S. Ravn, Y. Aizawa, G. D. Pollevick et al., "Gain of function in IKs secondary to a mutation in KCNE5 associated with atrial fibrillation," *Heart Rhythm*, vol. 5, no. 3, pp. 427–435, 2008.

[13] C. Fatini, E. Sticchi, M. Genuardi et al., "Analysis of minK and eNOS genes as candidate loci for predisposition to non-valvular atrial fibrillation," *European Heart Journal*, vol. 27, no. 14, pp. 1712–1718, 2006.

[14] R. L. Abraham, T. Yang, M. Blair, D. M. Roden, and D. Darbar, "Augmented potassium current is a shared phenotype for two genetic defects associated with familial atrial fibrillation," *Journal of Molecular and Cellular Cardiology*, vol. 48, no. 1, pp. 181–190, 2010.

[15] X. Ren, C. Xu, C. Zhan et al., "Identification of NPPA variants associated with atrial fibrillation in a Chinese GeneID population," *Clinica Chimica Acta*, vol. 411, no. 7-8, pp. 481–485, 2010.

[16] K. M. Brauch, L. Y. Chen, and T. M. Olson, "Comprehensive mutation scanning of LMNA in 268 patients with lone atrial fibrillation," *American Journal of Cardiology*, vol. 103, no. 10, pp. 1426–1428, 2009.

[17] D. M. Hodgson-Zingman, M. L. Karst, L. V. Zingman et al., "Atrial natriuretic peptide frameshift mutation in familial atrial fibrillation," *New England Journal of Medicine*, vol. 359, no. 2, pp. 158–165, 2008.

[18] T. Makiyama, M. Akao, S. Shizuta et al., "A novel SCN5A gain-of-function mutation M1875T associated with familial atrial fibrillation," *Journal of the American College of Cardiology*, vol. 52, no. 16, pp. 1326–1334, 2008.

[19] L. Shi, C. Li, C. Wang et al., "Assessment of association of rs2200733 on chromosome 4q25 with atrial fibrillation and ischemic stroke in a Chinese Han population," *Human Genetics*, vol. 126, no. 6, pp. 843–849, 2009.

[20] P. T. Ellinor, K. L. Lunetta, N. L. Glazer et al., "Common variants in KCNN3 are associated with lone atrial fibrillation," *Nature Genetics*, vol. 42, no. 3, pp. 240–244, 2010.

[21] C. Zhang, G. H. Yuan, Z. F. Cheng, M. W. Xu, L. F. Hou, and F. P. Wei, "The single nucleotide polymorphisms of Kir3.4 gene and their correlation with lone paroxysmal atrial fibrillation in Chinese Han population," *Heart Lung and Circulation*, vol. 18, no. 4, pp. 257–261, 2009.

[22] Z. Zeng, C. Tan, S. Teng et al., "The single nucleotide polymorphisms of IKs potassium channel genes and their association with atrial fibrillation in a Chinese population," *Cardiology*, vol. 108, no. 2, pp. 97–103, 2007.

[23] L. Y. Chen, J. D. Ballew, K. J. Herron, R. J. Rodeheffer, and T. M. Olson, "A common polymorphism in SCN5A is associated with lone atrial fibrillation," *Clinical Pharmacology and Therapeutics*, vol. 81, no. 1, pp. 35–41, 2007.

[24] P. T. Ellinor, V. I. Petrov-Kondratov, E. Zakharova, E. G. Nam, and C. A. MacRae, "Potassium channel gene mutations rarely cause atrial fibrillation," *BMC Medical Genetics*, vol. 7, article 70, 2006.

Hindawi Publishing Corporation
The Scientific World Journal
Volume 2013, Article ID 507872, 10 pages
http://dx.doi.org/10.1155/2013/507872

Research Article

Calcium Transient and Sodium-Calcium Exchange Current in Human versus Rabbit Sinoatrial Node Pacemaker Cells

Arie O. Verkerk,[1] Marcel M. G. J. van Borren,[2] and Ronald Wilders[1]

[1] *Department of Anatomy, Embryology and Physiology, Academic Medical Center, University of Amsterdam, Meibergdreef 15, 1105 AZ Amsterdam, The Netherlands*
[2] *Laboratory of Clinical Chemistry and Hematology, Jeroen Bosch Hospital, Henri Dunantstraat 1, 5223 GZ 's-Hertogenbosch, The Netherlands*

Correspondence should be addressed to Ronald Wilders; r.wilders@amc.uva.nl

Received 11 January 2013; Accepted 7 February 2013

Academic Editors: Y. Du and Y. Wang

There is an ongoing debate on the mechanism underlying the pacemaker activity of sinoatrial node (SAN) cells, focusing on the relative importance of the "membrane clock" and the "Ca^{2+} clock" in the generation of the small net membrane current that depolarizes the cell towards the action potential threshold. Specifically, the debate centers around the question whether the membrane clock-driven hyperpolarization-activated current, I_f, which is also known as the "funny current" or "pacemaker current," or the Ca^{2+} clock-driven sodium-calcium exchange current, I_{NaCa}, is the main contributor to diastolic depolarization. In our contribution to this journal's "Special Issue on Cardiac Electrophysiology," we present a numerical reconstruction of I_f and I_{NaCa} in isolated rabbit and human SAN pacemaker cells based on experimental data on action potentials, I_f, and intracellular calcium concentration ($[Ca^{2+}]_i$) that we have acquired from these cells. The human SAN pacemaker cells have a smaller I_f, a weaker $[Ca^{2+}]_i$ transient, and a smaller I_{NaCa} than the rabbit cells. However, when compared to the diastolic net membrane current, I_{NaCa} is of similar size in human and rabbit SAN pacemaker cells, whereas I_f is smaller in human than in rabbit cells.

1. Introduction

Animal studies have demonstrated that pacemaker activity of the sinoatrial node (SAN) is controlled by a complex system of "clocks" composed of voltage-dependent sarcolemmal currents—designated the "membrane clock," "voltage clock," or "ion channel clock"—and tightly coupled sarcoplasmic reticulum (SR) Ca^{2+} cycling molecules together with the electrogenic sodium-calcium exchanger, named the "Ca^{2+} clock" [1, 2]. There is an ongoing debate on the relative importance of the "membrane clock" and the "Ca^{2+} clock" in the generation of the small net membrane current underlying the spontaneous diastolic depolarization that drives the cell towards its action potential threshold [3–7]. This debate centers around the contribution of the hyperpolarization-activated current I_f, also known as "funny current" or "pacemaker current," as a member of the membrane clock, and the sodium-calcium exchange current I_{NaCa}, resulting from the electrogenic sodium-calcium exchange process and thus driven by the Ca^{2+} clock.

In contrast with the data collected in animal studies, the mechanism of SAN pacemaker activity in man is virtually unexplored. In a comprehensive study, Chandler et al. [8] characterized the "molecular architecture" of the human SAN based on messenger RNA (mRNA) levels of 120 ion channels and related proteins, and they concluded that the expression pattern was appropriate to explain pacemaking. They observed a prominent expression of HCN4 and, to a lesser extent, HCN1, which are both subunits of the I_f channel. We actually recorded I_f in voltage clamp experiments on single pacemaker cells isolated from the SAN of a patient who underwent SAN excision [9]. From these cells, we also acquired spontaneous action potentials, which showed a clear diastolic depolarization phase resulting in an intrinsic cycle length of ≈ 830 ms (72 beats/min). In addition, our voltage clamp experiments revealed the presence of a fast large

inward current with characteristics of the Na^+ current, I_{Na} [10].

Clinical data also point to a role for I_f and I_{Na} in human SAN pacemaker activity. Mutations in *HCN4* and *SCN5A*, encoding pore-forming subunits of the I_f and I_{Na} channel, respectively, have been linked to familial sick sinus syndrome (see [11, 12] and primary references cited therein), thus suggesting that I_f and I_{Na} indeed contribute to human SAN pacemaker activity. A further clinical indication regarding the role of a specific ion current in human SAN pacemaker activity involves the slowly activating delayed rectifier K^+ current (I_{Ks}) and comes from patients who suffer from the long-QT syndrome type 1 and carry a loss-of-function mutation in the *KCNQ1* (*KvLQT1*) gene, encoding the pore-forming α-subunit of the I_{Ks} channel. These patients have close-to-normal heart rates in rest [13], but their ability to increase heart rate during exercise is seriously impaired [14].

The aforementioned experimental and clinical observations all point to a role for important components of the "membrane clock" in human SAN pacemaker activity. There are also some clinical data in support of a contribution of the "Ca^{2+} clock" through patients with catecholaminergic polymorphic ventricular tachycardia (CPVT), who have an impaired Ca^{2+} clock due to mutations in the *RYR2* gene (CPVT1) or the *CASQ2* gene (CPVT2), encoding the cardiac ryanodine receptor isoform 2 (RyR2, responsible for Ca^{2+} release from the SR) and the cardiac calsequestrin isoform 2 protein (calsequestrin-2, responsible for calcium buffering in the SR), respectively [15]. Leenhardt et al. [16] observed a marked sinus bradycardia in a group of 21 nongenotyped CPVT patients. Sumitomo et al. [17] also reported sinus bradycardia in their group of 29 nongenotyped CPVT patients. At the time of the reports by Leenhardt et al. [16] and Sumitomo et al. [17], CPVT had not yet been associated with the *RYR2* and *CASQ2* genes. More recently, Postma et al. [18, 19] found a marked sinus bradycardia in both CPVT1 [18] and CPVT2 [19] patients.

Chandler et al. [8] observed various Ca^{2+}-handling proteins in the human SAN, albeit less abundant than in the surrounding right atrium, including NCX1 (responsible for sodium-calcium exchange in the heart), RyR2, and SERCA2a (responsible for Ca^{2+} uptake by the SR). They constructed a mathematical model of a human SAN cell by modification of the Courtemanche et al. [20] model of a human atrial myocyte, scaling ion current densities on the basis of the relative mRNA expression level in SAN and atrium and introducing the T-type Ca^{2+} current and I_f. Specifically, I_{NaCa} was scaled down to 74% of its value in the Courtemanche et al. [20] model. Recently, Allah et al. [21] published a study in which they used the same experimental approach as Chandler et al. [8] to determine the expression of ion channels and Ca^{2+} handling proteins in the SAN, right atrium, and left ventricle of the neonate and adult rabbit. From their Figure 6 [21], it appears that the mRNA expression level of the *NCX1* gene in the adult rabbit SAN is ≈ 78% and ≈ 69% of that in right atrium and left ventricle, respectively.

When we recorded action potentials from isolated human SAN pacemaker cells and carried out voltage clamp experiments [9], we also acquired some data on the intracellular free Ca^{2+} concentration ($[Ca^{2+}]_i$) of human SAN pacemaker cells using the fluorescent Ca^{2+} indicator Indo-1. In the present study, we use these thus far unpublished experimental data in a numerical reconstruction of I_{NaCa} in a human SAN pacemaker cell. The thus obtained I_{NaCa} is compared to the net membrane current (I_{net}) and to I_f, which are also obtained through a numerical reconstruction. In addition, we present data on I_f, I_{NaCa}, and I_{net} in rabbit SAN pacemaker cells, thus allowing a comparison of these currents between rabbit and human SAN pacemaker cells.

2. Materials and Methods

2.1. Cell Preparations. Single SAN cells were isolated by an enzymatic dissociation procedure as described previously [22] from New Zealand White rabbits and from a patient who underwent SAN excision because of inappropriate sinus tachycardias originating from the SAN region (see [9] for clinical details). In either case, cells were stored at room temperature for at least 45 min in modified Kraft-Brühe (KB) solution before they were put into a recording chamber on the stage of an inverted microscope and superfused with modified Tyrode's solution at 36 ± 0.2°C. KB solution contained (in mM) KCl 85, K_2HPO_4 30, $MgSO_4$ 5.0, glucose 20, pyruvic acid 5.0, creatine 5.0, taurine 30, β-hydroxybutyric acid 5.0, succinic acid 5.0, BSA 1%, and Na_2ATP 2.0; pH was set to 6.9 with KOH. Modified Tyrode's solution contained (in mM) NaCl 140, KCl 5.4, $CaCl_2$ 1.8, $MgCl_2$ 1.0, glucose 5.5, and HEPES 5.0; pH was set to 7.4 with NaOH. Spindle and elongated spindle-like cells displaying regular contractions were selected for measurements.

2.2. Cytosolic Ca^{2+} Measurements. Cytosolic Ca^{2+} concentration ($[Ca^{2+}]_i$) was measured in Indo-1 loaded cells as described previously [23]. In brief, cells were loaded with 5 μM of the fluorescent dye Indo-1-AM (Molecular Probes, Eugene, OR, USA) for 10 min at room temperature in KB solution and subsequently superfused with modified Tyrode's solution for 15 min at 36 ± 0.2°C to remove excess indicator and allow full deesterification. A rectangular adjustable slit was used to select a single cell and to reduce background fluorescence. Dual wavelength emission of Indo-1 upon excitation at 340 nm was recorded at 405–440 and 505–540 nm using photomultiplier tubes, and, after correction for background fluorescence, free $[Ca^{2+}]_i$ was calculated as described by van Borren et al. [23].

$[Ca^{2+}]_i$ transients were characterized by the minimum diastolic $[Ca^{2+}]_i$ (MDC), their amplitude (TA), their maximum rate of rise ($d[Ca^{2+}]_i/dt_{max}$), their duration measured at 20, 50, and 90% decay (TD_{20}, TD_{50}, and TD_{90}, resp.), and their frequency. Parameter values obtained from 10 consecutive $[Ca^{2+}]_i$ transients were averaged.

2.3. Action Potential Measurements. Action potentials from rabbit and human SAN cells were recorded with

the amphotericin-perforated and conventional whole-cell configuration of the patch-clamp technique, respectively, using an Axopatch 200B patch-clamp amplifier (Molecular Devices Corporation, Sunnyvale, CA, USA). For recording from rabbit SAN cells, pipettes (borosilicate glass; resistance 2–5 MΩ) were filled with solution containing (in mM) K-gluconate 120, KCl 20, NaCl 5, amphotericin B 0.22, NMDGCl (N-methyl-D-glucammonium chloride) 10, and HEPES 10; pH was set to 7.2 with KOH. For recording from human SAN cells, patch pipettes contained (in mM) K-gluconate 125, KCl 20, NaCl 5, $MgCl_2$ 1, MgATP 5, and HEPES 10; pH was set to 7.2 with KOH.

Action potentials were characterized by their frequency, their duration at 20, 50, and 90% repolarization (APD_{20}, APD_{50}, and APD_{90}, resp.), maximum diastolic potential (MDP), action potential amplitude (APA), maximum upstroke velocity (dV_m/dt_{max}), and diastolic depolarization rate measured over the 100 ms time interval starting at MDP+1 mV (DDR_{100}). Parameter values obtained from 10 consecutive action potentials were averaged. All membrane potential values were corrected for the calculated liquid junction potential.

2.4. Numerical Reconstruction of Hyperpolarization-Activated Current. For the numerical reconstruction of both rabbit and human I_f, we used a first-order Hodgkin and Huxley [24] type kinetic scheme. Accordingly, I_f is given by

$$I_f = y \times g_f \times \left(V_m - E_f\right), \tag{1}$$

in which g_f is the fully activated I_f conductance, V_m is the membrane potential, E_f is the I_f reversal potential, and the gating variable y, with $0 \le y \le 1$, obeys the first-order differential equation

$$\frac{dy}{dt} = \alpha \times (1 - y) - \beta \times y, \tag{2}$$

with voltage-dependent rate constants α and β, or, equivalently,

$$\frac{dy}{dt} = \frac{(y_\infty - y)}{\tau}, \tag{3}$$

with the steady-state activation y_∞ and time constant τ given by

$$y_\infty = \frac{\alpha}{(\alpha + \beta)}, \tag{4}$$

$$\tau = \frac{1}{(\alpha + \beta)}. \tag{5}$$

For rabbit I_f, we used the model by Dokos et al. [25], who based their equations on the comprehensive experimental study on rabbit I_f by van Ginneken and Giles [26], arriving at

$$\alpha = \frac{0.36 \times (V_m + 137.8)}{\{\exp[0.066 \times (V_m + 137.8)] - 1\}},$$
$$\beta = \frac{0.1 \times (V_m + 76.3)}{\{1 - \exp[-0.21 \times (V_m + 76.3)]\}}, \tag{6}$$

for the rate constants α and β, both expressed in s^{-1}. In our computations, we used a scaling factor of 0.71665 for the time constant τ (5) as a correction factor for the temperature of 30–33°C in the experiments of van Ginneken and Giles [26]. This correction factor was adopted from the SAN cell models by Kurata et al. [27] and Maltsev and Lakatta [28]. With the bath and pipette Na^+ and K^+ concentrations listed in Sections 2.1 and 2.3, the reversal potential of the Dokos et al. [25] model amounts to −21.0 mV. For the fully activated I_f conductance, we used a value of 0.218 pS/pF, based on the mean values of 12.0 nS and 55 pF for the fully activated conductance and membrane capacitance, respectively, reported by van Ginneken and Giles [26].

For human I_f, we used the model that we developed on the basis of our voltage clamp data on human SAN cells [9]. In this model [29, 30], y_∞ and τ (in ms) are given by

$$y_\infty = 0.01329 + \frac{0.99921}{\{1 + \exp[(V_m + 97.134)/8.1752]\}} \quad \text{if } V_m < -80 \text{ mV}, \tag{7}$$

$$y_\infty = 0.0002501 \times \exp\left(\frac{-V_m}{12.861}\right) \quad \text{if } V_m \ge -80 \text{ mV},$$

$$\tau = 1000 \times \left\{0.36 \times \frac{(V_m + 148.8)}{[\exp(0.066 \times (V_m + 148.8)) - 1]} + 0.1 \times \frac{(V_m + 87.3)}{[1 - \exp(-0.21 \times (V_m + 87.3))]}\right\}^{-1} - 54, \tag{8}$$

respectively. The fully activated I_f conductance g_f and the I_f reversal potential E_f were set to 0.075 nS/pF and −22 mV, respectively, in accordance with the fully activated I_f conductance of 75.2±3.8 pS/pF (mean±SEM, $n = 3$) and I_f reversal potential of −22.1 mV ± 2.4 mV (mean ± SEM, $n = 3$) determined experimentally [9].

The numerical reconstruction was carried out on an Intel Xeon based workstation using Compaq Visual Fortran 6.6C and employing a simple and efficient Euler-type integration scheme with a time step of 10 μs. Simulations were run for a sufficiently long time to achieve steady-state conditions.

2.5. Numerical Reconstruction of Sodium-Calcium Exchange Current. For the numerical reconstruction of human I_{NaCa} on the basis of the recorded data on V_m and $[Ca^{2+}]_i$ (combined voltage and calcium clamp [31]), we adopted the I_{NaCa} formulation of the Courtemanche et al. [20] model for a human atrial myocyte, with I_{NaCa} scaled down to 74% of its control value. We thus followed the approach by Chandler et al. [8] in their construction of a mathematical model of a human SAN cell by modification of the Courtemanche et al. [20] model, as set out in the Introduction.

We used a similar approach for the numerical reconstruction of rabbit I_{NaCa} on the basis of the acquired data on V_m

and $[Ca^{2+}]_i$. In this case, we adopted the I_{NaCa} formulation of the Lindblad et al. [32] model for a rabbit atrial myocyte. However, the original I_{NaCa} was scaled down to 78% of its control value, based on the mRNA data by Allah et al. [21], as detailed in the Introduction.

The Courtemanche et al. [20] and Lindblad et al. [32] equations not only require values for V_m and $[Ca^{2+}]_i$, but also for $[Ca^{2+}]_e$, $[Na^+]_e$ and $[Na^+]_i$, which denote the extracellular Ca^{2+} concentration, the extracellular Na^+ concentration, and the intracellular Na^+ concentration, respectively. For these ion concentrations, we used the bath and pipette solutions listed in Sections 2.1 and 2.3.

2.6. Statistics. Data are presented as mean ± SEM. Comparisons between groups were made using an unpaired t-test. The level of significance was set at $P < 0.05$.

3. Results

For the present study, we first characterized the action potentials and $[Ca^{2+}]_i$ transients that we recorded from single rabbit and human SAN pacemaker cells. Next, we used our experimental data for a numerical reconstruction of the hyperpolarization-activated current and the sodium-calcium exchange current associated with the recorded action potentials and $[Ca^{2+}]_i$ transients, thus allowing a comparison of these currents between rabbit and human SAN pacemaker cells.

3.1. Rabbit and Human Action Potentials. Figure 1(a) shows typical examples of the spontaneous action potentials of rabbit and human SAN pacemaker cells, recorded with the patch-clamp technique. Maximum diastolic potential (MDP) and action potential amplitude (APA) are remarkably similar, whereas the beating frequency is strikingly different, as confirmed by the mean value of 3.11 ± 0.24 Hz for the 7 rabbit cells versus 1.21 ± 0.02 Hz for the 3 human cells ($P < 0.05$) and illustrated in Figure 1(b).

Neither the action potential durations, for example, the APD_{90} of 144 ± 35 versus 113 ± 6 ms, nor the diastolic depolarization rate of 49 ± 18 versus 89 ± 19 mV/s differ significantly between human and rabbit SAN cells, which is likely due to the low number of cells of human origin. Nevertheless, from Figure 1(a), it is indicative that the longer cycle length of the human cells (828 ± 15 versus 337 ± 35 ms) is importantly due to longer diastolic depolarization rather than longer action potential duration. A further difference is found in the maximum rate of rise of the action potential, which is considerably larger in the rabbit cells (13.0 ± 1.6 versus 4.6 ± 1.2 V/s, $P < 0.05$; Figure 1(b)).

3.2. Rabbit and Human $[Ca^{2+}]_i$ Transients. In the 7 rabbit cells of Figure 1(b), we simultaneously recorded the membrane potential, using the perforated patch-clamp technique, and the $[Ca^{2+}]_i$ transient, using the fluorescent Ca^{2+} indicator Indo-1. A typical example of such $[Ca^{2+}]_i$ transient, recorded from the same cell and during the same period of time as used for Figure 1(a), is provided in Figure 1(c). Also shown in Figure 1(c) is the $[Ca^{2+}]_i$ transient that we were able to record from a single human SAN cell. Further attempts to acquire the $[Ca^{2+}]_i$ transient of human cells resulted in unstable recordings. Of note, no action potentials are available from the cell that we recorded the $[Ca^{2+}]_i$ transient from. So, in contrast with the rabbit data, the human data of Figures 1(a) and 1(c) are not simultaneously collected and are not from the same cell.

The minimum diastolic $[Ca^{2+}]_i$ level of the human cell is similar to that of the rabbit cells, but otherwise the $[Ca^{2+}]_i$ transients are widely different, with a smaller amplitude, longer duration, and smaller rate of rise in case of the human cell, as illustrated in Figure 1(d), in which the characteristics of the $[Ca^{2+}]_i$ transient of the human cell are compared to those of the mean characteristics in the 7 rabbit cells.

As illustrated in Figure 2(a) for the simultaneously recorded action potential (top) and $[Ca^{2+}]_i$ transient (bottom) of a rabbit SAN cell, the maximum rate of rise of the $[Ca^{2+}]_i$ transient, as determined from the time derivative of the $[Ca^{2+}]_i$ transient signal (Figure 2(b), bottom), occurs with a time lag relative to the maximum rate of rise of the associated action potential, as determined from the time derivative of the V_m signal (Figure 2(b), top). This time lag between the occurrence of dV_m/dt_{max} and $d[Ca^{2+}]_i/dt_{max}$ was determined for each of the 7 rabbit SAN cells tested and amounted to 21.3 ± 0.6 ms. The time lag ranged between 19 and 23 ms and showed no appreciable frequency dependence, as illustrated in Figure 2(c), in which the time lag is plotted versus the spontaneous beating frequency.

3.3. Numerical Reconstruction of Membrane Ionic Currents. Next, we carried out a numerical reconstruction of the hyperpolarization-activated current (I_f) and the sodium-calcium exchange current (I_{NaCa}) of rabbit and human SAN pacemaker cells based on the experimental data on their action potentials and $[Ca^{2+}]_i$ transients presented in Figures 1 and 2.

3.3.1. Experimental Data. For the reconstruction of rabbit membrane ionic currents, we used a 1-s simultaneous recording of V_m and $[Ca^{2+}]_i$ of one of the 7 rabbit cells that we digitized at 10 kHz through linear interpolation of the acquired data points. This 1-s recording contained three action potentials and associated $[Ca^{2+}]_i$ transients and was turned into a continuous signal by repeating the 1-s signal. Because of the repetition of the 1-s signal, the fourth and fifth action potentials of Figure 3(a) (left) are identical to the first and second, respectively. The same holds for the associated $[Ca^{2+}]_i$ transients, which are shown in Figure 3(b) (left).

A similar approach, now using a ≈1.6 s time frame, was used in case of the human cell data. However, because data on V_m and $[Ca^{2+}]_i$ were not simultaneously collected, we selected two consecutive action potentials with cycle lengths of 791 and 822 ms—human SAN pacemaker cells show a beat-to-beat fluctuation in cycle length as do rabbit cells [33]—and two consecutive $[Ca^{2+}]_i$ transients that, by coincidence, had identical cycle lengths. Furthermore, for the timing of the two signals, it was assumed that the time lag between the occurrence of dV_m/dt_{max} and $d[Ca^{2+}]_i/dt_{max}$ was 21 ms, as

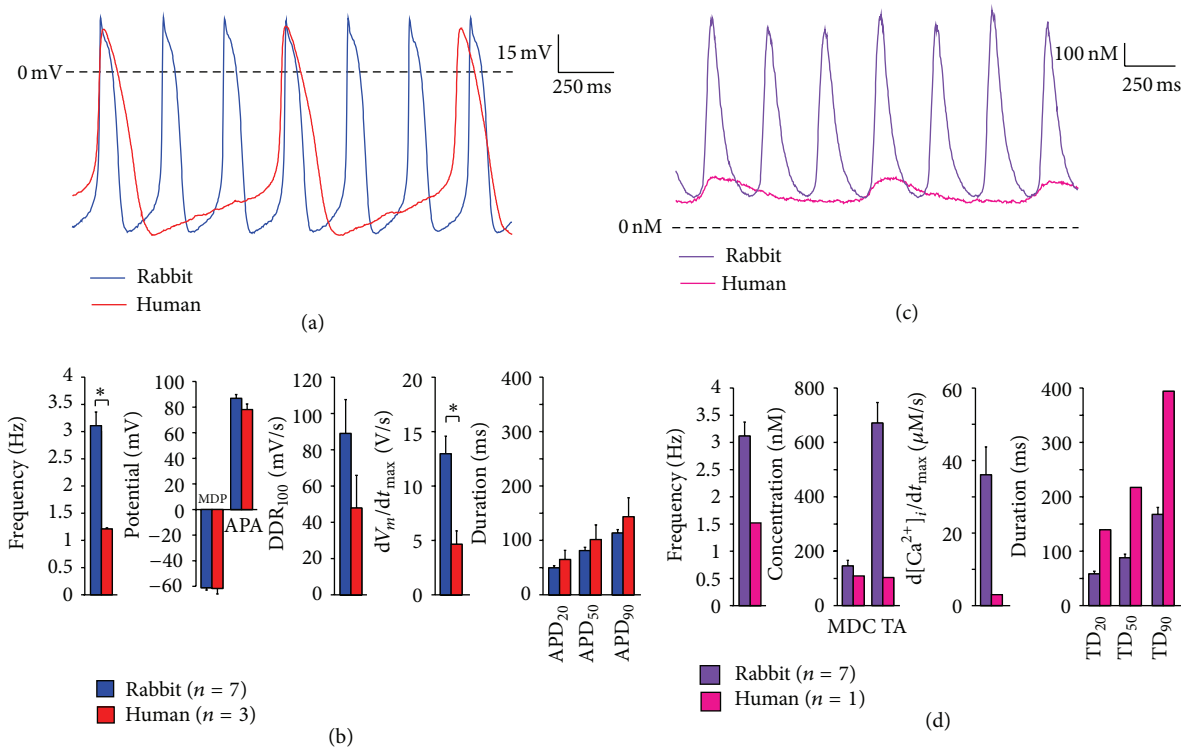

FIGURE 1: Spontaneous electrical activity of rabbit and human sinoatrial node (SAN) pacemaker cells. (a) and (b) Typical examples (a) and average characteristics (b) of action potentials. (c) and (d) Typical examples (c) and average characteristics (d) of the intracellular free Ca^{2+} concentration ($[Ca^{2+}]_i$). Data are mean ± SEM; n = number of cells; MDP = maximum diastolic potential; APA = action potential amplitude; DDR_{100} = diastolic depolarization rate over the 100 ms time interval starting at MDP + 1 mV; dV_m/dt_{max} = maximal upstroke velocity; APD_{20}, APD_{50}, and APD_{90} = action potential duration at 20, 50, and 90% repolarization; MDC = minimum diastolic $[Ca^{2+}]_i$; TA = $[Ca^{2+}]_i$ transient amplitude; $d[Ca^{2+}]_i/dt_{max}$ = maximum rate of rise of $[Ca^{2+}]_i$ transient; TD_{20}, TD_{50}, and TD90 = $[Ca^{2+}]_i$ transient duration at 20, 50, and 90% decay. $^*P < 0.05$.

observed in the rabbit cells (Figure 2(c)). The resulting V_m and $[Ca^{2+}]_i$ data are shown in the right panels of Figures 3(a) and 3(b).

3.3.2. Numerical Reconstruction of Net Membrane Current. As a reference for I_f and I_{NaCa}, we first determined the net membrane current (I_{net}) in both rabbit and human cells. Because $I_{net} = -C_m \times dV_m/dt$, where C_m denotes membrane capacitance, the current density of I_{net} is identical to $-dV_m/dt$ and thus readily follows from the time derivative of the action potential, which is shown in Figure 3(c) for the action potentials of Figure 3(a). In the diastolic voltage range, I_{net} is a small inward current with a density of ≈ 0.1 and ≈ 0.05 pA/pF in rabbit and human, respectively (Figures 3(d) and 3(e), gray traces), in line with the mean diastolic depolarization rate of 89 ± 19 and 49 ± 18 mV/s, respectively (Figure 1(b)). Figure 3(c) also confirms the data of Figure 1(b) regarding the smaller dV_m/dt_{max} in human versus rabbit SAN cells.

3.3.3. Numerical Reconstruction of Hyperpolarization-Activated Current. The action potentials of Figure 3(a) were applied as a voltage clamp signal in order to reconstruct the hyperpolarization-activated current I_f, as detailed in Section 2.4. The resulting I_f traces are shown in Figure 3(d). There is an almost 7-fold difference in diastolic I_f amplitude between rabbit and human, which becomes less pronounced when compared to the net membrane current, I_{net}, in each of the cell types. In rabbit, diastolic I_f is 2-3 times I_{net}, whereas diastolic I_f and I_{net} are of similar size in human.

3.3.4. Numerical Reconstruction of Sodium-Calcium Exchange Current. The V_m and $[Ca^{2+}]_i$ data of Figures 3(a) and 3(b) were applied as a combined voltage and calcium clamp signal in order to reconstruct the sodium-calcium exchange current I_{NaCa} in human and rabbit SAN cells, as detailed in Section 2.5. The resulting I_{NaCa} is smaller in amplitude in human than in rabbit (Figure 3(e)). However, in either case, the mid-diastolic I_{NaCa} amplitude is roughly twice that of I_{net}. The end-diastolic amplitude of I_{NaCa} at −45 mV is ≈ 0.07 pA/pF in human, which is ≈ 25% of the value of ≈ 0.28 pA/pF in rabbit.

3.3.5. Charge Carried by Individual Currents. From the current traces of Figures 3(d) and 3(e), one can compute the contribution to diastolic depolarization in terms of charge carried by I_{net}, I_f, and I_{NaCa} through integration of each of these currents over time. We carried out such computation for the 20 mV spontaneous depolarization from MDP + 1 mV

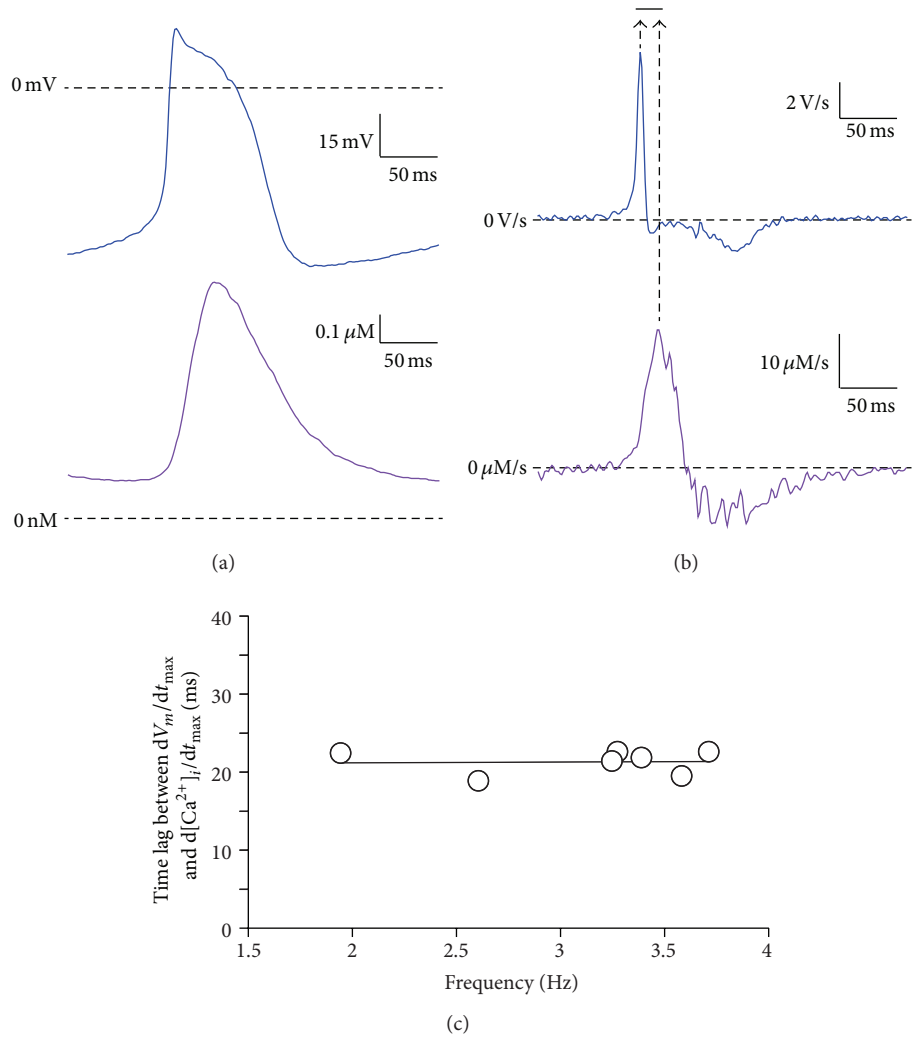

FIGURE 2: (a), Simultaneously recorded action potential (top) and $[Ca^{2+}]_i$ transient (bottom) of a rabbit SAN cell. (b) Time derivatives of the action potential (top) and $[Ca^{2+}]_i$ transient (bottom) traces shown in panel (a). Arrows indicate the timing of the maximum rate of change in membrane potential (dV_m/dt_{max}) and intracellular Ca^{2+} concentration ($d[Ca^{2+}]_i/dt_{max}$). Horizontal bar indicates the time lag of ≈20 ms. (c) Time lag between the occurrence of dV_m/dt_{max} and $d[Ca^{2+}]_i/dt_{max}$ versus beating frequency of the 7 cells measured. Solid line is the linear regression line (slope 0.1 ± 1.1; $R = 0.042$). Note the absence of an appreciable frequency dependence of the time lag.

of the rabbit and human action potentials of Figure 3(a). As shown in Figure 4 (left bars), the thus computed charge carried by $I_{net}(Q_{net})$ amounts to 0.020 pC/pF for both rabbit and human, as expected from the 20 mV depolarization, which is equivalent to a charge flow of 0.02 pC/pF. The charge carried by $I_f(Q_f)$ is 0.043 and 0.018 pC/pF for rabbit and human, respectively, whereas that carried by $I_{NaCa}(Q_{NaCa})$ amounts to 0.055 and 0.047 pC/pF, respectively (Figure 4, middle and right bars).

4. Discussion

In the present study, we first characterized the action potentials and $[Ca^{2+}]_i$ transients that we recorded from single rabbit and human SAN pacemaker cells. Next, we used our experimental data for a numerical reconstruction of the hyperpolarization-activated current and the sodium-calcium exchange current associated with the recorded action potentials and $[Ca^{2+}]_i$ transients.

4.1. Experimental Data. Human SAN pacemaker cells have a lower beating frequency and a lower maximum upstroke velocity than rabbit SAN pacemaker cells (Figures 1(a) and 1(b)). Also, they have a considerably weaker $[Ca^{2+}]_i$ transient (Figures 1(c) and 1(d)), which may, at least in part, be a frequency effect, as observed in rabbit cells [23]. The longer cycle length of the human cells is largely due to a longer diastolic phase (Figures 1(a) and 1(b)). In this respect, the recorded action potentials differ from those that Chandler et al. [8] computed by turning the Courtemanche et al. [20] human atrial cell model into a human SAN pacemaker cell model. On the other hand, the range of the computed calcium

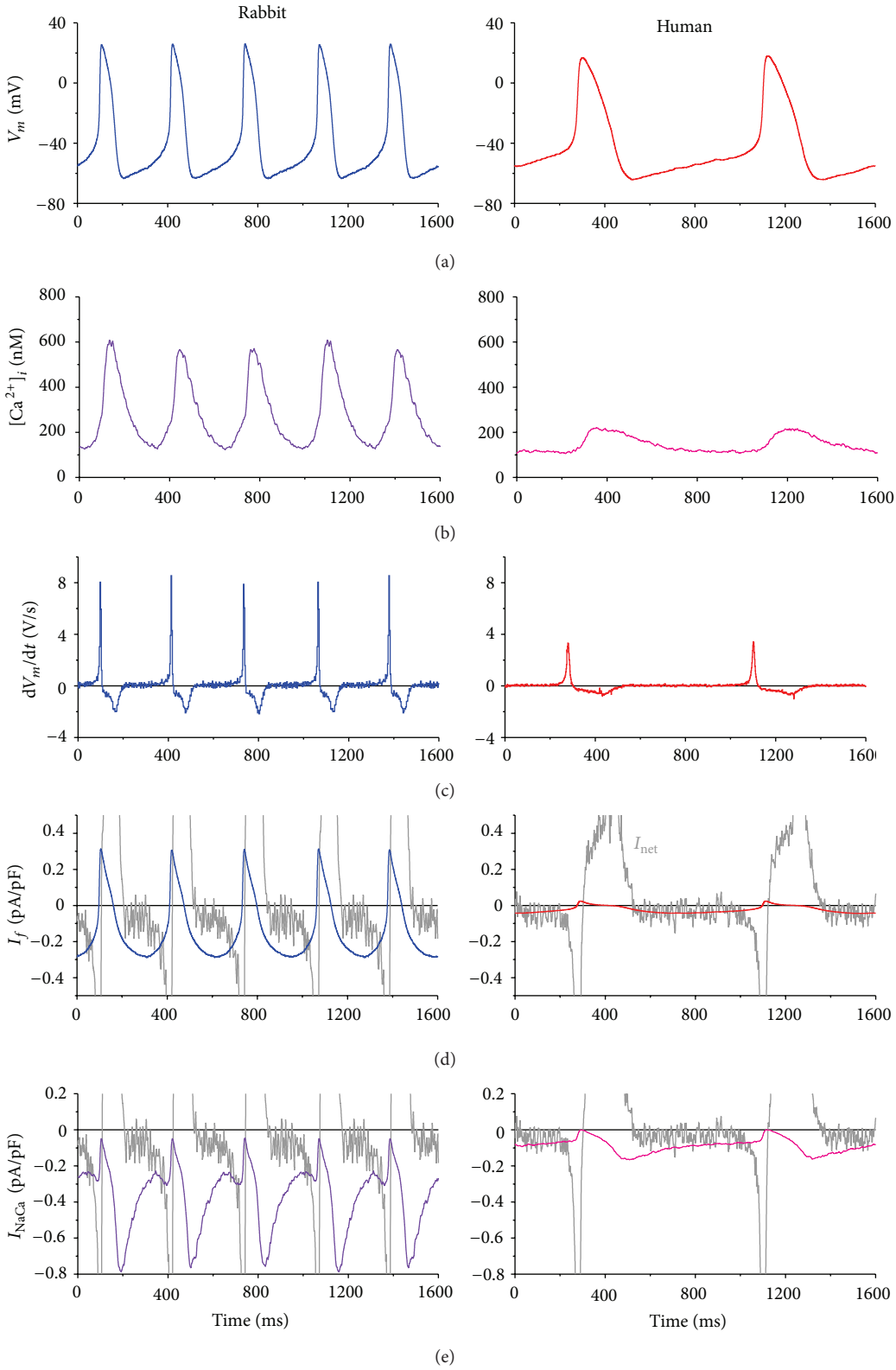

FIGURE 3: Action potential and calcium transient recordings from rabbit (left) and human (right) SA nodal myocytes and associated numerical reconstructions of membrane currents. (a) Recorded membrane potential V_m. (b) Recorded intracellular calcium concentration ($[Ca^{2+}]_i$). (c) Time derivative of V_m (dV_m/dt). (d) Reconstructed hyperpolarization-activated inward current (I_f). The noisy trace in gray is the net membrane current (I_{net}) computed from $I_{net} = -C_m \times dV_m/dt$, where C_m denotes membrane capacitance. (e) Reconstructed sodium-calcium exchange current (I_{NaCa}), with the net membrane current in gray.

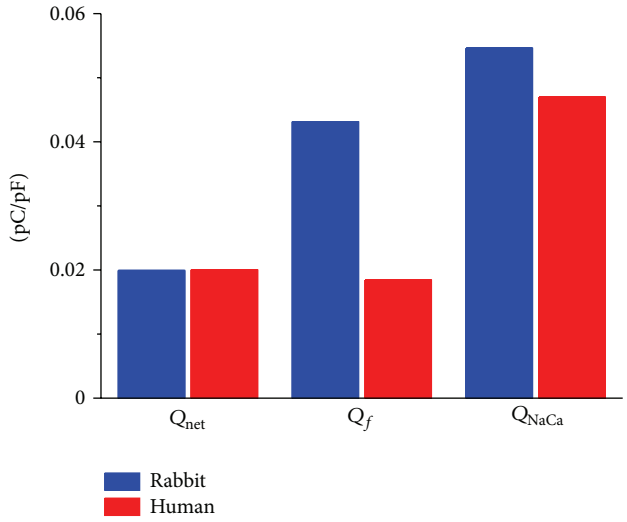

FIGURE 4: Charge carried by net membrane current (Q_{net}), reconstructed hyperpolarization-activated inward current (Q_f), and reconstructed sodium-calcium exchange current (Q_{NaCa}) during 20 mV spontaneous depolarization from MDP + 1 mV of the rabbit and human SA nodal action potentials of Figure 3.

signal (approximately 150–250 nM; Figure 8 of Chandler et al. [8]) compares reasonably well with the experimentally observed range (roughly 110–220 nM; Figures 1(c) and 1(d)).

As an important caveat, it should be noted that our data on human cells have been collected from only a small number of cells, all from a single patient who underwent SAN excision because of tachycardias [9]. Stable action potential recordings were obtained from three cells and a stable calcium transient recording from only one cell. Furthermore, although almost identical experimental methods were employed, the use of the perforated-patch configuration of the patch-clamp technique in case of the rabbit cells and the conventional whole-cell configuration in case of the human cells may have introduced deviations.

4.2. Numerical Reconstructions. In our numerical reconstruction of rabbit I_f, we used the Dokos et al. [25] equations based on a reanalysis of the data by van Ginneken and Giles [26] rather than the equations provided by van Ginneken and Giles [26] themselves. In the latter equations, the I_f deactivation rate is erroneously overestimated, as set out in detail by Dokos et al. [25]. As a result, the reconstructed I_f of Figure 3(d) (left) is larger than in rabbit SAN cell models that employ the van Ginneken and Giles equations, such as the models by Kurata et al. [27] and Maltsev and Lakatta [28]. Furthermore, the more negative maximum diastolic potential of the recorded action potentials adds to the larger I_f. The availability of I_f almost immediately after repolarization and its amplitude larger than that of I_{net} are in line with the data from action potential clamp experiments on rabbit SAN cells carried out by Zaza et al. [34]. The reconstructed human I_f trace compares well with the traces that we previously reconstructed for the other two human SAN pacemaker cells from which action potentials are available [12].

In our numerical reconstruction of I_{NaCa}, we used equations from rabbit and human atrial cell models—properly scaled to account for the reduced mRNA expression of *NCX1* in the SAN versus the atrium, both in human [8] and in rabbit [21]—that allowed the reconstruction of I_{NaCa} from the experimentally recorded membrane potential and global cytosolic $[Ca^{2+}]_i$. Today, there are highly detailed models of calcium handling in (rabbit) SAN cells [28, 35], but for a reconstruction of I_{NaCa}, these would require experimental data on $[Ca^{2+}]_i$ in submembrane spaces rather than global cytosolic $[Ca^{2+}]_i$. In human cells, the total charge carried by I_f during spontaneous diastolic depolarization is similar to that carried by I_{net}, whereas in rabbit it is approximately twice (Figure 4).

Of note, the diastolic I_{NaCa} amplitude at −45 mV of ≈0.28 pA/pF in rabbit (Figure 3(e), left) is identical to the value of 0.28 ± 0.03 pA/pF that Vinogradova et al. [36] observed experimentally. A highly similar amplitude is obtained (data not shown) if I_{NaCa} is not reconstructed from the Lindblad et al. [32] equations but from the equations for a ventricular cell provided by Faber and Rudy [37], scaled down to 69% to account for the mRNA data by Allah et al. [21].

Human I_{NaCa} is smaller than that of rabbit (Figure 3(e)). This is not only due to the smaller I_{NaCa} in the human versus the rabbit atrial cell model from which the equations were adopted for the reconstruction. What also plays a role is that the experimentally recorded $[Ca^{2+}]_i$ is smaller in human than in rabbit at all values of V_m. Yet, the total charge carried by I_{NaCa} during spontaneous diastolic depolarization is of similar magnitude in rabbit and human (Figure 4).

5. Conclusion

Human SAN pacemaker cells have a smaller I_f, a weaker $[Ca^{2+}]_i$ transient, and a smaller I_{NaCa} than rabbit SAN pacemaker cells. However, when compared to the diastolic net membrane current, I_{NaCa} is of similar size in human and rabbit cells, whereas I_f is smaller in human than in rabbit cells.

Conflict of Interests

The authors declare that they have no conflict of interests.

References

[1] M. E. Mangoni and J. Nargeot, "Genesis and regulation of the heart automaticity," *Physiological Reviews*, vol. 88, no. 3, pp. 919–982, 2008.

[2] E. G. Lakatta, V. A. Maltsev, and T. M. Vinogradova, "A Coupled SYSTEM of intracellular Ca^{2+} clocks and surface membrane voltage clocks controls the timekeeping mechanism of the heart's pacemaker," *Circulation Research*, vol. 106, no. 4, pp. 659–673, 2010.

[3] E. G. Lakatta and D. DiFrancesco, "What keeps us ticking: a funny current, a calcium clock, or both?" *Journal of Molecular and Cellular Cardiology*, vol. 47, no. 2, pp. 157–170, 2009.

[4] D. DiFrancesco and D. Noble, "The funny current has a major pacemaking role in the sinus node," *Heart Rhythm*, vol. 9, no. 2, pp. 299–301, 2012.

[5] V. A. Maltsev and E. G. Lakatta, "The funny current in the context of the coupled-clock pacemaker cell system," *Heart Rhythm*, vol. 9, no. 2, pp. 302–307, 2012.

[6] D. DiFrancesco and D. Noble, "Rebuttal: The funny current in the context of the coupled clock pacemaker cell system," *Heart Rhythm*, vol. 9, no. 3, pp. 457–458, 2012.

[7] E. G. Lakatta and V. A. Maltsev, "Rebuttal: what I_f the shoe doesn't fit? The funny current has a major pacemaking role in the sinus node," *Heart Rhythm*, vol. 9, no. 3, pp. 459–460, 2012.

[8] N. J. Chandler, I. D. Greener, J. O. Tellez et al., "Molecular architecture of the human sinus node insights into the function of the cardiac pacemaker," *Circulation*, vol. 119, no. 12, pp. 1562–1575, 2009.

[9] A. O. Verkerk, R. Wilders, M. M. G. J. van Borren et al., "Pacemaker current (I_f) in the human sinoatrial node," *European Heart Journal*, vol. 28, no. 20, pp. 2472–2478, 2007.

[10] A. O. Verkerk, R. Wilders, M. M. G. J. van Borren, and H. L. Tan, "Is sodium current present in human sinoatrial node cells?" *International Journal of Biological Sciences*, vol. 5, no. 2, pp. 201–204, 2009.

[11] H. Dobrzynski, M. R. Boyett, and R. H. Anderson, "New insights into pacemaker activity: promoting understanding of sick sinus syndrome," *Circulation*, vol. 115, no. 14, pp. 1921–1932, 2007.

[12] A. O. Verkerk, A. C. G. van Ginneken, and R. Wilders, "Pacemaker activity of the human sinoatrial node: role of the hyperpolarization-activated current, I_f," *International Journal of Cardiology*, vol. 132, no. 3, pp. 318–336, 2009.

[13] W. Zareba, A. J. Moss, P. J. Schwartz et al., "Influence of the genotype on the clinical course of the long-QT syndrome," *The New England Journal of Medicine*, vol. 339, no. 14, pp. 960–965, 1998.

[14] H. Swan, M. Viitasalo, K. Piippo, P. Laitinen, K. Kontula, and L. Toivonen, "Sinus node function and ventricular repolarization during exercise stress test in long QT syndrome patients with KvLQT1 and HERG potassium channel defects," *Journal of the American College of Cardiology*, vol. 34, no. 3, pp. 823–829, 1999.

[15] A. Leenhardt, I. Denjoy, and P. Guicheney, "Catecholaminergic polymorphic ventricular tachycardia," *Circulation Arrhythmia and Electrophysiology*, vol. 5, no. 5, pp. 1044–1052, 2012.

[16] A. Leenhardt, V. Lucet, I. Denjoy, F. Grau, Dien Do Ngoc, and P. Coumel, "Catecholaminergic polymorphic ventricular tachycardia in children: a 7-year follow-up of 21 patients," *Circulation*, vol. 91, no. 5, pp. 1512–1519, 1995.

[17] N. Sumitomo, K. Harada, M. Nagashima et al., "Catecholaminergic polymorphic ventricular tachycardia: electrocardiographic characteristics and optimal therapeutic strategies to prevent sudden death," *Heart*, vol. 89, no. 1, pp. 66–70, 2003.

[18] A. V. Postma, I. Denjoy, T. M. Hoorntje et al., "Absence of calsequestrin 2 causes severe forms of catecholaminergic polymorphic ventricular tachycardia," *Circulation Research*, vol. 91, no. 8, pp. e21–e26, 2002.

[19] A. V. Postma, I. Denjoy, J. Kamblock et al., "Catecholaminergic polymorphic ventricular tachycardia: RYR2 mutations, bradycardia, and follow up of the patients," *Journal of Medical Genetics*, vol. 42, no. 11, pp. 863–870, 2005.

[20] M. Courtemanche, R. J. Ramirez, and S. Nattel, "Ionic mechanisms underlying human atrial action potential properties: insights from a mathematical model," *American Journal of Physiology*, vol. 275, no. 1, pp. H301–H321, 1998.

[21] E. A. Allah, J. O. Tellez, J. Yanni et al., "Changes in the expression of ion channels, connexins and Ca^{2+}-handling proteins in the sino-atrial node during postnatal development," *Experimental Physiology*, vol. 96, no. 4, pp. 426–438, 2011.

[22] A. O. Verkerk, H. M. den Ruijter, J. Bourier et al., "Dietary fish oil reduces pacemaker current and heart rate in rabbit," *Heart Rhythm*, vol. 6, no. 10, pp. 1485–1492, 2009.

[23] M. M. G. J. van Borren, A. O. Verkerk, R. Wilders et al., "Effects of muscarinic receptor stimulation on Ca^{2+} transient, cAMP production and pacemaker frequency of rabbit sinoatrial node cells," *Basic Research in Cardiology*, vol. 105, no. 1, pp. 73–87, 2010.

[24] A. L. Hodgkin and A. F. Huxley, "A quantitative description of membrane current and its application to conduction and excitation in nerve," *The Journal of Physiology*, vol. 117, no. 4, pp. 500–544, 1952.

[25] S. Dokos, B. Celler, and N. Lovell, "Ion currents underlying sinoatrial node pacemaker activity: a new single cell mathematical model," *Journal of Theoretical Biology*, vol. 181, no. 3, pp. 245–272, 1996.

[26] A. C. G. van Ginneken and W. Giles, "Voltage clamp measurements of the hyperpolarization-activated inward current I_f in single cells from rabbit sino-atrial node," *Journal of Physiology*, vol. 434, pp. 57–83, 1991.

[27] Y. Kurata, I. Hisatome, S. Imanishi, and T. Shibamoto, "Dynamical description of sinoatrial node pacemaking: improved mathematical model for primary pacemaker cell," *American Journal of Physiology Heart and Circulatory Physiology*, vol. 283, no. 5, pp. H2074–H2101, 2002.

[28] V. A. Maltsev and E. G. Lakatta, "Synergism of coupled subsarcolemmal Ca^{2+} clocks and sarcolemmal voltage clocks confers robust and flexible pacemaker function in a novel pacemaker cell model," *American Journal of Physiology Heart and Circulatory Physiology*, vol. 296, no. 3, pp. H594–H615, 2009.

[29] A. O. Verkerk, M. M. G. J. van Borren, R. J. G. Peters et al., "Single cells isolated from human sinoatrial node: action potentials and numerical reconstruction of pacemaker current," in *Proceedings of the 29th Annual International Conference of Engineering in Medicine and Biology Society (EMBC '07)*, pp. 904–907, August 2007.

[30] A. O. Verkerk and R. Wilders, "Relative importance of funny current in human versus rabbit sinoatrial node," *Journal of Molecular and Cellular Cardiology*, vol. 48, no. 4, pp. 799–801, 2010.

[31] M. M. G. J. van Borren, J. G. Zegers, A. O. Verkerk, and R. Wilders, "Computational model of rabbit SA node pacemaker activity probed with action potential and calcium transient clamp," in *Proceedings of the 29th Annual International Conference of Engineering in Medicine and Biology Society (EMBC '07)*, pp. 156–159, August 2007.

[32] D. S. Lindblad, C. R. Murphey, J. W. Clark, and W. R. Giles, "A model of the action potential and underlying membrane currents in a rabbit atrial cell," *American Journal of Physiology*, vol. 271, no. 4, part 2, pp. H1666–H1696, 1996.

[33] R. Wilders and H. J. Jongsma, "Beating irregularity of single pacemaker cells isolated from the rabbit sinoatrial node," *Biophysical Journal*, vol. 65, no. 6, pp. 2601–2613, 1993.

[34] A. Zaza, M. Micheletti, A. Brioschi, and M. Rocchetti, "Ionic currents during sustained pacemaker activity in rabbit sinoatrial myocytes," *Journal of Physiology*, vol. 505, no. 3, pp. 677–688, 1997.

[35] M. S. Imtiaz, P. Y. von der Weid, D. R. Laver, and D. F. van Helden, "SR Ca^{2+} store refill-a key factor in cardiac pacemaking," *Journal of Molecular and Cellular Cardiology*, vol. 49, no. 3, pp. 412–426, 2010.

[36] T. M. Vinogradova, S. Sirenko, A. E. Lyashkov et al., "Constitutive phosphodiesterase activity restricts spontaneous beating rate of cardiac pacemaker cells by suppressing local Ca^{2+} releases," *Circulation Research*, vol. 102, no. 7, pp. 761–769, 2008.

[37] G. M. Faber and Y. Rudy, "Action potential and contractility changes $[Na^+]_i$ in overloaded cardiac myocytes: a simulation study," *Biophysical Journal*, vol. 78, no. 5, pp. 2392–2404, 2000.

Hindawi Publishing Corporation
The Scientific World Journal
Volume 2013, Article ID 837086, 6 pages
http://dx.doi.org/10.1155/2013/837086

Review Article

Predictors of Cardiac Resynchronization Therapy Response: The Pivotal Role of Electrocardiogram

Yahya S. Al Hebaishi,[1] Halia Z. Al Shehri,[2] and Abdulrahman M. Al Moghairi[1]

[1] *Adult Cardiology Department, Prince Sultan Cardiac Centre (PSCC), Prince Sultan Military Medical City, P.O. Box 27656, Riyadh 11427, Saudi Arabia*
[2] *Adult Cardiology Department, Prince Salman Heart Center, King Fahad Medical City, P.O. Box 59046, Riyadh 11525, Saudi Arabia*

Correspondence should be addressed to Abdulrahman M. Al Moghairi; aalmoghairi@pscc.med.sa

Received 25 January 2013; Accepted 21 February 2013

Academic Editors: Y. Du and Y. Wang

Heart failure affects millions of patients all over the world, and its treatment is a major clinical challenge. Cardiac dyssynchrony is common among patients with advanced heart failure. Resynchronization therapy is a major advancement in heart failure management, but unfortunately not all patients respond to this therapy. Hence, many diagnostic tests have been used to predict the response and prognosis after cardiac resynchronization therapy. In this paper we summarize the usefulness of different diagnostic modalities with special emphasis on the role of surface electrocardiogram as a major predictor of response to cardiac resynchronization therapy.

1. Introduction

Heart failure is estimated to affect more than 23 million people worldwide with an approximately 2 million new cases diagnosed annually [1]. In the United States it is estimated that 5.1 million people have HF [2]. The incidence of heart failure increases with age, with approximately 10 in every 1,000 at age above 65 years being affected [2, 3]. Left bundle branch block (LBBB) and wide QRS complex are surrogates of left ventricular dyssynchrony that are commonly found in heart failure patients, and their presences associated with increased mortality [4–6]. In addition to medical therapy, implantable device therapy has become a standard therapy for refractory heart failure. Cardiac resynchronization therapy (CRT) has been shown to improve symptoms, quality of life, and survival and to enhance reverse remodeling in appropriately selected patients [7–9]. The efficacy of such therapy was demonstrated in patients with moderate and severe heart failure and more recently patient with mild heart failure symptoms [7–13]. Albeit the clinical response to CRT is evident in the majority of case, the lack of response still seen in approximately one-third of patients [7]. In this paper we discuss the potential value of different imaging modalities and ECG parameters in predicting CRT response.

2. Patient's Selection for CRT: Is There Still a Role for Echo and Other Imaging Modalities?

Correction of left ventricular (LV) dyssynchrony is thought to be the main therapeutic effect of CRT. In the past decade several imaging techniques were used to quantify mechanical dyssynchrony and predict CRT response; these imaging techniques include M-mode echocardiography, Tissue Doppler imaging (TDI), Strain imaging, 3-dimensional echocardiography, magnetic resonance imaging, and nuclear cardiology. In addition to the technical difficulty and increased cost associated with the use of these imaging techniques, the accuracy of such modalities in predicting CRT is questionable.

Multiple echocardiographic parameters had been shown to correlate with the response to CRT in several trials; however, the PROSPECT, large, multicenter, and prospective study, of 498 patients demonstrated that the tested 12 different

echocardiographic dyssynchrony measures were unable to distinguish responders from nonresponders to a degree that may influence clinical decision [9, 14–16].

Real-time 3-dimensional echocardiography (RT3DE) is an emerging technique for left ventricular (LV) dyssynchrony assessment. The advantage of RT3DE is its ability to provide simultaneous information of the global LV contractility [17]. In a series of 57 consecutive heart failure patients scheduled for CRT, Marsan et al. evaluated the systolic dyssynchrony index (SDI) obtained by RT3DE. SDI cutoff value of 6.4% yielded a sensitivity of 88% and specificity of 85% to predict response to CRT [18]. In another study of sixty heart failure patients, triple plane TDI was able to predict six months clinical response and reverse LV remodeling after CRT implantation with a sensitivity of 89% and specificity of 82% [19]. Despite the promising early studies these techniques have their own limitations and need further validation.

Nuclear imaging with single photon emission computed tomography (SPECT) and magnetic resonance imaging (MRI) are another modalities, which have been used in the assessment of LV mechanical dyssynchrony. Additional advantage of both techniques is their ability to assess the presence and location of LV transmural scar, which may influence LV lead positioning Figure 1. Large-scale clinical trials are needed to evaluate the role of such modalities in predicting the long-term response to CRT [20–24].

3. 12 Leads ECG Remains the Gold Standard Test for CRT Patient Selection

Despite the wide availability of clinical and investigational imaging modalities to evaluate the patient response to CRT with variable accuracy, a simple 12-lead remains the standard test for patient selection. Several ECG parameters used to predict the response to CRT, including baseline rhythm, QRS duration, QRS morphology, LV activation sequence, and the PR interval.

3.1. QRS Duration. Prolonged QRS duration (≥120 ms) as measured on the standard 12-lead ECG is the most commonly used parameter in clinical practice to identify eligible candidates for CRT [25–28]. Despite the apparent simplicity and the reasonable reproducibility, accurate measurement of QRS duration remains a clinical challenge and an operator dependent. The main source of error seems to be in identifying the beginning and the end of QRS complex on surface ECG. The onset and the end of the QRS complex may be isoelectric, resulting in underestimation of the actual QRS duration. Other potential sources of error include fluctuation of the baseline and presence of a notch or a pacing spike at the onset of the QRS complex or contamination of the QRS complex by the repolarization changes. Computer measurements may provide more precise and more reproducible measurements in presence of a good quality 12-lead ECG [29].

3.2. Normal QRS Duration. More than 27% of heart failure patients with reduced left ventricular systolic function and QRS duration <120 ms have evidence of mechanical dyssynchrony by TDI, and the presence of which seems to be associated with increased mortality [30–32]. Few nonrandomized studies suggested a beneficial outcome from CRT in this patient population; however, the RethinQ study showed no benefit in 172 patients with QRS duration <130 ms and mechanical dyssynchrony randomized to biventricular implantable cardioverter defibrillator against the control group. Furthermore, at six months there was no difference in Peak VO2, 6-minute walk test, LV reverse remodeling and quality of life score between the treatment and control groups [33–35].

3.3. Intermediate QRS Duration. The degree of QRS duration prolongation is an indicator of severity of electrical dyssynchrony [30]. QRS duration of 120 milliseconds or greater had been used as an entry criteria of major clinical trials (COMPANION, CARE-HF, RAFT, and REVERSE) [25–28]. Small studies using hemodynamics or peak oxygen consumption endpoints suggest that patients with intermediate QRS duration (QRS between 120 and 150 milliseconds) may not benefit from CRT [36, 37]. However, a meta-analysis that included the COMPANION, CARE-HF, REVERSE, MADIT-CRT, and RAFT trials found that CRT was effective in reducing adverse clinical events in patients with heart failure and a baseline QRS interval of 150 milliseconds or greater, but not in patients with a QRS of <150 milliseconds, and this difference in response between these QRS subgroups was seen in all New York Heart Association (NYHA) functional classes [38].

3.4. QRS Morphology. Baseline QRS morphology is probably equally important as QRS duration to predict response to CRT. Patients with a prolonged QRS duration may have a left bundle-branch block (LBBB), right bundle-branch Block (RBBB), nonspecific intraventricular conduction delay (IVCD), or paced rhythm. The presence of typical LBBB morphology is a strong predictor of response compared with right bundle branch block (RBBB) morphology and nonspecific intraventricular conduction delay (IVCD) that has a much lower probability of CRT response [39, 40].

3.5. LBBB and LV Activation Patterns. In LBBB significant depolarization delay between the anteroseptal and posterolateral walls occurs which thought to explains the efficacy of CRT in this patients population. Careful evaluation of the QRS morphology in patients with apparent LBBB may yield important further information. An early report by Grant and Doge suggested that reversal of the intraventricular septal activation pattern should occur with the onset of LBBB, which is reflected in the initial 40 ms of the QRS complex; however, these expected changes were absent in 40% of the study patients who developed new LBBB [41]. Similarly Auricchio et al, using 3-dimensional (3D) nonfluoroscopic contact and noncontact mapping, studied the LV activation pattern (including LV endocardial breakthrough site, transseptal activation time, and duration of LV endocardial activation) and found that 32% of patients with apparent LBBB had <20 ms delay between the RV activation compared

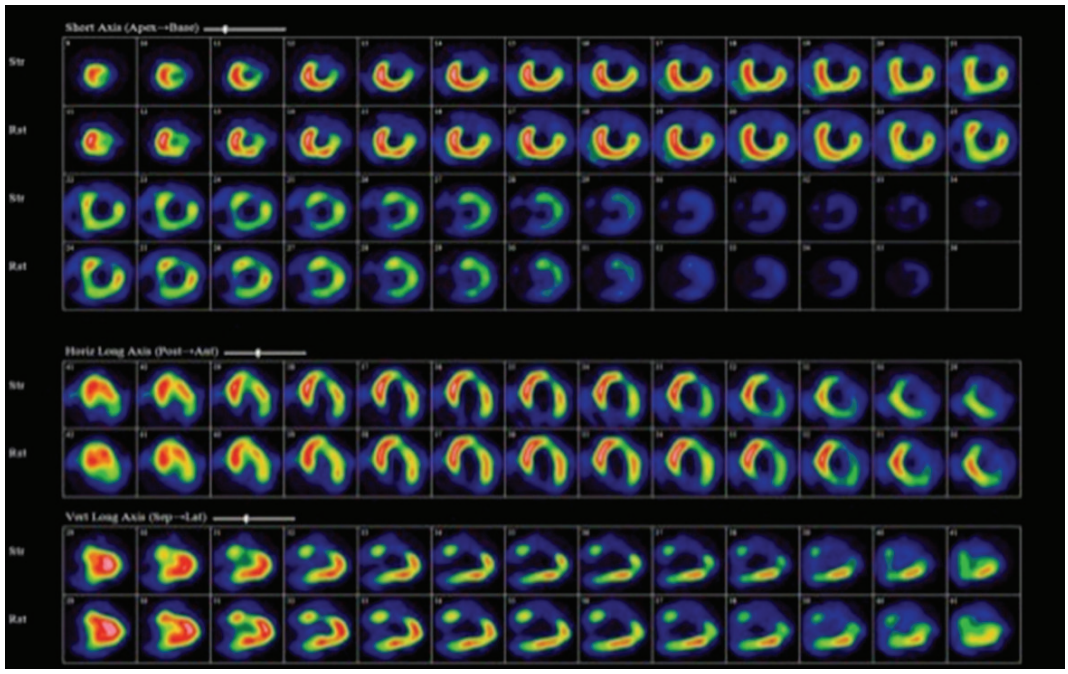

Figure 1: Baseline Tc-99m SPECT myocardial perfusions scan from CRT candidate demonstrating a fixed perfusion defect involving anterior and anterolateral wall consistent with transmural scar. Intraoperative testing demonstrated a high pacing threshold at anterolateral LV lead position; excellent pacing threshold was obtained from a posterolateral coronary sinus branch.

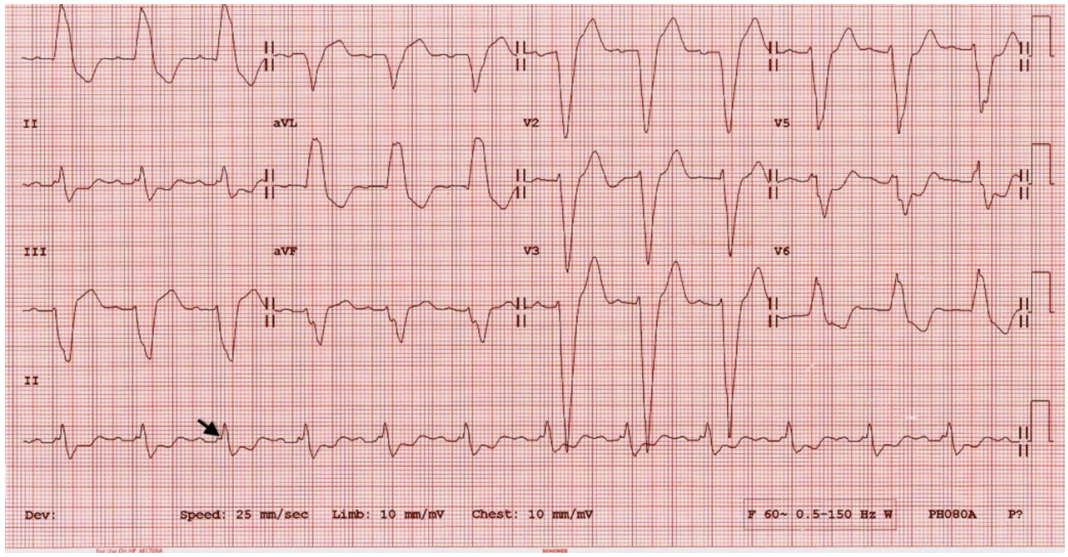

Figure 2: Baseline ECG from CRT super responder showing several predictors of good response including sinus rhythm, long PR interval, typical LBBB with mid-QRS slurring in lateral leads, QRS duration >200 ms, and long $LVAT_{max}$ measured by subtracting RVAT from the QRS duration. Arrow indicates the end of RVAT.

to LV endocardium and >40 ms in the remaining group, and the mean QRS duration was significantly different between the two groups (133 ± 28 ms, versus 170 ± 16 ms, resp.) [42]. Based on these observations and their own work Strauss and Sylvester argued that a QRS duration of 120–140 ms often represent left ventricular hypertrophy rather than a true LBBB and proposed that the criteria for complete LBBB should include QRS duration >140 ms in men or 130 ms in women. QS or rS in leads V1 and V2 and mid-QRS notching or slurring in at least two of leads V1, V2, V5, V6, I, and aVL [43].

In a study of 202 consecutive heart failure patients with LBBB, Sweeney et al. developed a predictive model to test the hypothesis that the probability of reverse volumetric remodeling could be predicted by the ventricular activation pattern on the 12-lead ECG before and after CRT. Their main

findings were that activation wave front fusion on the paced post-CRT ECG and prolonged maximum LV conduction time ($LVAT_{max}$) on baseline ECG are associated with higher probability of reverse remodeling. $LVAT_{max}$ is the difference between the total QRS duration and the right ventricular activation time (RVAT), where the RVAT represents the interval between the beginning of QRS and the early QRS notch (Figure 2) [44]. In the most recent ACCF/AHA/HRS guidelines update class I, indication for CRT was given only to symptomatic patients in sinus rhythm who have LBBB with a QRS duration greater than or equal to 150 ms and LV ejection fraction less than or equal to 35% [27].

3.6. RBBB and Nonspecific IVCD. Unlike LBBB, ventricular activation is not largely affected in RBBB, therefore from theoretical perspective CRT is not expected to be effective in this subgroup of patients [45]. Less than 15% of patients in the large controlled CRT trials had RBBB on baseline ECG, and as a result most available clinical data addressing the efficacy of CRT in RBBB are derived from retrospective data analyzing a relatively small number of patients [8, 9, 12, 13, 46]. Similarly, prospective studies included only a small number of patients with RBBB [47]. Systematic review of five studies which reported data on patients with RBBB including 259 patients randomized to CRT and 226 randomized to non-CRT showed unfavorable outcomes in patients with CRT [48]. Recently a meta-analysis of 5356 patients included in the major CRT trials, COMPANION, CARE-HF, MADIT-CRT, and RAFT trial, showed no benefit from CRT in patients with RBBB (RR: 0.91; 95% CI: 0.69–1.20; $P = 0.49$) or nonspecific IVCD (RR: 1.19; 95% CI: 0.87–1.63; $P = 0.28$) [40]. Furthermore, there was no heterogeneity among the clinical trials in the lack of benefit in non-LBBB patients. The benefit of CRT is significantly higher in LBBB compared with non-LBBB group; $P = 0.0001$ [40].

3.7. Patient Rhythm, P Wave Morphology and the PR Interval. Patient rhythm, interatrial conduction delay and the magnitude of atrioventricular delay, as represented by the native PR interval are additional valuable information that may influence CRT response and can be easily obtained from the baseline 12-lead ECG.

The role of CRT in patients with atrial fibrillation is not well established: major clinical trials of resynchronization included mainly patients in sinus rhythm. However, other studies suggested a positive outcome in AF patients [49–51]. A meta-analysis of 1,164 patients in five studies showed that patients in AF had a significant improvement after CRT, with similar or improved ejection fraction as sinus rhythm patients, but the functional improvement was less [52].

Interatrial conduction delay is characterized by a wide and notched P wave in lead II with a wide terminal negative deflection in lead V1. Significant interatrial delay may results in left atrial contraction during LV systole, which may negatively affect CRT outcome. In such cases simultaneous activation of both atria could be achieved by implantation of the atrial lead in the interatrial septum [53].

To ensure near 100% biventricular pacing in CRT, the programmed AV delay should be shorter than the native PR interval, this programming may truncate the left ventricular filling resulting in a suboptimal response to CRT; however, the presence of a long native PR interval may permit a more physiological AV delay programming. Subgroup analysis of patients in the COMPANION trial demonstrated that randomization to CRT was associated with a reduction in the endpoint, but the strength of the association was greater for those with prolonged PR (hazard ratio = 0.54; $P < 0.01$) versus normal PR (hazard ratio = 0.71; $P = 0.02$) intervals [54].

4. Conclusion

Prediction of CRT response is a complex and subject of extensive research over the past decade. Despite all we know about CRT, a significant proportion of heart failure patient dose not respond to CRT. However, careful analysis of simple 12-lead ECG can yield impressive data difficult to replace by any of the available more sophisticated clinical tools.

References

[1] J. J. V. McMurray, M. C. Petrie, D. R. Murdoch, and A. P. Davie, "Clinical epidemiology of heart failure: public and private health burden," *European Heart Journal*, vol. 19, supplement P, pp. P9–P16, 1998.

[2] A. S. Go, D. Mozaffarian, V. L. Roger et al. et al., "Heart disease and stroke statistics—2013 update: a report from the American heart association," *Circulation*, vol. 127, no. 1, pp. e6–e245, 2013.

[3] K. K. L. Ho, J. L. Pinsky, W. B. Kannel, and D. Levy, "The epidemiology of heart failure: the framingham study," *Journal of the American College of Cardiology*, vol. 22, no. 4, supplement A, pp. 6A–13A, 1993.

[4] F. A. Masoudi, E. P. Havranek, G. Smith et al., "Gender, age, and heart failure with preserved left ventricular systolic function," *Journal of the American College of Cardiology*, vol. 41, no. 2, pp. 217–223, 2003.

[5] K. D. Aaronson, J. S. Schwartz, T. M. Chen, K. L. Wong, J. E. Goin, and D. M. Mancini, "Development and prospective validation of a clinical index to predict survival in ambulatory patients referred for cardiac transplant evaluation," *Circulation*, vol. 95, no. 12, pp. 2660–2667, 1997.

[6] S. Baldasseroni, L. de Biase, C. Fresco et al., "Cumulative effect of complete left bundle-branch block and chronic atrial fibrillation on 1-year mortality and hospitalization in patients with congestive heart failure: a report from the Italian network on congestive heart failure (in-CHF database)," *European Heart Journal*, vol. 23, no. 21, pp. 1692–1698, 2002.

[7] J. G. F. Cleland, J. C. Daubert, E. Erdmann et al., "The effect of cardiac resynchronization on morbidity and mortality in heart failure," *The New England Journal of Medicine*, vol. 352, no. 15, pp. 1539–1549, 2005.

[8] C. Linde, W. T. Abraham, M. R. Gold, S. M. S. John, S. Ghio, and C. Daubert, "Randomized trial of cardiac resynchronization in mildly symptomatic heart failure patients and in asymptomatic patients with left ventricular dysfunction and previous heart failure symptoms," *Journal of the American College of Cardiology*, vol. 52, no. 23, pp. 1834–1843, 2008.

[9] C. Daubert, M. R. Gold, W. T. Abraham et al., "Prevention of Disease progression by cardiac resynchronization therapy in patients with asymptomatic or mildly symptomatic left ventricular dysfunction. Insights from the european cohort of the REVERSE (Resynchronization Reverses Remodeling in Systolic Left Ventricular Dysfunction) trial," *Journal of the American College of Cardiology*, vol. 54, no. 20, pp. 1837–1846, 2009.

[10] W. T. Abraham, W. G. Fisher, A. L. Smith et al., "Cardiac resynchronization in chronic heart failure," *The New England Journal of Medicine*, vol. 346, no. 24, pp. 1845–1853, 2002.

[11] M. R. Bristow, L. A. Saxon, J. Boehmer et al., "Cardiac-resynchronization therapy with or without an implantable defibrillator in advanced chronic heart failure," *The New England Journal of Medicine*, vol. 350, no. 21, pp. 2140–2150, 2004.

[12] A. J. Moss, W. J. Hall, D. S. Cannom et al., "Cardiac-resynchronization therapy for the prevention of heart-failure events," *The New England Journal of Medicine*, vol. 361, no. 14, pp. 1329–1338, 2009.

[13] A. S. L. Tang, G. A. Wells, M. Talajic et al., "Cardiac-resynchronization therapy for mild-to-moderate heart failure," *The New England Journal of Medicine*, vol. 363, no. 25, pp. 2385–2395, 2010.

[14] D. Mele, G. Pasanisi, F. Capasso et al., "Left intraventricular myocardial deformation dyssynchrony identifies responders to cardiac resynchronization therapy in patients with heart failure," *European Heart Journal*, vol. 27, no. 9, pp. 1070–1078, 2006.

[15] M. V. Pitzalis, M. Iacoviello, R. Romito et al., "Cardiac resynchronization therapy tailored by echocardiographic evaluation of ventricular asynchrony," *Journal of the American College of Cardiology*, vol. 40, no. 9, pp. 1615–1622, 2002.

[16] E. S. Chung, A. R. Leon, L. Tavazzi et al., "Results of the predictors of response to crt (prospect) trial," *Circulation*, vol. 117, no. 20, pp. 2608–2616, 2008.

[17] P. Sogaard, H. Egeblad, W. Y. Kim et al., "Tissue Doppler imaging predicts improved systolic performance and reversed left ventricular remodeling during long-term cardiac resynchronization therapy," *Journal of the American College of Cardiology*, vol. 40, no. 4, pp. 723–730, 2002.

[18] N. A. Marsan, G. B. Bleeker, C. Ypenburg et al., "Real-time three-dimensional echocardiography as a novel approach to assess left ventricular and left atrium reverse remodeling and to predict response to cardiac resynchronization therapy," *Heart Rhythm*, vol. 5, no. 9, pp. 1257–1264, 2008.

[19] N. R. van de Veire, C. M. Yu, N. Ajmone-Marsan et al., "Triplane tissue Doppler imaging: a novel three-dimensional imaging modality that predicts reverse left ventricular remodelling after cardiac resynchronisation therapy," *Heart*, vol. 94, no. 3, article e9, 2008.

[20] J. Chen, E. V. Garcia, R. D. Folks et al., "Onset of left ventricular mechanical contraction as determined by phase analysis of ECG-gated myocardial perfusion SPECT imaging: development of a diagnostic tool for assessment of cardiac mechanical dyssynchrony," *Journal of Nuclear Cardiology*, vol. 12, no. 6, pp. 687–695, 2005.

[21] M. M. Henneman, J. Chen, C. Ypenburg et al., "Phase analysis of gated myocardial perfusion single-photon emission computed tomography compared with tissue doppler imaging for the assessment of left ventricular dyssynchrony," *Journal of the American College of Cardiology*, vol. 49, no. 16, pp. 1708–1714, 2007.

[22] K. C. Bilchick, V. Dimaano, K. C. Wu et al., "Cardiac magnetic resonance assessment of dyssynchrony and myocardial scar predicts function class improvement following cardiac resynchronization therapy," *JACC: Cardiovascular Imaging*, vol. 1, no. 5, pp. 561–568, 2008.

[23] A. J. Taylor, M. Elsik, A. Broughton et al., "Combined dyssynchrony and scar imaging with cardiac magnetic resonance imaging predicts clinical response and long-term prognosis following cardiac resynchronization therapy," *Europace*, vol. 12, no. 5, pp. 708–713, 2010.

[24] E. C. Adelstein and S. Saba, "Scar burden by myocardial perfusion imaging predicts echocardiographic response to cardiac resynchronization therapy in ischemic cardiomyopathy," *The American Heart Journal*, vol. 153, no. 1, pp. 105–112, 2007.

[25] S. A. Hunt, W. T. Abraham, M. H. Chin et al., "2009 focused update incorporated into the ACC/AHA 2005 guidelines for the diagnosis and management of heart failure in adults. A report of the American college of cardiology foundation/American heart association task force on practice guidelines developed in collaboration with the international society for heart and lung transplantation," *Journal of the American College of Cardiology*, vol. 53, no. 15, pp. e1–e90, 2009.

[26] K. Dickstein, P. E. Vardas, A. Auricchio et al., "2010 focused update of ESC guidelines on device therapy in heart failure: an update of the 2008 ESC guidelines for the diagnosis and treatment of acute and chronic heart failure and the 2007 ESC guidelines for cardiac and resynchronization therapy—developed with the special contribution of the heart failure association and the european heart rhythm association," *Europace*, vol. 12, no. 11, pp. 1526–1536, 2010.

[27] C. M. Tracy, A. E. Epstein, D. Darbar et al. et al., "2012 ACCF/AHA/HRS focused update of the 2008 guidelines for device-based therapy of cardiac rhythm abnormalities: a report of the American college of cardiology foundation/American heart association task force on practice guidelines," *Journal of the American College of Cardiology*, vol. 60, no. 14, pp. 1297–1313, 2012.

[28] J. J. McMurray, S. Adamopoulos, S. D. Anker et al. et al., "ESC Guidelines for the diagnosis and treatment of acute and chronic heart failure 2012: the task force for the diagnosis and treatment of acute and chronic heart failure 2012 of the european society of cardiology. Developed in collaboration with the heart failure association (HFA) of the ESC," *European Heart Journal*, vol. 33, no. 14, pp. 1787–1847, 2012.

[29] M. de Guillebon, J. B. Thambo, S. Ploux et al., "Reliability and reproducibility of QRS duration in the selection of candidates for cardiac resynchronization therapy," *Journal of Cardiovascular Electrophysiology*, vol. 21, no. 8, pp. 890–892, 2010.

[30] G. B. Bleeker, M. J. Schalij, S. G. Molhoek et al., "Relationship between QRS duration and left ventricular dyssynchrony in patients with end-stage heart failure," *Journal of Cardiovascular Electrophysiology*, vol. 15, no. 5, pp. 544–549, 2004.

[31] R. Perry, C. G. de Pasquale, D. P. Chew, P. E. Aylward, and M. X. Joseph, "QRS duration alone misses cardiac dyssynchrony in a substantial proportion of patients with chronic heart failure," *Journal of the American Society of Echocardiography*, vol. 19, no. 10, pp. 1257–1263, 2006.

[32] G. Y. Cho, J. K. Song, W. J. Park et al., "Mechanical dyssynchrony assessed by tissue doppler imaging is a powerful predictor of mortality in congestive heart failure with normal QRS duration," *Journal of the American College of Cardiology*, vol. 46, no. 12, pp. 2237–2243, 2005.

[33] G. B. Bleeker, E. R. Holman, P. Steendijk et al., "Cardiac resynchronization therapy in patients with a narrow QRS complex," *Journal of the American College of Cardiology*, vol. 48, no. 11, pp. 2243–2250, 2006.

[34] C. M. Yu, Y. S. Chan, Q. Zhang et al., "Benefits of cardiac resynchronization therapy for heart failure patients with narrow QRS complexes and coexisting systolic asynchrony by echocardiography," *Journal of the American College of Cardiology*, vol. 48, no. 11, pp. 2251–2257, 2006.

[35] J. F. Beshai, R. A. Grimm, S. F. Nagueh et al., "Cardiac-resynchronization therapy in heart failure with narrow QRS complexes," *The New England Journal of Medicine*, vol. 357, no. 24, pp. 2461–2471, 2007.

[36] A. Auricchio, C. Stellbrink, M. Block et al., "Effect of pacing chamber and atrioventricular delay on acute systolic function of paced patients with congestive heart failure," *Circulation*, vol. 99, no. 23, pp. 2993–3001, 1999.

[37] A. Auricchio, C. Stellbrink, C. Butter et al., "Clinical efficacy of cardiac resynchronization therapy using left ventricular pacing in heart failure patients stratified by severity of ventricular conduction delay," *Journal of the American College of Cardiology*, vol. 42, no. 12, pp. 2109–2116, 2003.

[38] I. Sipahi, T. P. Carrigan, D. Y. Rowland, B. S. Stambler, and J. C. Fang, "Impact of QRS duration on clinical event reduction with cardiac resynchronization therapy: meta-analysis of randomized controlled trials," *Archives of Internal Medicine*, vol. 171, no. 16, pp. 1454–1462, 2011.

[39] W. Zareba, H. Klein, I. Cygankiewicz et al., "Effectiveness of cardiac resynchronization therapy by QRS morphology in the multicenter automatic defibrillator implantation trial-cardiac resynchronization therapy (MADIT-CRT)," *Circulation*, vol. 123, no. 10, pp. 1061–1072, 2011.

[40] I. Sipahi, J. C. Chou, M. Hyden, D. Y. Rowland, D. I. Simon, and J. C. Fang, "Effect of QRS morphology on clinical event reduction with cardiac resynchronization therapy: meta-analysis of randomized controlled trials," *The American Heart Journal*, vol. 163, no. 2, pp. 260.e3–267.e3, 2012.

[41] R. P. Grant and H. T. Dodge, "Mechanisms of QRS complex prolongation in man; left ventricular conduction disturbances," *The American Journal of Medicine*, vol. 20, no. 6, pp. 834–852, 1956.

[42] A. Auricchio, C. Fantoni, F. Regoli et al., "Characterization of left ventricular activation in patients with heart failure and left bundle-branch block," *Circulation*, vol. 109, no. 9, pp. 1133–1139, 2004.

[43] D. G. Strauss, R. H. Selvester, and G. S. Wagner, "Defining left bundle branch block in the era of cardiac resynchronization therapy," *The American Journal of Cardiology*, vol. 107, no. 6, pp. 927–934, 2011.

[44] M. O. Sweeney, R. J. van Bommel, M. J. Schalij, C. J. W. Borleffs, A. S. Hellkamp, and J. J. Bax, "Analysis of ventricular activation using surface electrocardiography to predict left ventricular reverse volumetric remodeling during cardiac resynchronization therapy," *Circulation*, vol. 121, no. 5, pp. 626–634, 2010.

[45] K. Kaszala and K. A. Ellenbogen, "When right may not be right: right bundle-branch block and response to cardiac resynchronization therapy," *Circulation*, vol. 122, no. 20, pp. 1999–2001, 2010.

[46] E. C. Adelstein and S. Saba, "Usefulness of baseline electrocardiographic QRS complex pattern to predict response to cardiac resynchronization," *The American Journal of Cardiology*, vol. 103, no. 2, pp. 238–242, 2009.

[47] H. Hara, O. A. Oyenuga, H. Tanaka et al., "The relationship of QRS morphology and mechanical dyssynchrony to long-term outcome following cardiac resynchronization therapy," *European Heart Journal*, vol. 33, no. 21, pp. 2680–2691, 2012.

[48] P. B. Nery, A. C. Ha, A. Keren, and D. H. Birnie, "Cardiac resynchronization therapy in patients with left ventricular systolic dysfunction and right bundle branch block: a systematic review," *Heart Rhythm*, vol. 8, no. 7, pp. 1083–1087, 2011.

[49] C. Linde, C. Leclercq, S. Rex et al., "Long-term benefits of biventricular pacing in congestive heart failure: results from the MUltisite STimulation In Cardiomyopathy (MUSTIC) study," *Journal of the American College of Cardiology*, vol. 40, no. 1, pp. 111–118, 2002.

[50] C. Leclercq, S. Walker, C. Linde et al., "Comparative effects of permanent biventricular and right-univentricular pacing in heart failure patients with chronic atrial fibrillation," *European Heart Journal*, vol. 23, no. 22, pp. 1780–1787, 2002.

[51] P. P. H. M. Delnoy, J. P. Ottervanger, H. O. Luttikhuis et al., "Comparison of usefulness of cardiac resynchronization therapy in patients with atrial fibrillation and heart failure versus patients with sinus rhythm and heart failure," *The American Journal of Cardiology*, vol. 99, no. 9, pp. 1252–1257, 2007.

[52] G. A. Upadhyay, N. K. Choudhry, A. Auricchio, J. Ruskin, and J. P. Singh, "Cardiac resynchronization in patients with atrial fibrillation. A meta-analysis of prospective cohort studies," *Journal of the American College of Cardiology*, vol. 52, no. 15, pp. 1239–1246, 2008.

[53] A. Dabrowska-Kugacka, E. Lewicka, A. Faran, D. Kozlowski, M. Kempa, and G. Raczak, "Right atrial appendage pacing in cardiac resynchronization therapy—haemodynamic consequences of interatrial conduction delay," *Archives of Medical Science*, vol. 7, no. 4, pp. 728–731, 2011.

[54] B. Olshansky, J. D. Day, R. M. Sullivan, P. Yong, E. Galle, and J. S. Steinberg, "Does cardiac resynchronization therapy provide unrecognized benefit in patients with prolonged PR intervals? The impact of restoring atrioventricular synchrony: an analysis from the COMPANION Trial," *Heart Rhythm*, vol. 9, no. 1, pp. 34–39, 2012.

Hindawi Publishing Corporation
The Scientific World Journal
Volume 2013, Article ID 209428, 6 pages
http://dx.doi.org/10.1155/2013/209428

Review Article

Mechanism of and Therapeutic Strategy for Atrial Fibrillation Associated with Diabetes Mellitus

Yubi Lin, Hairui Li, Xianwu Lan, Xianghui Chen, Aidong Zhang, and Zicheng Li

Department of Cardiology, The First Affiliated Hospital of Jinan University, Guangzhou 0086-510630, China

Correspondence should be addressed to Zicheng Li; zichengli@163.net

Received 11 January 2013; Accepted 19 February 2013

Academic Editors: Y. Du and Y. Wang

Diabetes mellitus (DM) is one of the most important risk factors for atrial fibrillation (AF) and is a predictor of stroke and thromboembolism. DM may increase the incidence of AF, and when it is combined with other risk factors, the incidence of stroke and thromboembolism may also be higher; furthermore, hospitalization due to heart failure appears to increase. Maintenance of well-controlled blood glucose and low levels of HbA1c in accordance with guidelines may decrease the incidence of AF. The mechanisms of AF associated with DM are autonomic remodeling, electrical remodeling, structural remodeling, and insulin resistance. Inhibition of the renin-angiotensin system is suggested to be an upstream therapy for this type of AF. Studies have indicated that catheter ablation may be effective for AF associated with DM, restoring sinus rhythm and improving prognosis. Catheter ablation combined with hypoglycemic agents may further increase the rate of maintenance of sinus rhythm and reduce the need for reablation.

1. Introduction

Atrial fibrillation (AF) is the most common sustained cardiac rhythm disorder and contributes to thromboembolism. The presence of AF is an independent risk factor for thromboembolism; especially stroke in association with AF increases mortality and morbidity, leading to greater disability, longer hospital stays, and worse quality of life [1, 2]. There are approximately 40 million people with diabetes mellitus (DM) and 10 million with AF in China, and morbidity from AF is increasing with the aging population. AF seriously affects people's health. The abnormal glucose metabolism and DM can facilitate the occurrence and development of AF and are associated with a worse prognosis.

2. DM Is a Strong Risk Factor for AF

2.1. DM Increases the Incidence of AF. AF commonly coexists with cardiovascular risk factors and disorders, which in turn increase the risk of the complications associated with the arrhythmia. The common risk factors for AF are cardiovascular, including hypertension, congestive heart failure, valvular heart disease, and vascular disease. As a cardiovascular risk factor, DM may be associated with the development and progression of AF. Investigators in the VHAH study reported the incidence of AF in patients with DM to be 14.9%, which was significantly higher than that in patients with hypertension but not DM ($P < 0.0001$). DM is a strong and independent risk factor for the occurrence of AF, with an odds ratio (OR) of 2.13 ($P < 0.0001$) [3]. The VALUE trial showed that new onset DM could be attributed to a significant increase in the new onset of AF (relative risk (RR) 1.49, $P = 0.0031$) and a higher risk of developing persistent AF (RR 1.87, $P = 0.0014$). When patients with new onset DM developed AF, the occurrence of heart failure was much higher (RR 3.56, $P < 0.0001$) [4]. In Nichols' 7.2 ± 2.8-year follow-up study, the age- and gender-adjusted incidence of AF in DM patients (9.1/1000 person-years) was greater than that in non-DM patients (6.6/1000 person-years). Sex is an independent risk factor for AF; women with DM have about a 26% increased risk of developing AF [5]. A meta-analysis [6] of seven prospective cohort studies and four case-control studies included 1,686,097 cases, of which 108,703 had AF. The study indicated that DM was associated with about a 40% increased risk of AF compared with non-DM patients (RR 1.39, $P < 0.001$). After adjusting for multiple risk factors

for AF, the RR of AF in patients with DM was still 1.24, and the population-attributable fraction of AF owing to DM was 2.5%. Among 75-year-old patients, occurrence of AF was associated with long-term hyperglycemia, and it was suggested that proactive screening for DM or prediabetes should be performed in patients with a history of AF more than 5 years [7].

2.2. DM Increases the Incidence of AF When Accompanied by Other Diseases. DM with hypertension further increased the OR of AF to 3.3, from 0.7 in patients with hypertension only and 2.0 in those with DM only, though this increase had no statistical significance after adjusting for insulin resistance, suggesting that insulin resistance may be the underlying mechanism of AF [8]. The population-attributable fraction of AF owing to metabolic syndrome (hypertension, increased low-density lipoprotein, hypertriglyceridemia, and impaired glucose metabolism) was 22% and the RR was 4.40 in patients with all five components of this syndrome compared with those without the disorder; the more the components, the higher the RR. The multivariate-adjusted RR for impaired glucose tolerance was 1.16. This indicates that the risk of AF increases significantly when DM is combined with other risk factors [9].

2.3. Poorly Controlled Blood Glucose Increases the Risk of AF. The risk of AF is increased by 3%/year with prolonged DM. Compared with people without DM, the adjusted ORs for DM patients with average HbA1c ≤ 7, 7-8, 8-9, or >9 were 1.06, 1.48, 1.46, and 1.96, respectively [10], in a prospective cohort study involving 13,025 participants. There was a positive linear association between HbA1c and the risk of AF in patients with or without DM, with hazard ratios of 1.13 and 1.05, respectively. Fasting blood glucose and insulin level were correlated with the risk of AF in DM patients, but not in people without DM. For every 1% increase in HbA1c, the risk of AF increased by 5% in non-DM individuals, but by 13% in those with DM. The risk of AF has also been shown to increase with the duration of DM, high HbA1c levels, and poor blood glucose control [11].

3. Prognostic Evaluation of DM Patients with AF

AF is a marker of poor prognosis in patients with DM and increases the risk of cardiovascular events and all-cause mortality. Diabetic neuropathy may mask the cardiac symptoms of first-recorded AF, making it asymptomatic, which may increase the risk of further cardiovascular events and mortality [12]. The ADVANCE study showed a 61% ($P < 0.0001$) increase of multivariate-adjusted all-cause mortality in DM patients with AF during the 4.3-year follow-up period compared with those without AF, and cardiovascular mortality, risk of stroke, and heart failure increased significantly (all $P < 0.001$). Routine treatment with a fixed combination of perindopril and indapamide reduced blood pressure by 5.3/2.3 mmHg and by 5.9/2.3 mmHg more than placebo in patients with AF, significantly decreasing the risk of cardiovascular events and all-cause mortality. Thus, a comprehensive therapeutic strategy that aggressively targets all cardiovascular risk factors is very important for DM patients with AF [13].

DM was an independent risk factor for the recurrence of AF in patients with persistent AF who underwent successful synchronization with current cardioversion, over a median follow-up period of 74 days. In patients with DM, the sinus rhythm maintenance rate was 45.2%, which was lower than that of patients without DM (66.8%, $P < 0.0001$) [14]. A study [15] reported that even after successful direct current cardioversion in DM patients with persistent AF, there was no significant improvement of endothelial responsiveness to supine shear stress or orthostatic modulation, which may be associated with DM-induced endothelial relaxation-constriction dysfunction. In patients with AF alone or in association with hypertension, endothelial dysfunction improved significantly after successful direct current cardioversion. DM-induced oxidative stress injury may be an underlying mechanism of AF [16].

4. Underlying Mechanisms of Diabetes-Induced AF

The precise pathophysiologic mechanisms that cause AF in DM patients are unknown [17]. The proposed mechanisms include autonomic remodeling, structural remodeling, electrical remodeling, and insulin resistance. There have been no studies of the role of DM-associated atrial inflammatory reaction and stress reaction in the occurrence of AF.

4.1. Autonomic Remodeling. Cardiac autonomic neuropathy (CAN) is a common complication of DM that significantly increases mortality. Reports of the morbidity from CAN in DM patients are inconsistent, which may be related to variations in the populations studied and the methods used to screen for CAN [18]. The morbidity from CAN was low (2.5%) in patients undergoing primary prevention, but very high (90%) in those with long-term type 1 DM awaiting pancreas transplantation [19, 20]. Based on heart rate variability (HRV) tests and spectral analysis of RR intervals, the morbidity from CAN in type 2 DM (T2DM) was 34.3%. Age, sex, and other risk factors may be associated with the progression of CAN [21]. A recent report showed that CAN was common in patients with T2DM, with a morbidity of 44.3%; CAN was associated with modifiable factors such as carotid lipid deposition, hypertension, dyslipidemia, smoking, poorly controlled glycemia, and microvasculopathy. Management of these risk factors can prevent the occurrence and progression of CAN [22], which is closely related to the effects of risk factors such as poor glycemic control, a history of hyperglycemia, age-related neural injury, and high blood pressure. Hyperglycemia plays an important role in the pathogenesis of CAN by impairing nerve blood perfusion and activating cellular metabolism and redox-associated biologic pathways.

The autonomic dysfunction in DM patients can be caused by hyperglycemia-related pathophysiologic pathways such as

the formation of advanced glycation end products, elevated oxidative/nitrosative stress with increased production of free radicals, and activation of the polyol and protein kinase C pathway, as well as poly-ADP ribosylation and neuronal damage-associated genes [18]. Most DM patients have autonomic imbalance—that is, enhanced sympathetic activity and decreased parasympathetic activity—regardless of whether they have DM neuropathy. Well-controlled blood glucose and use of angiotensin converting enzyme inhibitors have a beneficial effect on HRV [23]. A DM rat model established by intravenous injection of streptozotocin indicated that sympathetic stimulation increased the incidence of AF in DM rats but not in controls ($P < 0.01$). Sympathetic stimulation significantly shortened the effective refractory period (ERP) of atrial cells in both groups, but the heterogeneity of the atrial ERP increased in the DM rats only. Parasympathetic stimulation also increased the incidence of AF via shortening of the atrial ERP in both DM rats and controls. Immunohistochemical staining of the right atrium aimed at determining the distribution of sympathetic nerves revealed that tyrosine hydroxylase positive nerves were significantly more heterogeneous in DM rats than in control rats, whereas the heterogeneity of acetylcholine esterase positive nerves did not differ between the two groups. This evidence indicates that cardiac adrenergic nerve stimulation in individuals with DM can lead to AF. The heterogeneity of sympathetic innervation is increased in DM, which suggests that autonomic remodeling may increase susceptibility to AF in this group [24]. Animal studies have indicated that sympathetic nerve remodeling may play an important role in the development and progression of AF in DM patients.

4.2. Electrical and Structural Remodeling. DM cardiomyopathy (i.e., DM-related cardiac structural and functional changes that are not caused by coronary atherosclerosis or hypertension) can lead to left ventricular hypertrophy and increased susceptibility to ischemic injury and the morbidity of heart failure, thereby increasing mortality. Possible pathophysiologic mechanisms of DM cardiomyopathy include myocardial hypertrophy, myocardial lipotoxicity, oxidative stress, cellular apoptosis, interstitial fibrosis, contraction-relaxation dysfunction, impaired myocardial contractile reserve, mitochondrial dysfunction, and disorders of myocardial metabolism [25]. A study employing the genetic T2DM (Goto-Kakizaki) rat model found no difference in ERP between DM and control rats, but the intra-atrial activation time of the DM group was much longer. In a DM rat model, a single premature electrical stimulation induced large numbers of repetitive atrial responses [26]. During catheter ablation, using a three-dimensional mapping system, the activation time of both atria was significantly longer, and the bipolar voltage significantly decreased in a DM group [27]. Maximal P-P interval and the degree of P wave dispersion were significantly increased in prediabetic patients without a history of coronary heart disease, hypertension, or left ventricular hypertrophy, and the latter was positively related to fasting blood glucose level [28].

Atrial fibrosis is also an important mechanism for cardiac structural and electrical remodeling. In a DM rat model, there are widespread fibrotic deposits in the atria that are prone to the formation of anchoring points for reentry circuits and changes in the forward propagation of fibrillatory wavelets and thus cause atrial fractionated potentials and conduction delay [26]. Oxidative stress may also be involved in the formation of hyperglycemia-associated AF substrates, leading to atrial fibrosis. A study in which atrial tissue was collected from DM patients during coronary artery bypass graft surgery found that mitochondrial dysfunction in the atrial myocardium can cause excessive oxidative stress [29]. In DM rats, the expression of connexin-43 was elevated, whereas its phosphorylation was decreased in the atrial myocardium, which leads to disorders of intercellular electrical coupling and atrial arrhythmia [30]. Advanced glycation end products (AGEs) and AGE receptors (RAGEs) (the AGE-RAGE system) mediate the diffuse interstitial fibrosis of the atrial myocardium in DM rats through upregulation of the expression of growth factors by connective tissue, and cause structural remodeling. AGE inhibitors can downregulate the expression of growth factors and significantly inhibit the progression of DM-induced atrial fibrosis [31]. AGE inhibitors may be used in the upstream therapy of DM-related fibrosis in the future.

4.3. Insulin Resistance. Previous studies have demonstrated that patients with insulin-dependent DM suffer AF attacks while hypoglycemic. Some experts consider the cause of such AF attacks to be fluctuations in glycemia rather than the hyperglycemic state itself [17]. A study has found that blood glucose is significantly elevated during an AF attack and that a high dose of insulin (10 times the daily dose) is required to control it. After successful cardioversion of AF, the insulin dose required is significantly decreased [32].

5. Therapeutic Strategy

5.1. Anticoagulation Therapy. AF is a major risk factor for stroke and thromboembolism. The mortality, disability rate, and risk of stroke recurrence are all higher in stroke caused by AF than in that due to other causes. The risk of stroke varies among DM patients with AF, and treatment relies on risk evaluation and appropriate anticoagulation therapy. The simplest way to assess the risk of stroke is the $CHADS_2$ scoring system. The European Society of Cardiology Guidelines for the Management of Atrial Fibrillation (2010 ESC) recommended the use of a more appropriate system, the CHA_2DS_2-VASc. In AF patients with DM, if the risk of major bleeding is low or the benefit/risk ratio is considered high, an oral anticoagulant such as a vitamin K antagonist (VKAs) is the first choice independent of rate control or rhythm control. The dose of VKAs depends on the target intensity INR (International Normalized Ratio) of 2.0–3.0, with a target value of 2.5. New anticoagulants (e.g., Dabigatran etexilate, Apixaban) are alternatives to VKAs [33].

5.2. Upstream Therapy. Atrial structural remodeling or fibrosis can decrease the conduction speed of the atrial myocardium, which may be the underlying mechanism of

DM-related AF. Angiotensin II receptor blockers (ARBs) may play an important role in the upstream therapy of AF through the following mechanisms: decreasing atrial fibrosis and delaying atrial structural remodeling; inhibiting the production and facilitating the degradation of collagen fibers, thereby decreasing the left atrial overload that is the major reason for the development and progression of AF [26]; modifying the potassium channel current and downregulating the Ito current, the latter of which plays an important role in atrial electrical remodeling [34]; exerting various effects on the subunits of the potassium channel (e.g., losartan blocks the HERG, KvLQT1, mink, and hKv1.5 subunits) [35]; regulating L-type and T-type calcium channels and inhibiting the progression of AF substrates [36, 37]; prolonging the ERP and increasing the frequency adaptability of atria; and decreasing the hyperactivity of the sympathetic nerve system caused by angiotensin II [38]. In hypertensive DM patients with paroxysmal AF, the blood pressure lowering effect is similar in both groups. In patients treated with valsartan/amlodipine, the rate of recurrence of AF is significantly decreased compared with that in patients treated with atenolol/amlodipine, especially those given amiodarone or propafenone compared with those who take other or no antiarrhythmic agents [39].

Several studies indicated thiazolidinedione as a class of peroxisome proliferator-activated receptor-γ activator, may potentially benefit for AF prevention [40–42], especially pioglitazone, due to attenuate atrial fibrosis, inflammation activation, oxidative stress, and apoptosis in the atrium of experiment models [43–47]. The thiazolidinedione may be a novel upstream therapy for AF in DM patients, but still needs further large-scale randomized, controlled trials with long-term follow-up period to evaluate the potential role of AF prevention [48].

5.3. Antiarrhythmic Therapy and Catheter Ablation. Antiarrhythmic treatment in AF patients includes rate control and rhythm control; the choice of drug should be individualized. Commonly used antiarrhythmic drugs that control heart rate in AF patients are β-blockers, nondihydropyridine calcium channel blockers, and digitalis glycosides. Drugs commonly used to control heart rhythm are amiodarone and dronedarone. After treatment with the full dose of an antiarrhythmic drug, catheter ablation may be of further benefit in the treatment of AF [33]. A large prospective study enrolled 263 patients receiving first-time ablation for encircling pulmonary veins guided by the CARTO system; 31 of these had DM. Although the age, duration of AF, left atrial size, incidence of hypertension, and proportion with underlying heart disease were significantly higher in the DM patients compared with the non-DM patients, the rate of recurrence of AF after first-time ablation was similar in the two groups (32.3% versus 22.4%, $P = 0.24$). The possibility of an episode of asymptomatic AF caused by DM neuropathy cannot be excluded in this study, so the success rate of the AF ablation may have been overestimated. This study also suggested that the incidence of procedure-associated complications was higher in the DM patients (29% versus 8.2%, $P = 0.002$). The major complications were hemorrhage and thromboembolism. When hemorrhage was excluded, the incidence of complications was 6.4%. There was an increased tendency to develop cardiac tamponade and thromboembolism in the DM patients; possible reasons include the following: AF is a risk factor for cerebral embolism; DM can cause both prothrombotic and proinflammatory states; and hyperinsulinemia can induce a prothrombotic state that is closely related to metabolic disorders (postprandial hyperglycemia, high levels of free fatty acids, and hypertriglyceridemia) involving platelets, the coagulation cascade, and fibrinolysis [49]. Another study included 70 DM patients with AF (including paroxysmal and persistent AF) and assigned catheter ablation (one ablation procedure without drug treatment) or antiarrhythmic agents randomly. After 1 year of followup, sinus rhythm was maintained in 42.3% and 80% of patients treated with drugs or catheter ablation, respectively ($P = 0.001$). The Life Quality Scale score was significantly higher in the ablation group than in the drug group; 17.1% of patients developed obvious drug-associated side effects, and the hospitalization rate was significantly higher in the drug treatment group ($P = 0.01$). The major complication of catheter ablation was puncturing site bleeding. This evidence suggests that catheter ablation can significantly improve the prognosis of DM patients with AF compared with drug treatment alone [50]. Assessment of DM patients with AF 18.8 ± 6.4 months after catheter ablation showed that, though the recurrence rate was higher in patients with glucose metabolism derangement than in those without DM ($P = 0.02$), it still reached 18.5%, which may be associated with intra-atrial conduction delay and decreased voltage [27].

Pioglitazone is a commonly prescribed drug in clinical practice with anti-inflammatory and antioxidative effects. In a contrast study, 150 selected T2DM patients with paroxysmal AF were divided into two groups depending on whether pioglitazone was given after catheter ablation. Antiarrhythmic drugs were discontinued in patients who remained in sinus rhythm. After an average 15-month followup, compared with the control group, the rate of maintenance of sinus rhythm was higher (86.3% versus 70.7%, $P = 0.03$) and the proportion that underwent a second ablation was lower (9.8% versus 24.2%, $P = 0.03$) among patients treated with pioglitazone. This evidence indicates that, in T2DM with paroxysmal AF, pioglitazone can significantly increase the success rate of catheter ablation and decrease the recurrence of AF. Left atrial size is associated with recurrence of atrial arrhythmia, which can be decreased by both pioglitazone and ARBs [51].

6. Conclusion

DM is one of the most important risk factors for the development and progression of AF and can predict the occurrence of stroke and thromboembolism. Long-term anticoagulation therapy with VKAs is recommended in AF patients with DM. DM can increase the incidence of AF, and when it is combined with other risk factors, the incidence of stroke and thromboembolism may be even higher. The incidence and rate of hospitalization due to heart failure may be increased.

Maintenance of well-controlled blood glucose and low HbA1c according to guidelines may decrease the incidence of AF. The mechanisms of AF associated with DM are autonomic remodeling, electrical remodeling, structural remodeling, and insulin resistance; there are few studies concerning the role of inflammation and oxidative stress in the pathogenesis of AF. Inhibition of the renin-angiotensin system is expected to be an upstream therapy for this type of AF. Some studies have indicated that catheter ablation may be effective in AF associated with DM, restoring sinus rhythm and improving prognosis. Catheter ablation combined with hypoglycemic agents may further increase the rate of maintenance of sinus rhythm and also reduce the risk of need for reablation.

Acknowledgments

This work was supported by grants from the Fundamental Research Funds for the Central Universities (no. 21611333), the Science and Technological Program of Guangdong Province (no. 2010-1096-136), the Science and Technological Projects of Guangzhou (no. 2010Y1-C941), and the Key Disciplines' Funds and Special Research Funds (no. 2012207) of the First Clinical Medical College of Jinan University, Basic Research Expenses of Jinan University.

References

[1] T. Watson, E. Shantsila, and G. Y. Lip, "Mechanisms of thrombogenesis in atrial fibrillation: virchow's triad revisited," *The Lancet*, vol. 373, no. 9658, pp. 155–166, 2009.

[2] C. Steger, A. Pratter, M. Martinek-Bregel et al., "Stroke patients with atrial fibrillation have a worse prognosis than patients without: data from the Austrian Stroke registry," *European Heart Journal*, vol. 25, no. 19, pp. 1734–1740, 2004.

[3] M. R. Movahed, M. Hashemzadeh, and M. Mazen Jamal, "Diabetes mellitus is a strong, independent risk for atrial fibrillation and flutter in addition to other cardiovascular disease," *International Journal of Cardiology*, vol. 105, no. 3, pp. 315–318, 2005.

[4] T. A. Aksnes, R. E. Schmieder, S. E. Kjeldsen, S. Ghani, T. A. Hua, and S. Julius, "Impact of new-onset diabetes mellitus on development of atrial fibrillation and heart failure in high-risk hypertension (from the VALUE Trial)," *American Journal of Cardiology*, vol. 101, no. 5, pp. 634–638, 2008.

[5] G. A. Nichols, K. Reinier, and S. S. Chugh, "Independent contribution of diabetes to increased prevalence and incidence of atrial fibrillation," *Diabetes Care*, vol. 32, no. 10, pp. 1851–1856, 2009.

[6] R. R. Huxley, K. B. Filion, S. Konety, and A. Alonso, "Meta-analysis of cohort and case-control studies of type 2 diabetes mellitus and risk of atrial fibrillation," *American Journal of Cardiology*, vol. 108, no. 1, pp. 56–62, 2011.

[7] O. E. Johansen, E. Brustad, S. Enger, and A. Tveit, "Prevalence of abnormal glucose metabolism in atrial fibrillation: a case control study in 75-year old subjects," *Cardiovascular Diabetology*, vol. 7, article 28, 2008.

[8] C. J. Östgren, J. Merlo, L. Råstam, and U. Lindblad, "Atrial fibrillation and its association with type 2 diabetes and hypertension in a Swedish community," *Diabetes, Obesity and Metabolism*, vol. 6, no. 5, pp. 367–374, 2004.

[9] A. M. Chamberlain, S. K. Agarwal, M. Ambrose, A. R. Folsom, E. Z. Soliman, and A. Alonso, "Metabolic syndrome and incidence of atrial fibrillation among blacks and whites in the Atherosclerosis Risk in Communities (ARIC) Study," *American Heart Journal*, vol. 159, no. 5, pp. 850–856, 2010.

[10] S. Dublin, N. L. Glazer, N. L. Smith et al., "Diabetes mellitus, glycemic control, and risk of atrial fibrillation," *Journal of General Internal Medicine*, vol. 25, no. 8, pp. 853–858, 2010.

[11] R. R. Huxley, A. Alonso, F. L. Lopez et al., "Type 2 diabetes, glucose homeostasis and incident atrial fibrillation: the Atherosclerosis Risk in Communities study," *Heart*, vol. 98, no. 2, pp. 133–138, 2012.

[12] K. Sugishita, E. Shiono, T. Sugiyama, and T. Ashida, "Diabetes influences the cardiac symptoms related to atrial fibrillation," *Circulation Journal*, vol. 67, no. 10, pp. 835–838, 2003.

[13] X. Du, T. Ninomiya, B. De Galan et al., "Risks of cardiovascular events and effects of routine blood pressure lowering among patients with type 2 diabetes and atrial fibrillation: results of the ADVANCE study," *European Heart Journal*, vol. 30, no. 9, pp. 1128–1135, 2009.

[14] H. Soran, N. Younis, P. Currie, J. Silas, I. R. Jones, and G. Gill, "Influence of diabetes on the maintenance of sinus rhythm after a successful direct current cardioversion in patients with atrial fibrillation," *Quarterly Journal of Medicine* , vol. 101, no. 3, pp. 181–187, 2008.

[15] M. Guazzi, S. Belletti, L. Lenatti, E. Bianco, and M. D. Guazzi, "Effects of cardioversion of atrial fibrillation on endothelial function in hypertension or diabetes," *European Journal of Clinical Investigation*, vol. 37, no. 1, pp. 26–34, 2007.

[16] M. Guazzi, S. Belletti, E. Bianco, L. Lenatti, and M. D. Guazzi, "Endothelial dysfunction and exercise performance in lone atrial fibrillation or associated with hypertension or diabetes: different results with cardioversion," *American Journal of Physiology*, vol. 291, no. 2, pp. H921–H928, 2006.

[17] G. Y. H. Lip and G. I. Varughese, "Diabetes mellitus and atrial fibrillation: perspectives on epidemiological and pathophysiological links," *International Journal of Cardiology*, vol. 105, no. 3, pp. 319–321, 2005.

[18] R. Pop-Busui, "Cardiac autonomic neuropathy in diabetes: a clinical perspective," *Diabetes Care*, vol. 33, no. 2, pp. 434–441, 2010.

[19] The Diabetes Control and Complications Trial Research Group, "The effect of intensive diabetes therapy on measures of autonomic nervous system function in the Diabetes Control and Complications Trial (DCCT)," *Diabetologia*, vol. 41, no. 4, pp. 416–423, 1998.

[20] W. R. Kennedy, X. Navarro, and D. E. R. Sutherland, "Neuropathy profile of diabetic patients in a pancreas transplantation program," *Neurology*, vol. 45, no. 4, pp. 773–780, 1995.

[21] D. Ziegler, K. Dannehl, H. Muhlen, M. Spuler, and F. A. Gries, "Prevalence of cardiovascular autonomic dysfunction assessed by spectral analysis, vector analysis, and standard tests of heart rate variation and blood pressure responses at various stages of diabetic neuropathy," *Diabetic Medicine*, vol. 9, no. 9, pp. 806–814, 1992.

[22] C. Voulgari, M. Psallas, A. Kokkinos, V. Argiana, N. Katsilambros, and N. Tentolouris, "The association between cardiac autonomic neuropathy with metabolic and other factors in subjects with type 1 and type 2 diabetes," *Journal of Diabetes and its Complications*, vol. 25, no. 3, pp. 159–167, 2011.

[23] V. Urbančič-Rovan, B. Meglič, A. Stefanovska, A. Bernjak, K. Ažman-Juvan, and A. Kocijančič, "Incipient cardiovascular

autonomic imbalance revealed by wavelet analysis of heart rate variability in type 2 diabetic patients," *Diabetic Medicine*, vol. 24, no. 1, pp. 18–26, 2007.

[24] H. Otake, H. Suzuki, T. Honda, and Y. Maruyama, "Influences of autonomic nervous system on atrial arrhythmogenic substrates and the incidence of atrial fibrillation in diabetic heart," *International Heart Journal*, vol. 50, no. 5, pp. 627–641, 2009.

[25] S. Boudina and E. D. Abel, "Diabetic cardiomyopathy, causes and effects," *Reviews in Endocrine and Metabolic Disorders*, vol. 11, no. 1, pp. 31–39, 2010.

[26] T. Kato, T. Yamashita, A. Sekiguchi et al., "What are arrhythmogenic substrates in diabetic rat atria?" *Journal of Cardiovascular Electrophysiology*, vol. 17, no. 8, pp. 890–894, 2006.

[27] T. F. Chao, K. Suenari, S. L. Chang et al., "Atrial substrate properties and outcome of catheter ablation in patients with paroxysmal atrial fibrillation associated with diabetes mellitus or impaired fasting glucose," *American Journal of Cardiology*, vol. 106, no. 11, pp. 1615–1620, 2010.

[28] T. Karabag, M. Aydin, S. M. Dogan et al., "Prolonged P wave dispersion in pre-diabetic patients," *Kardiologia Polska*, vol. 69, no. 6, pp. 566–571, 2011.

[29] E. J. Anderson, A. P. Kypson, E. Rodriguez, C. A. Anderson, E. J. Lehr, and P. D. Neufer, "Substrate-specific derangements in mitochondrial metabolism and redox balance in the atrium of the type 2 diabetic human heart," *Journal of the American College of Cardiology*, vol. 54, no. 20, pp. 1891–1898, 2009.

[30] M. Mitašíková, H. Lin, T. Soukup, I. Imanaga, and N. Tribulová, "Diabetes and thyroid hormones affect connexin-43 and PKC-ε expression in rat heart atria," *Physiological Research*, vol. 58, no. 2, pp. 211–217, 2009.

[31] T. Kato, T. Yamashita, A. Sekiguchi et al., "AGEs-RAGE system mediates atrial structural remodeling in the diabetic rat," *Journal of Cardiovascular Electrophysiology*, vol. 19, no. 4, pp. 415–420, 2008.

[32] V. Rigalleau, L. Baillet, M. Hocini, and H. Gin, "Atrial fibrillation can cause major hyperglycemia," *Diabetes and Metabolism*, vol. 28, no. 3, pp. 239–240, 2002.

[33] A. J. Camm, P. Kirchhof, G. Y. Lip et al., "Guidelines for the management of atrial fibrillation: the Task Force for the Management of Atrial Fibrillation of the European Society of Cardiology (ESC)," *Europace*, vol. 12, no. 10, pp. 1360–1420, 2010.

[34] J. R. Ehrlich, S. H. Hohnloser, and S. Mattel, "Role of angiotensin system and effects of its inhibition in atrial fibrillation: clinical and experimental evidence," *European Heart Journal*, vol. 27, no. 5, pp. 512–518, 2006.

[35] R. Caballero, E. Delpón, C. Valenzuela, M. Longobardo, and J. Tamargo, "Losartan and its metabolite E3174 modify cardiac delayed rectifier K+ currents," *Circulation*, vol. 101, no. 10, pp. 1199–1205, 2000.

[36] W. C. De Mello, "Intracellular angiotensin II regulates the inward calcium current in cardiac myocytes," *Hypertension*, vol. 32, no. 6, pp. 976–982, 1998.

[37] S. Fareh, A. Bénardeau, B. Thibault, and S. Nattel, "The T-type Ca2+ channel blocker mibefradil prevents the development of a substrate for atrial fibrillation by tachycardia-induced atrial remodeling in dogs," *Circulation*, vol. 100, no. 21, pp. 2191–2197, 1999.

[38] T. Unger, "Neurohormonal modulation in cardiovascular disease," *American Heart Journal*, vol. 139, no. 1, pp. S2–S8, 2000.

[39] R. Fogari, A. Zoppi, A. Mugellini et al., "Comparative evaluation of effect of valsartan/amlodipine and atenolol/amlodipine combinations on atrial fibrillation recurrence in hypertensive patients with type 2 diabetes mellitus," *Journal of Cardiovascular Pharmacology*, vol. 51, no. 3, pp. 217–222, 2008.

[40] T. Liu, P. Korantzopoulos, G. Li, and J. Li, "The potential role of thiazolidinediones in atrial fibrillation," *International Journal of Cardiology*, vol. 128, no. 1, pp. 129–130, 2008.

[41] T. F. Chao, H. B. Leu, C. C. Huang et al., "Thiazolidinediones can prevent new onset atrial fibrillation in patients with non-insulin dependent diabetes," *International Journal of Cardiology* , vol. 156, no. 2, pp. 199–202, 2012.

[42] M. W. Anglade, J. Kluger, C. M. White, J. Aberle, and C. I. Coleman, "Thiazolidinedione use and post-operative atrial fibrillation: a US nested case-control study," *Current Medical Research and Opinion*, vol. 23, no. 11, pp. 2849–2855, 2007.

[43] M. Shimano, Y. Tsuji, Y. Inden et al., "Pioglitazone, a peroxisome proliferator-activated receptor-gamma activator, attenuates atrial fibrosis and atrial fibrillation promotion in rabbits with congestive heart failure," *Heart Rhythm*, vol. 5, no. 3, pp. 451–459, 2008.

[44] O. Kume, N. Takahashi, O. Wakisaka et al., "Pioglitazone attenuates inflammatory atrial fibrosis and vulnerability to atrial fibrillation induced by pressure overload in rats," *Heart Rhythm*, vol. 8, no. 2, pp. 278–285, 2011.

[45] A. G. Vaiopoulos, K. Marinou, C. Christodoulides et al., "The role of adiponectin in human vascular physiology," *International Journal of Cardiology*, vol. 155, no. 2, pp. 188–193, 2012.

[46] G. Li and T. Liu, "The therapeutic strategies of enhancing adiponectin and lowering leptin may be benefit to controlling atrial fibrillation," *Medical Hypotheses*, vol. 73, no. 1, p. 122, 2009.

[47] D. Xu, N. Murakoshi, M. Igarashi et al., "PPAR-gamma activator pioglitazone prevents age-related atrial fibrillation susceptibility by improving antioxidant capacity and reducing apoptosis in a rat model," *Journal of Cardiovascular Electrophysiology*, vol. 23, no. 2, pp. 209–217, 2012.

[48] T. Liu and G. Li, "Thiazolidinediones as novel upstream therapy for atrial fibrillation in diabetic patients: a review of current evidence," *International Journal of Cardiology*, vol. 156, no. 2, pp. 215–216, 2012.

[49] R. B. Tang, J. Z. Dong, X. P. Liu et al., "Safety and efficacy of catheter ablation of atrial fibrillation in patients with diabetes mellitus—single center experience," *Journal of Interventional Cardiac Electrophysiology*, vol. 17, no. 1, pp. 41–46, 2006.

[50] G. B. Forleo, M. Mantica, L. De Luca et al., "Catheter ablation of atrial fibrillation in patients with diabetes mellitus type 2: results from a randomized study comparing pulmonary vein isolation versus antiarrhythmic drug therapy," *Journal of Cardiovascular Electrophysiology*, vol. 20, no. 1, pp. 22–28, 2009.

[51] J. Gu, X. Liu, X. Wang et al., "Beneficial effect of pioglitazone on the outcome of catheter ablation in patients with paroxysmal atrial fibrillation and type 2 diabetes mellitus," *Europace*, vol. 13, no. 9, pp. 1256–1261, 2011.